Final Report

Practical Cost-Optimization of Characterization and Remediation Decisions at DNAPL Sites with Consideration of Prediction Uncertainty

SERDP Project ER-1611

May 2011

Jack Parker
Ungtae Kim
University of Tennessee at Knoxville

Peter Kitanidis
Mike Cardiff
Xiaoyi Liu
Jonghyun Lee
Standford University

This document has been cleared for public release

SERDP
DOD ▪ EPA ▪ DOE

Report Documentation Page

Form Approved
OMB No. 0704-0188

Public reporting burden for the collection of information is estimated to average 1 hour per response, including the time for reviewing instructions, searching existing data sources, gathering and maintaining the data needed, and completing and reviewing the collection of information. Send comments regarding this burden estimate or any other aspect of this collection of information, including suggestions for reducing this burden, to Washington Headquarters Services, Directorate for Information Operations and Reports, 1215 Jefferson Davis Highway, Suite 1204, Arlington VA 22202-4302. Respondents should be aware that notwithstanding any other provision of law, no person shall be subject to a penalty for failing to comply with a collection of information if it does not display a currently valid OMB control number.

1. REPORT DATE	2. REPORT TYPE	3. DATES COVERED
MAY 2011	**N/A**	**-**

4. TITLE AND SUBTITLE	5a. CONTRACT NUMBER
Practical Cost-Optimization of Characterization and Remediation Decisions at DNAPL Sites with Consideration of Prediction Uncertainty	5b. GRANT NUMBER
	5c. PROGRAM ELEMENT NUMBER
6. AUTHOR(S)	5d. PROJECT NUMBER
	5e. TASK NUMBER
	5f. WORK UNIT NUMBER
7. PERFORMING ORGANIZATION NAME(S) AND ADDRESS(ES) **University of Tennessee at Knoxville**	8. PERFORMING ORGANIZATION REPORT NUMBER
9. SPONSORING/MONITORING AGENCY NAME(S) AND ADDRESS(ES)	10. SPONSOR/MONITOR'S ACRONYM(S)
	11. SPONSOR/MONITOR'S REPORT NUMBER(S)

12. DISTRIBUTION/AVAILABILITY STATEMENT
Approved for public release, distribution unlimited

13. SUPPLEMENTARY NOTES
The original document contains color images.

14. ABSTRACT
The goal of this project was to develop a practical tool for optimizing the design and operation of groundwater remediation systems that explicitly considers uncertainty in site and remediation system characteristics, performance and cost model limitations, and measurement uncertainties that affect predictions of remediation performance and cost. The project was specifically focused on chlorinated solvent contaminated sites with dense nonaqueous phase liquid (DNAPL) sources.

15. SUBJECT TERMS

16. SECURITY CLASSIFICATION OF:			17. LIMITATION OF ABSTRACT	18. NUMBER OF PAGES	19a. NAME OF RESPONSIBLE PERSON
a. REPORT	b. ABSTRACT	c. THIS PAGE			
unclassified	**unclassified**	**unclassified**	**SAR**	**91**	

Acknowledgements

The idea for this project grew from a 2006 SERDP/ESTCP workshop on *Reducing the Uncertainty of DNAPL Source Zone Remediation*, which crystallized the need for an integrated approach to site remediation that uses models coupled with calibration, error propagation, and stochastic optimization methods to evaluate complex tradeoffs and interactions among various remediation technologies and operational strategies, characterization and monitoring data availability and plans for additional measurements, sampling and measurement uncertainty, intrinsic model uncertainty, cost estimation uncertainty, and the detailed statistical formulation of compliance rules.

Encouragement for this formidable undertaking – before and during the project – by Andrea Leeson (SERDP/ESTCP), Beth Moore (USDOE), Dave Becker (USACE), and Kyle Gorder (Hill AFB) was greatly appreciated. Completion of the project would not have been possible without the efforts of many other people. Aleisa Bloom and Bill Ahlers (ORNL) and Bob Lyon (USR Corp.) provided valuable practical insight, technical details and cost parameters on bioremediation using emulsified vegetable oil injection and site data for Dover AFB. Information on historical remedial actions and ongoing investigations and issues at the Fort Lewis EGDY site was provided by Jim Gillie (IMCOM), Mike Truex (PNNL), Mike Annable (University of Florida) and Tamzen Macbeth (CDM). Greg Beyke (TRS Group) provided much guidance on cost and implementation details for source zone mass reduction using electrical resistance heating and Ralph Baker (TerraTherm) provided information on conductive heating and steam injection.

Ungtae Kim (University of Tennessee) implemented the initial semi-analytical solution for DNAPL source depletion and dissolved transport and added many refinements through the project to simulate electron donor-limited biodecay, thermal remediation, and other processes. Mike Cardiff, under the direction of Peter Kitanidis at Stanford University, implemented version 1.0 of the coupled calibration and stochastic cost optimization code, which served as a platform for several further versions implemented by Ungtae Kim that incorporated many refinements in the forward model, cost functions, and optimization code. Kim also formulated and calibrated a model for Dover AFB and conducted analyses of the Fort Lewis site. Xiaoyi Liu and Jonghyun Lee at Stanford implemented improvements in the stochastic optimization code, investigated monetary quantification of additional site characterization data (value of information), and performed design optimization simulations of the Dover AFB site.

This work was performed under contract number W912HQ-08-C-0009 administered by the U.S. Army Corps of Engineers.

Jack Parker
Knoxville, Tennessee
May 2011

Abstract

Objective. The goal of this project was to develop a practical tool for optimizing the design and operation of groundwater remediation systems that explicitly considers uncertainty in site and remediation system characteristics, performance and cost model limitations, and measurement uncertainties that affect predictions of remediation performance and cost. The project was specifically focused on chlorinated solvent contaminated sites with dense nonaqueous phase liquid (DNAPL) sources.

Technical Approach. The method is based on a semi-analytical mathematical model to simulate DNAPL source depletion and dissolved phase transport in response to natural and engineered conditions. The performance model is coupled with cost functions for thermal source zone treatment and enhanced bioremediation. Compliance criteria are defined by statistical rules. The performance model is also coupled with an inverse solution to estimate model parameters, parameter covariances, and residual prediction error. A stochastic cost optimization (SCO) algorithm is used to determine values for design variables that minimize expected net present value cost over Monte Carlo realizations. The method is implemented in SCOToolkit software. The method was applied to two well-characterized sites where different remedial technologies were used, to evaluate its ability to reduce costs and improve remedial designs.

Results. Stochastic cost optimization of design and monitoring variables was found to reduce expected costs by 50% or more relative to conventional design methods, and to substantially increase the probability of meeting compliance targets. Although additional field applications to demonstrate the method are needed, along with development of a “user friendly” interface, the method was shown to be highly effective for two field test sites.

At the first site, the Fort Lewis East Gate Disposal Yard (EGDY) site, optimization of thermal source treatment indicated a need for a much larger treatment area than was actually employed, to avoid a high failure probability associated with source delineation uncertainty based on available source characterization data. Source treatment may be cost effective if additional characterization were undertaken to reduce source zone uncertainty. The method was also used to optimize source and plume bioremediation at the EGDY site, using whey injection without additional source reduction. The results indicated that this remedial strategy should achieve the maximum contaminant limit by 2110, with a 93% probability of success when using relatively low whey injection rates.

The methodology was applied to Dover AFB Area 5 to optimize enhanced bioremediation. The results suggested that electron donor injection may be needed indefinitely in the future to meet remediation criteria, as a result of the uncertainty associated with the source mass estimates, and the difficulties in characterizing and treating source zones without disrupting base operations. Optimization analyses to minimize long term operating costs indicated compliance criteria could be met using only five of the current ten emulsified vegetable oil injection galleries, with operating costs approximately half current costs. Recalibration and optimization after 50 years, using additional data from this period, was projected to further reduce operating costs.

Benefits. The results indicate that SCOToolkit has a potential to significantly improve remediation performance and reduce costs. Use of the method also can identify the most critical data gaps and the uncertainties that will most affect costs and performance projections.

Table of Contents

List of Figures

List of Tables

List of Acronyms and Symbols

AAB	accelerated anaerobic bioremediation
AFB	air force base
A_{TSRi}	areal extent of the thermal treatment zone [m^2]
$A_{\backslash L}$	longitudinal dispersivity [m]
A_T	transverse dispersivity [m]
BTEX	benzene, toluene, ethylbenzene, and xylene
B	lumped parameter defined as $B = J_{cal} / M_{cal}^{\beta}$
CDM	Camp Dresser McKee
CH	chlorinated hydrocarbon
COC	contaminants of concern
COD	chemical oxygen demand
C	dissolved concentration [µg/L]
C_{EDi}^{norx}	ED concentration associated with ED gallery *i* prior to reactions [µg/L]
C_{EDi}^{avail}	ED concentration associated with ED gallery *i* available for reactions [µg/L]
$C'_{CH(\text{serial})}$	aqueous CH concentration after serial reaction path [µg/L]
C_{ED}^{avail}	aqueous concentration of injected ED available for reactions [µg/L]
$C_{ED}^{H\ nat}$	background H-equivalent ED concentration in the aquifer [µg/L]
C_{EA}^{H}	background H-equivalent concentration all EA species in the aquifer [µg/L]
$C_{CH(parallel)}^{'}$	aqueous CH concentration after parallel reaction path [µg/L]
C_{ED}^{net}	aqueous ED concentration after reactions [µg/L]
$C_{CH(mixed)}^{'}$	aqueous CH concentration after mixed reaction path [µg/L]
C_{NPV}^{all}	total NPV remediation and penalty cost [$K]
C_{NPV}^{SWtot}	total NPV site-wide cost [$K]
C_{NPV}^{EDtot}	total NPV ED injection system cost [$K]
C_{NPV}^{TRtot}	total NPV thermal remediation cost [$K]
C_{total}^{PTcap}	total PT fixed cost [$K]
C_{total}^{PTop}	total PT operating cost per year [$K/yr]
C_{NPV}^{pen}	NPV penalty cost [$K]
C_{NPV}^{SWcap}	total NPV site-wide fixed cost [$K]
C_{well}^{SWcap}	fixed cost for monitoring well construction [$K/well]
C_{other}^{SWcap}	any other site-wide fixed costs [$K]
C_{total}^{SWop}	total NPV operating cost for site-wide monitoring and reporting [$K]
C_{samp}^{SWop}	cost per sample for site-wide monitoring [$K/sample]
C_{other}^{SWop}	other annual site-wide operating costs [$K/yr]

C_{NPV}^{EDtot}	the total NPV cost for ED injection [$K]
C_{NPV}^{EDcap}	total NPV fixed ED cost [$K]
C_{width}^{EDcap}	fixed cost per ED gallery width [$K/m]
C_{mw}^{EDcap}	construction cost per operational ED monitoring well [$K/well]
C_{other}^{EDcap}	other fixed ED costs [$K]
C_{NPV}^{EDop}	total NPV operating cost for ED injection [$K]
C_{width}^{EDop}	operating cost per ED gallery width for maintenance etc. [$K/m]
C_{mass}^{EDop}	operating cost per unit ED mass injection [$K/kg]
C_{samp}^{EDop}	collection and analysis cost per ED monitoring sample [$K/sample]
C_{other}^{EDop}	other ED operating costs per gallery per year for reporting etc. [$K/gallery/yr]
C_{all}^{EDop}	other ED operating costs regardless of the number of galleries [$K/yr]
C_{NPV}^{TRtot}	total NPV cost for thermal treatment for all sources [$K]
C_{site}^{TR}	fixed cost for all sources at a site [$K]
$C_{vol_i}^{TR}$	cost multiplier per unit area of the treatment zone to reach design energy [$K/m^3]
$C_{area_i}^{TR}$	cost multiplier per unit area of the treatment zone to reach design energy [$K/m^2]
C_{mob}^{TR}	mobilization cost for each sampling event [$K/event]
$C_{well_i}^{TR}$	installation cost per monitoring well [$K/well]
C_{GWsamp}^{TR}	sampling and analysis cost per groundwater sample [$K/sample]
$C_{bore_i}^{TR}$	cost per soil boring [$K/boring]
$C_{SOILsamp}^{TR}$	cost per soil sample analyzed [$K/sample]
d	annual discount rate [-]
DNAPL	dense nonaqueous phase liquid
(E_0, N_0)	raw easting and northing field coordinates [m]
(E*, N*)	raw easting and northing field coordinates to evaluate [m]
EA	electron acceptor
ED	electron donor
EGDY	East Gate Disposal Yard
ERH	electrical resistance heating
ESTCP	Environmental Security Technology Certification Program
EVO	emulsified vegetable oil
EXV	extreme value compliance rule
E_{eff}	fractional energy yield for biologically-mediated reaction after energy for cell synthesis [-]
E_{frac}	ratio of actual energy consumed when TSR terminates versus the design estimate [-]
$E_{frac(init)}$	cumulative fraction of estimated total energy requirement at which the first samples are taken during TSR [-]
f'_{CH}	H-equivalent react with a unit contaminant concentration [-]
f'_{ED}	H-equivalents to react with a unit ED concentration [-]

f'_{EA}	H-equivalents to react with a unit EA concentration [-]
f_{samp}^{ED}	number of samples per well per year for ED operational monitoring
f_{samp}^{SW}	number of samples per well per year for site-wide monitoring [#/well/yr]
f_{mt}	mass transfer enhancement concentration coefficient [m^3/kg]
f_E	fraction of non-monitoring variable costs attributable to energy use [-]
F_i	total soil and/or groundwater samples divided by pre-treatment sampling number [-]
F_{mt}	mass transfer enhancement factor [-]
F_{miss}	fraction of pre-remediation mass outside thermal treatment zone [-]
F_{serial}	fraction of reductive dechlorination that follows serial pathway [-]
I_{pen}	1 if a penalty cost is triggered else 0 [-]
I_{PT}	1 if PT implementation is triggered else 0 [-]
I_i^{ED}	indicator that is 1 if gallery *i* is actually implemented else 0
IMCOM	US Army Installation Management Command
ISCO	in situ chemical oxidation
IWCD	Industrial waste collection drain
I_i^{TR}	1 if thermal treatment is performed for source i else 0 [-]
J_i	contaminant mass dissolution rate for source i [kg/d]
J_{cal}	contaminant mass dissolution rate for source on calibration date [kg/d]
$J_{treatment\ zone}$	discharge rate from mass within thermal treatment zone [kg/d]
L_z	aquifer thickness [m]
L_i^{ED}	width of ED gallery *i* perpendicular to the flow direction [m]
MCL	maximum contaminant level
M	contaminant mass in source [kg]
M_{cal}	contaminant mass on calibration date [kg]
M_{EDi}	mass injection rate of ED for gallery *i* [kg/d]
M_{miss}	initial mass outside the thermal treatment zone [kg]
M_{ref}	contaminant mass on reference date [kg]
M_{TSRo}	source mass at the commencement of thermal treatment [kg]
$M_{treatment\ zone\ o}$	initial mass within the thermal treatment zone [kg]
NC	non-compliance condition
NFA	no further action compliance condition
N_{source}	number of individual source zones [-]
$N_{well_i}^{TR}$	number of source zone groundwater monitoring wells [-]
$N_{samp/well_i}^{TR}$	number of sampling depths per well [-]
$N_{bore_i}^{TR}$	number of soil boring locations for each sampling time [-]
$N_{samp/bore_i}^{TR}$	number of depth intervals sampled per boring [-]
N_{well}^{SW}	number of site-wide monitoring wells including compliance wells [-]
$N_{lookback}$	moving time window for compliance evaluation [yr]
N_{mw}^{ED}	number of operational monitoring wells [not injection wells] per ED gallery
N_{gal}^{ED}	number of potential ED galleries

O_{ti}^{ED}	indicator that is 1 if gallery *i* is operating in year t else 0
ORNL	Oak Ridge National Laboratory
PNNL	Pacific Northwest National Laboratory
PCE	tetrachloroethylene
PICT	permanent injection circulation transects
PT	conditional containment condition implemented (compliance condition)
q	darcy velocity [m/d]
R	retardation factor [-]
RCL	regression confidence limit compliance rule
$R_{TSR(soil)}$	target soil concentration reduction fraction for thermal treatment [-]
$R_{TSR(gw)}$	target groundwater concentration reduction fraction for thermal treatment [-]
SERDP	Strategic Environmental Research and Development Program
SCOToolkit	Stochastic Cost Optimization Toolkit
S_{lnC}	standard deviation of ln-transformed variable [-]
TCE	trichloroethene
TSR	thermal source reduction
t_{oi}^{ED}	start date for ED gallery *i* [yr]
t_{ref}	reference date for NPV adjustment [yr]
t_{max}	maximum simulation date [yr]
t_{PT}	year that PT is triggered [yr]
t_{start}	first year capital costs are incurred [yr]
$t_{penalty}$	date when penalty cost is incurred [yr]
t_{nfa}	earliest date when no further action conditions may be met [yr]
t_{TSRo}	date thermal treatment begins [yr]
t_{TSRf}	date when thermal treatment is completed [yr]
t_{TSR}	date that thermal treatment is performed [yr]
t_{ref}	basis date for present value [yr]
t_o	source release date [yr]
t_{cal}	calibration date [yr]
t_{ref}	reference date [yr]
t_{rem}	date remedial action commences [yr]
USDOE	US Department of Energy
USACE	US Army Corps of Engineers
UST	underground storage tank
VC	vinyl chloride
v	superficial pore water velocity [m/d]
X_i	binary switch [= 0 or 1] to select/deselect thermal treatment for source i [-]
(x, y)	local easting and northing coordinates along streamline from source origin [m]
Z_{TSR}	vertical extent of the thermal treatment zone [m]
β	source mass depletion exponent [-]
ΔE_{frac}	incremental energy fraction between thermal sampling events [-]
ϕ	aquifer porosity [-]
λ_i	first-order decay coefficient for zone i [d^{-1}]

Chapter 1
Introduction

1.1 Background

In the last 25 years, there have been a number of studies on remediation design optimization, which reflect an increasing appreciation for the importance of cost optimization. Teutsch et al. (2001) emphasize the need to combine physically based simulation models and economic models for quantitative decision-making. Becker et al. (2006) reported that simulation-optimization methods were able to identify solutions that cost 5% to 50% less than trial-and-error results, translating to cost savings of $600K to $10M for sites studied.

Much of the early optimization work focused on pump-and-treat system design with the objective to minimize total pumping as a surrogate for operating cost. Gorelick et al. (1984) was the first to combine simulation models with nonlinear optimization methods to identify optimal design variables. McKinney and Lin (1996) argued for incorporating fixed as well as operating costs, leading to solutions with fewer wells and higher pumping rates. Regulatory compliance (e.g., plume containment) has been variously treated as an optimization constraint (Wagner and Gorelick, 1987; McKinney and Lin, 1996), as a "penalty cost" for noncompliance included in the objective function (Rizzo and Dougherty, 1996; Chan-Hilton and Culver, 2005), or as a component in multi-objective programming (e.g., Erickson et al., 2002).

Many remediation optimization studies disregard uncertainty in simulated performance resulting in overly optimistic estimates of cost and success probability. Wagner and Gorelick (1987) considered uncertainty in parameters using a linearized chance-constraint formulation. A number of studies treated uncertainty explicitly by optimizing the expectation of system performance over an ensemble (Andricevic and Kitanidis, 1990; Lee and Kitanidis, 1991; Tucciarelli and Pinder, 1991; Wagner et al., 1992; Aly and Peralta, 1999; Teutsch and Finkel, 2002; Mugunthan and Shoemaker, 2004; Chan-Hilton and Culver, 2005; Feyen and Gorelick, 2005).

Although pump-and treat methods have been widely used, they are more realistically regarded as containment rather than a remediation measures. This is particularly true for sites with dense nonaqueous phase liquid (DNAPL) source zones, because of their low solubility and very long persistence (e.g., Cohen and Mercer, 1993; National Research Council, 1994). A number of remediation strategies have been developed in recent years to deal with DNAPL sites. These include source mass reduction via thermal or chemical oxidation or surfactant flushing (e.g., Liang and Falta, 2008; Heron et al., 2009; Thompson et al., 2007) and introduction of electron donors (EDs) and other amendments in wells or trenches to enhance in situ contaminant biodecay within the source and/or dissolved plume (Wymore et al., 2006).

Effective remediation may require a combination of technologies, thus complicating the optimization problem. Furthermore, a more complex simulation model will be required that is capable of describing the individual remediation strategies of interest. This will introduce additional model parameters with attendant uncertainty, which will propagate to performance predictions. Mayer and Endres (2007) studied cost tradeoffs associated with source mass removal and dissolved plume remediation measures under deterministic conditions. Cardiff et al. (2010) presented a semi-analytical model for DNAPL site remediation using thermal source reduction (TSR) and/or ED injection for enhanced dissolved plume biodecay, coupled with an

inverse solution to estimate model parameters and their uncertainty from measured site data; a cost module to compute net present value (NPV) cost to meet specific objectives and constraints considering fixed and operating costs; an error propagation module to determine expected cost; and an optimization module to determine design variables that minimize the expected cost. A simple test problem was presented to illustrate the methodology.

1.2 Objectives and Overview of Approach

The goal of this project was to develop a practical tool for optimizing the design and operation of groundwater remediation systems that explicitly takes into consideration uncertainty in site and remediation system characteristics and inherent model limitations that affect predictions of remediation performance and cost – with a specific focus on chlorinated solvent contaminated sites with DNAPL sources.

The general approach for the Stochastic Cost Optimization Toolkit (SCOToolkit) described in this report is depicted in flowchart form in Figure 1-1. The central component of the method is a semi-analytical mathematical model to simulate DNAPL source depletion and dissolved phase transport of a target chlorinated hydrocarbon over time in response to natural and engineered conditions. Currently, the performance model is coupled with cost functions for thermal source zone treatment and enhanced bioremediation using ED injection.

In the inverse modeling mode, historical site data is used to calibrate the simulation model and to estimate parameter covariances and residual prediction error. Forward predictions of remediation performance and cost are performed for defined remediation strategies, operating rules and remediation criteria. A Monte Carlo (MC) method is used to quantify uncertainty in performance and cost attributable considering uncertainty in model parameters, measurements employed for real-time decisions, and cost function variables.

Design optimization is performed to determine values of design variables that minimize the expected value (average over MC realizations) of NPV, which may include “penalty costs” for failure to achieve defined remediation objectives within a specified time period.

Chapter 2 of this report describes the basic transport model. Chapters 3 and 4 describe the enhanced bio and thermal cost/performance models, respectively. Chapter 5 outlines calibration and uncertainty analysis methods. Chapter 6 presents the stochastic design optimization approach and Chapters 7 – 9 document practical applications of the program. A program user guide for SCOToolkit is available in a separate document.

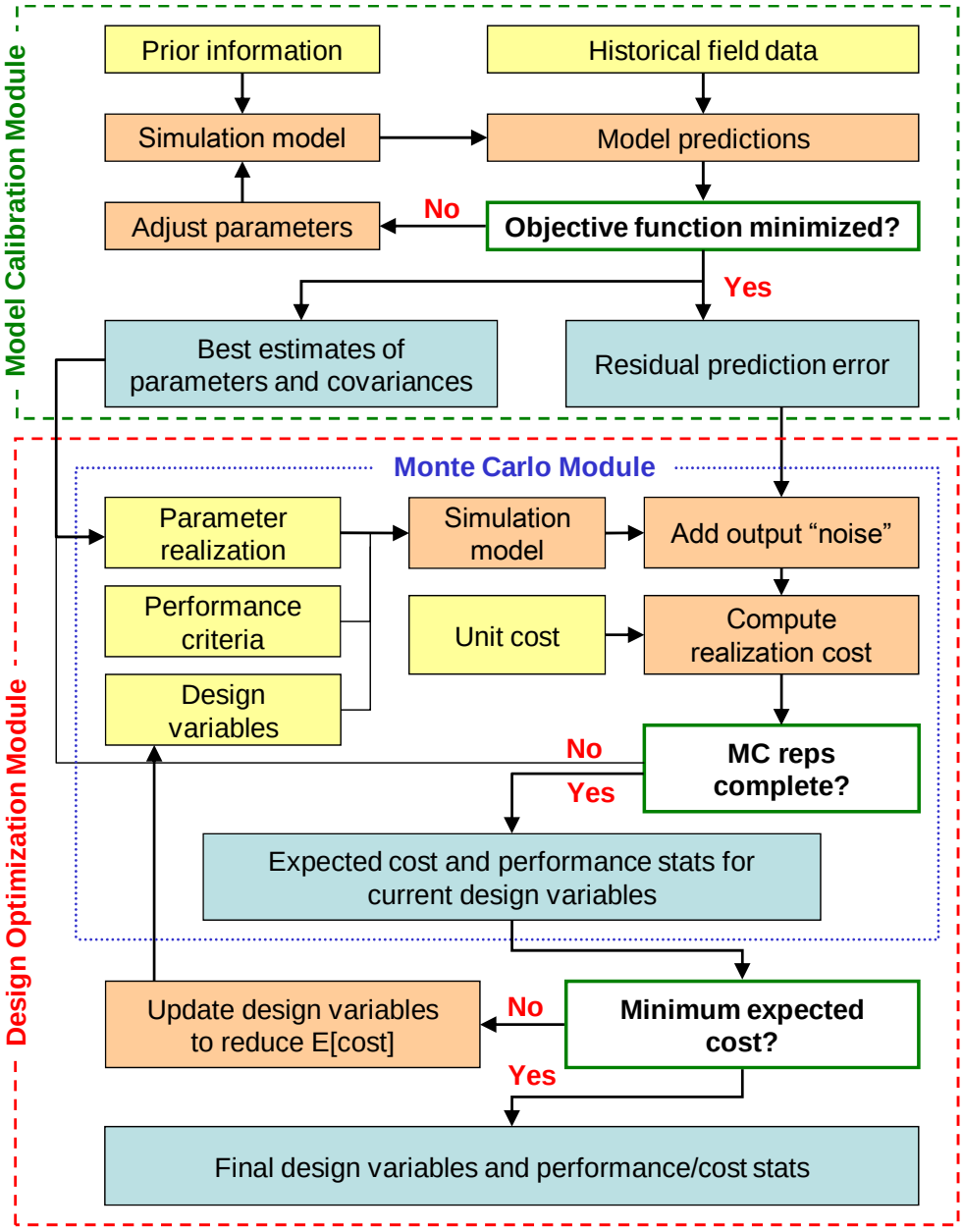

Figure 1-1. Procedural flowchart for SCOToolkit.

Chapter 2
Contaminant Transport Model Formulation

2.1 DNAPL Source Model

Field-scale DNAPL source dissolution and mass depletion over time is described by the model of Parker and Park (2004) and Park and Parker (2005). Considering the possibility of engineered manipulation in mass transfer kinetics, we describe the rate of contaminant mass dissolution in a source zone, J_i [M T^{-1}], versus time, t, by

$$J(t) = F_{mt} J_{cal} \left(\frac{M(t)}{M_{cal}} \right)^{\beta} \tag{2.1}$$

where $J_{cal} = J(t=t_{cal})$ and $M_{cal} = M(t=t_{cal})$ in which t_{cal} denotes a reference time selected for model calibration, M is the source contaminant mass remaining, β is a depletion exponent that reflects the DNAPL source "architecture," and F_{mt} is a time-dependent dimensionless mass transfer enhancement factor.

Integration of the source mass balance equation employing (2.1) as described by Park and Parker (2005) yields source mass remaining versus time after the release date t_o for $\beta \neq 1$

$$M(t) = \left[M_{ref}{}^{1-\beta} - F_{mt} B(1-\beta)(t - t_{ref}) \right]^{1/(1-\beta)} \tag{2.2}$$

where $B = J_{cal} / M_{cal}^{\beta}$. Considering remedial actions at dates $t_{rem\,1}$, $t_{rem\,2}$…$t_{rem\,n}$ when partial source mass removal and/or step changes in F_{mt} occur and stipulating that $t_o < t_{cal} < t_{rem\,1}$, values of M_{ref}, t_{ref} and F_{mt} in (2.2) are assumed to vary with time as follows

Time Period	F_{mt}	t_{ref}	M_{ref}
$t_o < t \leq t_{rem\,1}$	$F_{mt\,0} = 1$	$t_{ref\,0} = t_{cal}$	$M_{ref\,0} = M_{cal}$
$t_{rem\,1} < t \leq t_{rem\,2}$	$F_{mt\,1}$	$t_{ref\,1} = t_{rem\,1}$	$M_{ref\,1}$
$t_{rem\,n-1} < t \leq t_{rem\,n}$	$F_{mt\,n-1}$	$t_{ref\,n-1} = t_{rem\,n-1}$	$M_{ref\,n-1}$
$t > t_{rem\,n}$	$F_{mt\,n}$	$t_{ref\,n} = t_{rem\,n}$	$M_{ref\,n}$

in which $M_{ref\,n}$ for $n > 0$ is given by

$$\begin{aligned} M_{ref\ n} &= M_{remo\ n} - \Delta M_{rem\ n} \\ M_{remo\ n} &= \left[M_{rem\ n-1}{}^{1-\beta} - F_{mt\ n-1} B(1-\beta)(t_{rem\ n} - t_{rem\ n-1}) \right]^{1/(1-\beta)} \end{aligned} \tag{2.3}$$

where $\Delta M_{rem\ n}$ is the mass removed from the source at time $t_{rem\ n}$ regarded as instantaneous. Sorenson (2006) reported that enhanced source zone biodecay caused dissolution rate coefficients to increase by factors of 2 to 6 in laboratory studies and 3 to 8 in field studies. Parker and Park (2004) also have shown that field-scale dissolution rate coefficients will vary inversely with changes in source zone darcy flux (e.g., due to engineered or inadvertent permeability decreases due to amendment injection). Changes in F_{mt} due to ED injection upgradient of DNAPL sources are described in Chapter 3.

2.2 Mapping of Groundwater Flow Field

We consider multiple chlorinated hydrocarbon (CH) sources that may occur within an aquifer characterized by a Cartesian coordinate system in field mapping units (E, N) – e.g., northing and easting. Flow paths will generally be nonlinear. To apply a semi-analytical solution for contaminant transport to mildly nonlinear flow fields, we define a coordinate transformation for each DNAPL source (and later for ED injection galleries) to convert from field coordinates to linearized local coordinates (x, y) and back.

For each source *j* we define the origin of the local coordinate system to be at the center of the downgradient plane of the source – (E_0, N_0) in field coordinates. A streamline may be drawn through (E_0, N_0) using water level contours and dissolved plume data and selected coordinates along the streamline are used to fit a cubic polynomial of the form $N = N_0 + a(E-E_0) + b(E-E_0)^2 + c(E-E_0)^3$. The polynomial function is used to define the (E, N)→(x, y) mapping where x is the distance along the centerline and y is the transverse distance orthogonal to the centerline. Given a location in field coordinates (E*, N*) local coordinates can be found as follows (Figure 2-1):

1) The orthogonal line that passes through (E*, N*) and intersects the streamline at $E = E_{cross}$ may be described by $N = A+BE$ where $A = N^* + BE_{cross}$ and $B = -(a+2b+3cX^2)^{-1}$,
2) Solve recursively for E_{cross} using $E_{cross} = E^*$ initially then solve the cubic equation for E where the orthogonal line intersects the streamline,
3) Compute y as the distance from (E*, N*) to (E_{cross}, N_{cross}), and
4) Compute x as distance along streamline from (E_0, N_0) to (E_{cross}, N_{cross}) by integrating $[1 + N'(E)^2]^{1/2}dE$ from E_0 to E_{cross} where $N'(E)=dN/dE$. Calculate numerically using dE = 10 m.

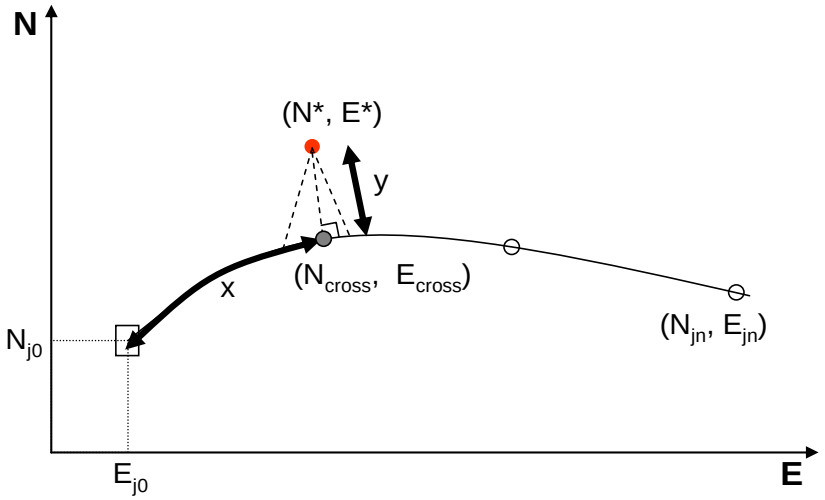

Figure 2-1. Curvilinear streamline in (E, N) field coordinates and mapping to local (x, y) coordinates for source j.

2.3 Dissolved Plume Transport

Dissolved phase transport of contaminants emanating from DNAPL source zones in an unconfined aquifer is described by a 2-D vertically-averaged semi-analytical solution that employs the source zone function described in section 2-1. The solution considers linear sorption and first-order decay. Spatially-variable decay within the aquifer can be described with up to three "zones" at different distances from the source that are characterized by different decay coefficients. Zone 1 represents the region $x < L_{12}$, Zone 2 is $L_{12} < x \le L_{23}$, and Zone 3 is $x > L_{23}$. Extension of the model to simulate ED-limited biodecay is discussed in Chapter 3. Leakage of contamination from the unconfined aquifer (unit A) to an underlying semi-confined aquifer (unit B) and dissolved transport in the lower aquifer due to the secondary source can be optionally considered. The solution for a single DNAPL source in the unconfined aquifer is

$$C_{Ai}(x,y,t) = \int_0^{t-t_o} \frac{J_{Ai}(t-t_o-\tau)}{4L_{zA}L_{yA}\phi_A(\pi R_A A_L v_A \tau)^{1/2}} \exp\left(-\frac{\lambda_{Ai}\tau}{R_A} - \frac{(R_A x - v_A\tau)^2}{4R_A A_L v_A \tau}\right) \times\left[erfc\left(-\frac{y+L_{yA}/2}{2(A_T v_A \tau / R_A)^{1/2}}\right) - erfc\left(-\frac{y-L_{yA}/2}{2(A_T v_A \tau / R_A)^{1/2}}\right)\right] d\tau \quad (2.4)$$

where (x, y) are local coordinates indexed to the source, t is Julian date, t_o is the source release date, τ is a dummy integration variable, $R_A = 1+\rho k_d/\phi$ is the retardation factor in which ρk_d is a dimensionless sorption coefficient, v_A is pore velocity, A_{LA} is longitudinal dispersivity, A_{TA} is transverse dispersivity, L_{zA} is aquifer thickness, L_{yA} is width of the source, ϕ_A is porosity, and λ_{Ai} is a first-order decay coefficient for Zone i. Integration of (2.4) is performed numerically.

For Zone 1 $\lambda_{Ai} = \lambda_{A1}$ and computed from (2.1) with "normal" calibrated values for J_{cal} and M_{cal}. For Zone 2 $\lambda_{Ai} = \lambda_{A2}$ and $J_{Ai}(t) = J_{A2}(t) = J$ computed from (2.1) with values for J_{cal} and M_{cal} multiplied by a scaling factor S_2 defined as

$$S_2 = \frac{C_{A1}(x = L_{12}, y = 0, t; \lambda_{A1}, J_{A1})}{C_{A1}(x = L_{12}, y = 0, t; \lambda_{A2}, J_{A1})} \quad (2.5)$$

For Zone 3 $\lambda_{Ai} = \lambda_{A3}$ and $J_{Ai}(t) = J_{A3}(t) = J$ computed from (2.1) with values for J_{cal} and M_{cal} multiplied by a scaling factor S_3 defined as

$$S_3 = \frac{C_{A1}(x = L_{23}, y = 0, t; \lambda_{A2}, J_{A2})}{C_{A1}(x = L_{23}, y = 0, t; \lambda_{A3}, J_{A1})} \quad (2.6)$$

If leakage from aquifer A to B is considered, Zone 2 can be treated as a leakage window and the decay coefficient is computed as $\lambda_{A2} = q_v/\phi_A L_{zA}$ where q_v is the vertical darcy velocity in the leakage "window".

The solution for aquifer B, which is characterized by a single uniform decay coefficient, is

$$C_B(x,y,t) = \int_0^{t-t_o} \frac{J_B(t-t_o-\tau)}{4L_{zB}L_{yB}\phi_B(\pi R_B A_{LB} v_B \tau)^{1/2}} \exp\left(-\frac{\lambda_B \tau}{R_B} - \frac{(R_B x - v_B \tau)^2}{4R_B A_{LB} v_B \tau}\right) \times \left[erfc\left(-\frac{y + L_{yB}/2}{2(A_{TB} v_B \tau / R_B)^{1/2}}\right) - erfc\left(-\frac{y - L_{yB}/2}{2(A_{TB} v_B \tau / R_B)^{1/2}}\right)\right] d\tau \quad (2.7)$$

where J_B(t) is the mass leakage rate [M T^{-1}] from Aquifer A to Aquifer B computed as

$$J_B(t) = q_v \bar{C}_A A \quad (2.8)$$

where A is the area [L^2] of the "window" in plan view (or part of the window if divided into multiple "panes"), and $\bar{C}_A$ is the average concentration in the window (or pane) computed in the A unit aquifer from (2.4) at the x midpoint of the window or pane (i.e., compute C_A for several points on a transect through the window and average them). The computed J_B values are stored at fixed delta t increments and the resulting look-up table is used to solve (2.7).

Contaminant concentrations resulting from multiple sources in the A or B aquifers are computed by superposition of the individual source solutions after reverting back to field coordinates as

$$C(E,N,t) = \sum_{j=1}^{N_{source}} C_j(E,N,t) \quad (2.9)$$

Note that function calls on the RHS of (2.9) require (E, N)→(x, y) mapping for each source j as illustrated in Figure 2-2.

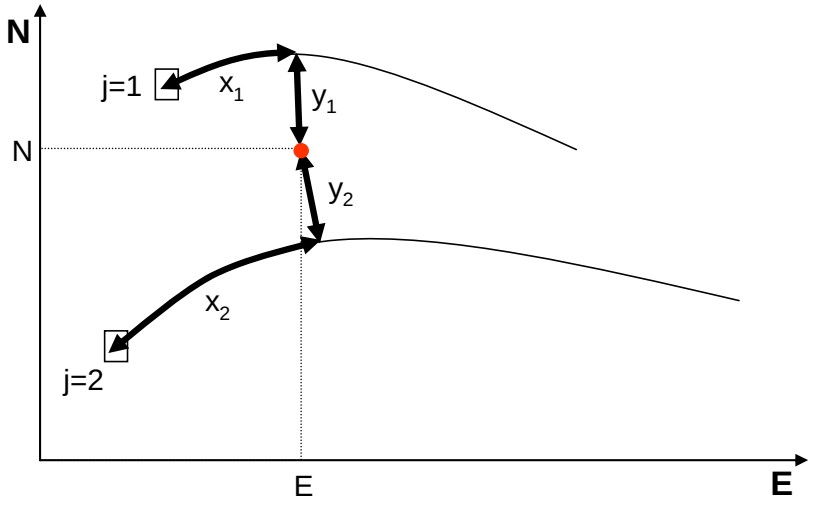

Figure 2-2. Mapping of well location to linearized coordinates for two adjacent nonlinear streamlines in field coordinates for solution superposition.

Chapter 3
Enhanced Bioremediation Cost-Performance Model

3.1 Electron Donor Transport

ED injection is assumed to be performed in one or more injection well galleries of width L_{ED} perpendicular to the groundwater flow direction. The flow field for each ED gallery is characterized by a polynomial streamline. Field coordinates (E, N) are mapped to a linearized local coordinate system (x, y) for each gallery with the local coordinate origin at the center of the ED gallery as described in Chapter 2.

To maximize computational efficiency, ED injection for each gallery *i* is approximated as a constant mass injection rate, M_{EDi} [M T^{-1}] from start date t_{EDo} to stop date t_{EDf} with M_{ED} = 0 otherwise. Actual aqueous phase ED injection will generally be pulsed to reduce well fouling problems and injection of nonaqueous phase ED will be performed with a frequency that depends on the dissolution rate of ED material. As a result, temporal variations in ED concentrations will occur near injection galleries. However, since these variations will diminish markedly with distance from the galleries, modeling ED injection with a time-averaged rate will generally not affect ED available to drive biodecay through most of the aquifer. For the assumed step function injection, the ED concentration before reactions in the aquifer attributable to gallery *i* in local coordinates is

$$\begin{aligned} C_{EDi}^{norx}(x,y,t) &= 0 && \text{for } t < t_{EDo} \\ C_{EDi}^{norx}(x,y,t) &= C(x,y,t-t_{EDo}) && \text{for } t_{EDo} < t < t_{EDf} \\ C_{EDi}^{norx}(x,y,t) &= C(x,y,t-t_{EDo}) - C(x,y,t-t_{EDf}) && \text{for } t > t_{EDf} \end{aligned} \tag{3-1}$$

where C_{EDi}^{norx} is the ED concentration attributable to ED gallery *i* prior to any reactions and $C(x,y,t)$ is the continuous injection solution of Domenico (1987)

$$C(x,y,t) = \frac{f_x f_y M_{EDi}}{4 L_{EDi} L_z q}$$

$$f_x = \text{erfc}\left(\frac{x - v_R(t-t_{EDo})}{2(A_L v_R(t-t_{EDo}))^{0.5}}\right) + \exp\left(\frac{x}{A_L}\right)\text{erfc}\left(\frac{x + v_R(t-t_{EDo})}{2(A_L v_R(t-t_{EDo}))^{0.5}}\right) \tag{3-2}$$

$$f_y = \text{erf}\left(\frac{y + L_{ED}/2}{2(A_T x)^{0.5}}\right) - \text{erf}\left(\frac{y - L_{ED}/2}{2(A_T x)^{0.5}}\right)$$

in which L_{ED} is the ED gallery width perpendicular to the groundwater flow direction, L_z is the effective aquifer thickness, q is the darcy velocity, $v_R = q/(\phi R_{ED})$ is the mean retarded ED plume velocity, and A_L and A_T are longitudinal and transverse dispersivity, respectively.

Kinetics of ED reactions is approximated assuming the fraction of injected ED concentration that is reactive varies exponentially with travel time as

$$C_{EDi}^{avail}(x,y,t) = \left(1 - \exp\frac{-\alpha_{ED} x R_{ED}}{v}\right) C_{EDi}^{norx}(x,y,t) \tag{3-3}$$

where (x, y) are local coordinates for ED gallery i, α_{ED} is a reaction rate coefficient [T^{-1}], v is groundwater pore velocity [$L\ T^{-1}$], and R_{ED} is the ED retardation factor [-].

For multiple ED galleries, the total ED concentration prior to reactions C_{ED}^{norx} at a given location and time is computed by superposition in field coordinates as

$$C_{ED}^{norx}(E,N,t) = \sum_i C_{EDi}^{norx}(E,N,t) \tag{3-4}$$

and the total ED concentration available for reactions is computed similarly as

$$C_{ED}^{avail}(E,N,t) = \sum_i C_{EDi}^{avail}(E,N,t) \tag{3-5}$$

where i denotes solutions for individual ED injection galleries.

The foregoing implicitly treats introduced ED as an aqueous phase material. Nevertheless, nonaqueous or emulsified ED (e.g., various vegetable oil formulations) can be simulated within this mathematical construct by suitable adjustment of α_{ED} and R_{ED} – e.g. by calibration to pilot test data.

3.2 Electron Donor Reactions with Electron Acceptors and Contaminants

Biodecay of CH species is assumed to be limited by the quantity of ED species relative to electron acceptor (EA) species (Kamanth et al., 2006). To estimate the attenuation of CH due to ED addition, a superposition method is used that is analogous to that described by Borden and Bedient (1986). If redox reactions occur serially in order of decreasing reaction free energy (e.g., $O_2 > NO_3 > SO_4 >$ Fe(III) > CH), then an electron balance yields

$$C'_{CH\,(\text{serial})} = \max\left[0, C_{CH} - \max\left(0, \frac{R_{ED} f'_{ED} C_{ED}^{avail} + R_{ED} C_{ED}^{H\ nat} - C_{EA}^{H}}{R_{CH} f'_{CH}}\right)\right] \tag{3-6}$$

where $C'_{CH(\text{serial})}$ is the aqueous CH concentration <u>after</u> serial ED reactions, C_{CH} is the computed CH concentration <u>before</u> ED reactions in the A or B aquifer as needed (as described in Chapter 2), C_{ED}^{avail} is the aqueous concentration of injected ED available for reactions, $C_{ED}^{H\ nat}$ is the background H-equivalent ED concentration in the aquifer, C_{EA}^{H} is the background H-equivalent concentration all EA species in the aquifer, f'_{CH} is the ratio of H-equivalent to actual contaminant concentration, f'_{ED} is the ratio of H-equivalent to actual injected ED concentration, R_{CH} is the CH retardation factor, and R_{ED} is the ED retardation factor (no retardation is assumed for EA species).

H-equivalent ratios (H_{stoch}) for common groundwater ED, EA, and solvent species are summarized in Table 3-1. H-equivalent ratios for EAs are estimated as $f'_{EA} = f_{EA}/E_{eff}$ where f_{EA} is the stoichiometric ratio for complete EA reduction and E_{eff} is fractional energy yield for the biologically-mediated reaction after deducting energy consumed for cell synthesis. The H-equivalent ratio for CH is similarly computed as $f'_{CH} = f_{CH}/E_{eff}$, while H-equivalent ratios for ED species are computed as $f'_{ED} = f_{ED}E_{eff}$, since ED occurs on the opposite side of the EA-ED balance ledger.

Table 3-1. H-equivalent conversion factors for selected ED, EA and CH.

Species	H_{stoch}[1]	E_{eff}[2]	f'[3]
Chlorinated solvents[4]			
PCE (tetrachloroethene)	0.058	0.9	0.064
TCE (trichloroethene)	0.046	0.9	0.051
DCE (cis-1,2-dichloroethene)	0.042	0.9	0.038
VC (vinyl chloride)	0.032	0.9	0.024
Electron donors			
Acetate	0.13	0.6	0.078
Butyrate	0.21	0.6	0.126
Ethanol	0.26	0.6	0.156
HRC	0.12	0.6	0.072
Lactate	0.13	0.6	0.078
Methanol	0.19	0.6	0.114
Molasses	0.14	0.6	0.084
Propionate	0.18	0.6	0.108
Vegetable oil	0.39	0.6	0.234
Whey	0.13	0.6	0.078
Electron acceptors			
Oxygen	0.125	0.51	0.245
Sulfate	0.081	0.43	0.188
Nitrate	0.083	0.92	0.091
Iron (II)	0.018	0.9	0.020

[1] H_{stoch} is the H-equivalent ratio computed for the simple chemical redox reactions (Kamanth et al., 2006)

[2] E_{eff} is the energy conversion efficiency to adjust yield for cell synthesis for relevant microbial populations (Rittman and McCarty, 2001)

[3] f' is the net H-equivalent mass ratio = $H_{stoch}E_{eff}$ for electron donors and H_{stoch}/E_{eff} for electron acceptors.

[4] Stoichiometry based on conversion to ethene.

If reductive dechlorination of CH is assumed to occur under anaerobic conditions with competition among microbial populations responsible for reduction of NO_3, SO_4, etc., an electron balance yields

$$C'_{CH(parallel)} = \min\left[1, \max\left(0, \frac{R_{CH} f'_{CH} C_{CH} + C^H_{EA} - R_{ED} f'_{ED} C^{avail}_{ED} - R_{ED} C^{H\ nat}_{ED}}{R_{CH} f'_{CH} C_{CH} + C^H_{EA} - C^H_{O2}}\right)\right] C_{CH} \qquad (3\text{-}7)$$

where no retardation is assumed for O_2. Assuming that actual biodecay can be approximated as a linear combination of the foregoing pathways, then

$$C'_{CH(mixed)} = F_{serial} C'_{CH(serial)} + (1 - F_{serial}) C'_{CH(parallel)} \qquad (3\text{-}8)$$

where F_{serial} is the fraction of reductive dechlorination that follows the serial pathway. The ED concentration remaining in solution after reactions with EA and CH may be computed by

$$C_{ED}^{net} = C_{ED}^{norx} - \frac{\min\left(R_{ED} f_{ED}^{'} C_{ED}^{avail} + R_{ED} C_{ED}^{H\ nat}, C_{EA}^{H} + R_{CH} f_{CH}^{'} \left(C_{CH} - C_{CH\,(\text{mixed})}^{'}\right)\right)}{R_{CH} f_{CH}^{'}} \tag{3-9}$$

which is used to determine effects of ED injection on mass transfer enhanced in (2.4).

3.3 DNAPL Source Mass Transfer Enhancement Due to ED Injection

The current version of SCOToolkit considers changes in DNAPL mass transfer rate by a factor F_{mt} (see Chapter 2) due to ED injection upgradient of DNAPL sources. Whey injection studies at the Fort Lewis, Washington East Gate Disposal Yard (EGDY) DNAPL site by Macbeth and Sorenson (2008) indicate an approximately linear mass transfer enhancement with ED concentration in the source zone (measured as COD) that may be described by

$$F_{mt} = 1 + f_{mt} C_{ED}^{net} \tag{3-10}$$

where C_{ED}^{net} is the net aqueous ED concentration in the source zone and f_{mt} is a mass transfer enhancement coefficient. If increases in source zone dissolved concentrations are observed during an ED injection pilot test, f_{mt} may be calibrated by adjusting the model input value until the computed F_{mt} value agrees with observed mass transfer enhancement.

The value of C_{ED}^{net} is computed as described in Chapter 3 at coordinates corresponding to the center of the DNAPL source zone at a date equal to the injection start date plus a duration t_{lag} to allow the ED concentration to reach about 99% of the steady-state value estimated as $t_{lag} = xR/v + 3(2A_L xR)^{1/2}/v$ where x is the travel distance from the ED injection gallery to the center of the DNAPL source, R is the ED retardation factor, v is the mean groundwater pore velocity, and A_L is the aquifer longitudinal dispersivity.

3.4 Electron Donor Injection Cost Function

Capital and operating costs for implementation of enhanced bioremediation by injection of ED and other amendments in injection well galleries are described as follows:

$$\begin{aligned}
C_{NPV}^{EDtot} &= C_{NPV}^{EDcap} + C_{NPV}^{EDop} \\
C_{NPV}^{EDcap} &= C_{width}^{EDcap} \sum_{i=1}^{N_{gali}^{ED}} I_i^{ED} L_1^{ED} (1-d)^{t_{oi}^{ED} - t_{ref}} + C_{mw}^{EDcap} N_{mw}^{ED} \sum_{i=1}^{N_{gali}^{ED}} I_i^{ED} (1-d)^{t_{oi}^{ED} - t_{ref}} + \max_i \left(I_i^{ED}\right) C_{other}^{EDcap} (1-d)^{\min_i (t_{oi}^{ED}) - t_{ref}} \\
C_{NPV}^{EDop} &= \sum_{t=t_{ref}}^{t_{max}} \left(C_{width}^{EDop} \sum_{i=1}^{N_{gali}^{ED}} O_{ti}^{ED} L_1^{ED} + C_{mass}^{EDop} \sum_{i=1}^{N_{gali}^{ED}} O_{ti}^{ED} M_{EDi} + C_{samp}^{EDop} f_{samp}^{ED} \sum_{i=1}^{N_{gali}^{ED}} O_{ti}^{ED} N_{mw}^{ED} + C_{other}^{EDop} \sum_{i=1}^{N_{gali}^{ED}} O_{ti}^{ED} + C_{all}^{EDop} \max_i \left(O_{ti}^{ED}\right) \right) (1-d)^{t-t_{ref}}
\end{aligned} \tag{3-11}$$

where the time summation is over integer values of time in years,

C_{NPV}^{EDtot} is the total NPV cost for ED injection ($K),

C_{NPV}^{EDcap} is the total NPV fixed ED cost ($K),

C_{width}^{EDcap} is the fixed cost per ED gallery width ($K/m),

C_{mw}^{EDcap} is the construction cost per operational ED monitoring well ($K/well),

C_{other}^{EDcap} is any other fixed ED costs,

C_{NPV}^{EDop} is the total NPV operating cost for ED injection ($K),

C_{width}^{EDop} is the operating cost per ED gallery width for maintenance etc. ($K/m),

C_{mass}^{EDop} is the operating cost per unit ED mass injection ($K/kg),

C_{samp}^{EDop} is the collection and analysis cost per ED monitoring sample ($K/sample),

C_{other}^{EDop} is other ED operating costs per gallery per year for reporting etc. ($K/gallery/yr),

C_{all}^{EDop} is other ED operating costs regardless of the number of galleries ($K/yr),

d is the annual discount rate (fraction),

f_{samp}^{ED} is the number of samples per well per year for ED operational monitoring,

I_i^{ED} is an indicator that is 1 if gallery i is actually implemented else 0,

L_i^{ED} is the width of ED gallery i perpendicular to the flow direction (m),

M_{EDi} is the mass injection rate of ED for gallery i (kg/yr),

N_{mw}^{ED} is the number of operational monitoring wells (not injection wells) per ED gallery,

N_{gal}^{ED} is the number of potential ED galleries,

O_{ti}^{ED} is an indicator that is 1 if gallery i is operating in year t else 0,

t_{oi}^{ED} is the start date for ED gallery i (yr),

t_{ref} is the reference date for NPV adjustment (yr), and

t_{max} is the maximum simulation date (yr).

3.5 Electron Donor Injection Design Variables

The current version of SCOToolkit allows multiple ED injection galleries to be considered. Each ED gallery can have different gallery coordinates, width, start date, and a constant (average) ED injection rate. Termination of ED injection may be specified as a fixed date or the end date can be based on operational monitoring of contaminant concentrations (C_{ED}) in a nearby well. For ED galleries downgradient of a DNAPL source intended to enhance dissolved plume remediation, ED injection is terminated when the annually-averaged measured contaminant concentration in a designated well location (or locations) upgradient of the ED gallery is less than a specified value C_{ED} (provided any other upgradient ED galleries have terminated injection earlier than the travel time between the galleries prior to present). For ED galleries placed immediately upgradient of a DNAPL source to enhance source zone remediation, an operational monitoring well is designated downgradient of the source to monitor total solvents and decay products as an indicator of source zone DNAPL dissolution rate. When the total concentration is less than a stipulated C_{ED} value, ED injection is terminated. Lognormal noise is applied to simulated annually averaged "measurements" with a ln-standard error equal to $S_{lnCED}\, f_{samp}^{ED\ 1/2}$ where S_{lnCED} is the ln-error for single measurements and f_{samp}^{ED} is the number of measurements per year (number of ED monitoring wells per gallery times annual sampling frequency).

Design variables that may warrant optimization for ED injection galleries include the following:

M_{EDi} is the ED mass injection rate for gallery i (m),

L_{EDi} is the width of gallery i (m),
t_{EDoi} is the start date for ED injection in gallery i,
C_{EDi} is the contaminant concentration at designated operational monitoring location(s) below which ED injection will be terminated, and
f_{samp}^{ED} is the number of measurements per gallery per year for ED operational monitoring.

ED injection gallery coordinates may be optimized directly or several potential locations can be pre-selected and optimization used to determine which are most effective.

If the value of M_{EDi} is below a specified lower cutoff, the gallery is treated as inoperative and no capital or operating costs are applied to it.

Chapter 4
Thermal Source Remediation Model

4.1 Overview

Source mass reduction is a key component of many DNAPL site remediation strategies. Options include excavation, soil vapor extraction, chemical oxidation and thermal treatment. Our focus here will be on electrical resistance heating (ERH) systems, which have broad applicability for saturated and unsaturated zone DNAPL sources. Unlike methods that depend on efficient advective mass transfer, ERH is relatively insensitive to heterogeneity in aquifer permeability, and is capable of removing a high percentage of mass from the treatment volume. The main limitation of ERH, which it shares with most source reduction methods, is that mass reduction is largely limited to the treatment zone (some increase in biotic and abiotic decay may occur downgradient due to elevated temperatures during and for a time after thermal treatment). Hence, its overall effectiveness is highly dependent on the reliability of DNAPL source identification and delineation.

ERH utilizes an array of electrodes installed within the identified treatment zone, which may be placed at discrete depth intervals in increments of the electrode length. Soil and/or groundwater concentrations within the source zone are generally determined prior to commencing treatment to establish baseline conditions and monitoring during treatment is performed to decide when to shut off electrodes to achieve a target reduction in soil and/or groundwater concentrations within the treatment zone. In this chapter, we present a cost estimation formula, alternative operational monitoring methods to manage the ERH system, and the modeling approach employed to assess mass and flux reduction effectiveness, including impacts of uncertainty in source zone delineation.

4.2 Thermal Cost Model

A cost estimation formula for ERH as a function of treatment zone area and volume was provided by TRS Group, Inc. (Greg Beyke, personal communication) that considers capital and operating costs based on energy requirements computed to reach a specified relative contaminant mass reduction. We modified the formula to explicitly consider variations in operational sampling costs and energy costs and their dependence on real-time monitoring for aquifers with multiple NAPL sources as follows

$$C_{NPV}^{TRtot} = \left(\begin{array}{l} C_{site}^{TR} + \sum_{i=1}^{N_{source}} \left\{ I_i^{TR} (1 - f_E + f_E E_{frac_i})(C_{vol_i}^{TR} A_{TSR_i} Z_{TSR_i} + C_{area_i}^{TR} A_{TSR_i}) R_{TSR(soil)i}^{\ -0.0626} + F_i C_{mob}^{TR} \right. \\ \left. + N_{well_i}^{TR} C_{well_i}^{TR} + F_i N_{well_i}^{TR} N_{samp/well_i}^{TR} C_{GWsamp}^{TR} + F_i N_{bore_i}^{TR} C_{bore_i}^{TR} + F_i N_{bore_i}^{TR} N_{samp/bore_i}^{TR} C_{SOILsamp}^{TR} \right\} \end{array} \right) (1-d)^{t_{TSR} - t_{ref}} \tag{4-1}$$

where

A_{TSRi} is the areal extent of the thermal treatment zone (m^2),

C_{NPV}^{TRtot} is the total NPV cost for thermal treatment for all sources ($K),

C_{site}^{TR} is a fixed cost for all sources at a site ($K),

$C_{vol_i}^{TR}$ is a cost multiplier per unit volume of the treatment zone to reach design energy ($K/m^3),

$C_{area_i}^{TR}$ is a cost multiplier per unit area of the treatment zone to reach design energy ($K/m^2),

C_{mob}^{TR} is the mobilization cost for each sampling event ($K/event),

$C_{well_i}^{TR}$ is the installation cost per monitoring well ($K/well),

C_{GWsamp}^{TR} is the sampling and analysis cost per groundwater sample ($K/sample),

$C_{bore_i}^{TR}$ is the cost per soil boring ($K/boring),

$C_{SOILsamp}^{TR}$ is the cost per soil sample analyzed ($K/sample),

E_{fraci} is the ratio of actual energy consumed when TSR terminates versus the design estimate (model-computed as described in section 4.4),

f_E is the fraction of non-monitoring variable costs attributable to energy use (~0.22),

F_i is the total number of soil and/or groundwater samples divided by the number in the pre-treatment sampling round (model-computed as described in section 4.4),

I_i^{TR} is 1 if thermal treatment is performed for source i, else 0,

N_{source} is the number of individual source zones,

$N_{well_i}^{TR}$ is the number of source zone groundwater monitoring wells,

$N_{samp/well_i}^{TR}$ is the number of sampling depths per well,

$N_{bore_i}^{TR}$ is the number of soil boring locations for each sampling time,

$N_{samp/bore_i}^{TR}$ is the number of depth intervals sampled per boring,

$R_{TSR(soil)i}$ is target ratio of source mass remaining following thermal treatment to the mass immediately prior to treatment,

t_{TSR} is the date that thermal treatment is performed (yr),

t_{ref} is the basis date for present value (yr),

X_i is a binary switch (= 0 or 1) to select/deselect thermal treatment for specific sources, and

Z_{TSRi} is the vertical extent of the thermal treatment zone (m).

Typical values for C_{site}^{TR}, $C_{vol_i}^{TR}$ and $C_{area_i}^{TR}$ are $320,000, $25/m^3 and $188/m^2 (in 2009), respectively, for a source consisting predominantly of TCE excluding design and oversight. Unit costs will vary with the spatial configuration of the source region (e.g., increasing with the ratio of source perimeter length to source area), source composition (e.g., solvent species, content of oil, grease and fuel hydrocarbons in mixture), local labor and electricity costs (based on $0.08 per kWh), groundwater velocity, and containment measures required. A remediation contractor should be consulted to develop unit costs for site-specific conditions.

In certain instances, a given source region may be characterized by two or more source functions representing different DNAPL "architectures" – for example, pools and residual DNAPL with different mass, depletion exponents, etc. For such co-located sources, the total source zone thickness should be divided among the various for the co-located sources architecture and the source area similarly divided among the sources. Well installation and soil boring costs for collocated sources must be computed in a manner that does not double count drilling through shallower source zones.

4.3 Operational Methods for Real Time Monitoring

The cost function in the preceding section is based on an estimate of the energy requirement to achieve a target contaminant mass reduction considering the heat capacity of the aquifer, advective heat loss, latent heat of volatilization of water and contaminants, and planned operating temperature. In practice, it is advantageous to base decisions on when to terminate thermal treatment on real-time data from operational monitoring during remediation. The following monitoring and system operation strategies are considered here.

Method 1a – Prior to heating, $N^{TR}_{bore_i}$ soil borings with $N^{TR}_{samp/bore_i}$ samples per boring are collected and average initial soil concentration is computed for each source treatment zone *i*. After a period of time when a fraction $E_{frac(init)i}$ of the theoretical energy requirement has been applied, the same number of soil samples as in the pre-heating round are collected and analyzed. If the *average* measured soil concentration is less than $R_{TSRi(soil)i}$ x the initial average, heating is terminated for all heating elements within the source. Otherwise, the sampling procedure is repeated at time intervals corresponding to a fractional energy use E_{frac} until the criteria are met.

Method 1b – Same as Method 1a except $N^{TR}_{well_i}$ groundwater monitoring wells with $N^{TR}_{samp/well_i}$ sampling depths per well are employed rather than soil samples with an operational objective to reduce groundwater concentration by a factor $R_{TSR(gw)i}$.

Method 1c – Same as Method 1a and 1b but soil and groundwater samples are taken at each sampling event and heating is terminated when both the average measured soil concentration is less than $R_{TSR(soil)i}$ x the initial average soil concentration and the average measured groundwater concentration is less than $R_{TSR(gw)i}$ x the initial average groundwater concentration.

Method 2a – This is similar to Method 1a but individual electrodes are turned off when the measured soil concentration for a sample within the zone heated by the electrode is less than $R_{TSR(soil)i}$ x the average pre-heating concentration. A one-to-one relation between electrodes and sampling regions is assumed. After an electrode is turned off, no further sampling is performed in this region.

Method 2b – Same as Method 2a using groundwater rather than soil samples with a target groundwater concentration reduction factor $R_{TSR(gw)i.}$

Method 2c – Same as Method 2a and 2b but both soil and groundwater samples are taken at each sampling event. Electrodes are shut off incrementally when both the local measured soil concentration is less than $R_{TSR(soil)i}$ x the initial average soil concentration and the average measured groundwater concentration is less than $R_{TSR(gw)i}$ x the initial average groundwater concentration.

4.4 Thermal Source Reduction Model

The model for source mass reduction versus time due to mass transfer to the dissolved phase was described in Chapter 2. Here we focus on source mass reduction during thermal treatment between time $t_{TSRo\ i}$ when thermal treatment begins for source *i* to $t_{TSRf\ i}$ when thermal treatment is completed. The source mass at the commencement of thermal treatment ($M_{TSRo\ i}$) is computed from (2.2) at $t = t_{TSRo\ i}$.

To consider the effects of imperfect source delineation and uncertainty in the area requiring thermal treatment, we divide $M_{TSRo\,i}$ into (1) mass within the treatment zone ($M_{treatment\ zone\ o\,i}$) and (2) mass outside the treatment zone ($M_{miss\,i}$), such that

$$M_{treatment\ zone\ o\,i} = M_{TSR\ o\,i} - M_{miss\,i}\ . \tag{4-2}$$

Assuming $M_{miss\,i}$ does not change substantially during thermal treatment, the total source mass remaining after thermal treatment is

$$M_{TSR\,fi} = M_{treatment\ zone\ fi} + M_{miss\,i} \tag{4-3}$$

where $M_{treatment\ zone\ fi}$ is the treatment zone mass following source heating. The "missing" mass is described by

$$M_{miss\,i} = F_{miss\,i} M_{TSRoi} \tag{4-4}$$

where $F_{miss\,i}$ is the fraction of the pre-remediation source mass that is outside the thermal treatment zone for source *i*, i.e., $F_{miss\,i} > 0$ indicates that a fraction $F_{miss\,i}$ of the estimated source mass is not within the treatment volume and hence will not be treated by source heating.

We treat $F_{miss\,i}$ as a stochastic variable controlled by uncertainty in the actual source volume approximated as

$$F_{miss\,i} = 1 - \min\left(1, \frac{V_{TSR\,i}}{V_{source\,i}}\right) \tag{4-5}$$

where $V_{TSR\,i}$ is the soil volume treated by the thermal system for source *i* and $V_{source\,i}$ is the actual volume of contaminated soil for source *i*. The latter is taken as a stochastic variable by virtue of uncertainty in source zone dimensions based on field investigations and/or model calibration. The "actual" source volume is computed in MC simulations as the product of source dimensions L_x, L_y and L_z generated from their respective best estimates and covariances (or log-transforms if uncertainty is regarded as log-normally distributed).

Source mass within the ERH treatment zone is assumed to decrease with cumulative applied energy as

$$M_{treatment\ zone\,i}(t) = M_{treatment\ zone\,oi}\left(R_{TSR(soil)i}\right)^{E_{frac\,i}(t)} \qquad t_{TSRo\,i} < t \le t_{TSRf\,i} \tag{4-6}$$

where $M_{treatment\ zone\,i}(t)$ is the mass within the treatment zone at time *t* during treatment at which a fraction (or multiple) $E_{frac\,i}(t)$ of the estimated total energy has been applied. The treatment duration, Δt_{TSR}, in years is approximated as

$$\Delta t_{TSRi} = 0.3 E_{frac\,f}\left(R_{TSR(soil)i}\right)^{-0.087} \tag{4-7}$$

with a ln standard deviation of ~0.25. Assuming that $E_{frac\,i}(t) = (t\text{-}t_{TSRoi})/\Delta t_{TSRi}$ then

$$M_{treatment\ zone\,i}(t) = M_{treatment\ zone\,oi}\left(R_{TSR(soil)i}\right)^{(t-t_{TSRo\,i})/\Delta t_{TSR\,i}} \qquad t_{TSRo\,i} < t \le t_{TSRf\,i} \tag{4-8}$$

with $\Delta t_{TSR\,i}$ given by (4-7) with noise. From (2.1), the total mass discharge rate from the source during thermal treatment is described by

$$J_{total\ i}(t) = J_{cal\ i}\left(\frac{M_{treatment\ zone\ i}(t) + M_{miss\ i}}{M_{cal\ i}}\right)^{\beta_i} \tag{4-9}$$

while the discharge rate from the treatment zone alone is only

$$J_{treatment\ zone\ i}(t) = J_{cal\ i}\left(\frac{M_{treatment\ zone\ i}(t)}{M_{cal\ i}}\right)^{\beta_i} \tag{4-10}$$

Average treatment zone dissolved concentrations can be inferred from (4-10) assuming aqueous concentration is approximately proportional to $J_{treatement\ zone\ i}$ and the darcy velocity, indicating

$$R_{TSR(gw)i} = R_{TSR(soil)i}^{\beta_{cal\ i}} \tag{4-11}$$

where $\beta_{cal\ i}$ is the best estimate of the source depletion exponent for source *i*. Note that for MC analyses, although β is generally a stochastic variable, $R_{TSR(gw)}$ and $R_{TSR(soil)}$ are design variables, which must be deterministic. Hence, conversion between soil and groundwater cleanup levels must be made using the best estimate of beta that is available to the user.

Note that average soil and/or groundwater concentrations may be less than their target values due to overshoot at discrete sampling intervals (including use of a value for $E_{frac(init)i}$ that overshoots the target on the first operational sampling). Furthermore, for Methods 1a–1c, positive or negative deviations can occur due to biases in average measured concentrations before and during thermal treatment operation and to biases in average concentrations before treatment. For Methods 2a–2c, positive or negative deviations in individual concentrations associated with each electrode volume may occur. Also, although Methods 2a–2c will generally result in reductions in energy and sampling costs, they will exhibit greater variability in actual cleanup levels because individual samples will exhibit greater variance than averaged values.

To simulate thermal treatment performance for the various methods, we compute average treatment zone soil and/or groundwater concentrations at the beginning of thermal treatment and at specified cumulative energy fractions from (4-2) – (4-6) and (4-10) and apply log-normal "noise" to represent individual measurement variability within the source zone. Uncertainty in averaged soil or dissolved concentrations are taken as the uncertainty in individual values (from calibration results or statistical analysis of field data) times $N^{-1/2}$ where N is the number of samples averaged. When simulated measurements indicate that remediation criteria have been met for Methods 1a–1c, the "actual" treatment zone mass remaining is taken as the noise-free treatment zone mass. For Methods 2a–2c in which electrodes are turned off incrementally, the mass in each "cell" within the treatment zone is simulated and the total source zone remaining when all electrodes have been shut down is computed by summing the final mass in each cell. Note that reduced energy and monitoring costs associated with incremental electrode shutdown may be offset by the greater uncertainty in individual measurements than site averages, which may necessitate operating longer to meet more stringent nominal cleanup levels that provide a safety factor against performance uncertainty.

4.5 Thermal System Design Variables

Design variables that may warrant optimization include the following for each identified DNAPL source:

A_{TSR} is the total soil area treated by the thermal system,
Operational monitoring method used to shut off TSR (i.e., Method 1 or 2),
$R_{TSR(soil)}$ is the ratio of final soil concentration in the source zone to the initial concentration,
$E_{frac(init)}$ is the cumulative fraction of estimated total energy requirement at which the first samples are taken (after pre-remediation baseline),
ΔE_{frac} is the incremental fraction of estimated total energy for subsequent sampling events,
$N_{well_i}^{TR}$ is the number of source zone groundwater monitoring wells,
$N_{samp/well_i}^{TR}$ is the number of sampling depths per well (if $N_{well_i}^{TR} > 0$),
$N_{bore_i}^{TR}$ is the number of soil boring locations for each sampling time, and
$N_{samp/bore_i}^{TR}$ is the number of depth intervals sampled per boring (if $N_{bore_i}^{TR} > 0$).

Note that if groundwater measurements are used to decide when to terminate thermal treatment, then the ratio of final groundwater concentration in the source zone to the initial groundwater concentration ($R_{TSR(gw)}$) is computed internally from (4-11). The value of $R_{TSR(gw)}$ corresponding to a specified $R_{TSR(soil)}$ is printed by the code for field use in making system termination decisions from source zone groundwater monitoring data.

Chapter 5
Model Calibration and Uncertainty Analysis

5.1 Overview

Before a model can be used to evaluate effects of various design variables on the expected performance and cost of remediation strategies of interest, a number of site-specific parameters must be estimated from data available from site characterization investigations. Most model parameters will be subject to more or less uncertainty, depending on the quality and quantity of data available. In addition to parametric uncertainty, models are, by definition, simplifications of reality, and thus are subject to intrinsic model formulation errors associated with explicit or implicit simplifying assumptions that have been invoked. Measurements used to estimate model parameters are themselves subject to sampling and analytical errors, which also contribute to prediction uncertainty.

Therefore, the first step that must be undertaken prior to employing a model to evaluate design options is to perform model calibration using all available data and then to quantify parametric, intrinsic and measurement uncertainty. The model can then be used to make forward estimates of performance and cost and to quantify the prediction uncertainty.

5.2 Model Calibration and Error Analysis

The purpose of the calibration/uncertainty analysis module is to determine best estimates of key model parameters and to quantify parametric and residual model uncertainty. The model calibration process utilizes field measurements (which may comprise various types of data, e.g., contaminant concentrations, ED concentrations, and contaminant fluxes at various locations and times), and prior information about parameter values and their uncertainty. Assuming Gaussian (or log-Gaussian) measurement errors and prior parameter distributions, we seek to minimize the negative log of the posterior distribution, *L*, described by

$$L = \frac{1}{2}\mathbf{w}^T\mathbf{w}\left(\mathbf{y}-\mathbf{h}(\mathbf{s})\right)^T\mathbf{R}(\boldsymbol{\theta})^{-1}\left(\mathbf{y}-\mathbf{h}(\mathbf{s})\right)+\frac{1}{2}\left(\mathbf{s}-\mathbf{s}^*\right)^T\mathbf{Q}^{-1}\left(\mathbf{s}-\mathbf{s}^*\right) \qquad (5\text{-}1)$$

where **y** is a vector of field measurements, **s** is a vector of parameter values, **s*** is a vector of prior parameter estimates, **h**(**s**) is a vector of model predictions corresponding to the field measurements, **R** is a matrix of measurement covariances corresponding to the vector of data types $\boldsymbol{\theta}$ (e.g., measured contaminant concentration, source mass, source mass discharge rate, etc.), **w** is a user-defined weighting matrix, and **Q** is the covariance matrix of prior parameter estimates. Off-diagonal terms are disregarded for **w**, **R** and **Q**.

Each model parameter and each data type may be log-transformed prior to application of (5-1). For parameters or data types that are physically constrained to be non-negative and that are expected to exhibit a coefficient of uncertainty greater than ~20%, log-transformation is advisable. Also, calibration data types that exhibit ranges in the data set that extend over several orders-of-magnitude, log-transformation may be desirable if comparable relative error (as opposed to absolute error) is desired over the measurement range. Otherwise, the regression results will likely be controlled by absolute errors from a small number of large data values.

The magnitude of each data type's uncertainty (i.e., diagonal terms in **R**) is generally not known *a priori*, but a posterior estimate can be made using the Restricted Maximum Likelihood (RML) algorithm (Kitanidis, 1987). Note that the final estimate of residual prediction uncertainty **R** for each data type represents the portion of data variability that cannot be accounted for by the model, which may be due to sampling or measurement errors and/or to intrinsic limitations of the model to represent all processes in the field. For simplicity, we will refer to this uncertainty as the "residual" error. A gradient-based nonlinear optimization algorithm is used to find the solution that minimizes (5-1).

A linearized approximation of the parameter posterior covariance matrix is computed from the final results as

$$\mathrm{cov}(\mathbf{s}) \approx \left(\mathbf{H}^T\mathbf{R}(\boldsymbol{\theta})^{-1}\mathbf{H} + \mathbf{Q}^{-1}\right)^{-1} \tag{5-2}$$

where $H_{ij} = \partial h_i / \partial s_j$ is a sensitivity matrix. Incorporating prior estimates of parameters and their uncertainty into the regression objective function greatly reduces nonuniqueness problems in the inverse solution and allows many more parameters to be calibrated than would be possible with unconstrained optimization. This not only allows refinement of parameters with relatively low uncertainty that may otherwise be assumed at their prior estimates, but allows interactions among more parameters, through the covariance matrix, to be taken into consideration in the error analysis. In addition to variable constraints on parameters associated with the stipulation of prior parameter uncertainty, absolute upper and lower constraints may also be placed on any parameters.

5.3 Monte Carlo Model

Uncertainty in forward simulations of remediation performance and cost is characterized using a MC modeling approach. Liu et al. (2010) have shown that linearized uncertainty methods compare well with more rigorous and much more computationally intensive than Markov Chain Monte Carlo (MCMC) methods when data is not inordinately noisy and reasonable prior information is available to condition parameter estimates. Thus, we utilize linearized uncertainty propagation methods to generate conditional parameter realizations.

The first step in performing MC simulations is to generate N_{mc} equiprobable realizations of calibrated model parameters for the problem under consideration using standard methods for multivariate Gaussian distributions (e.g., Press et al, 2007) based on parameter best estimates and covariances determined from the calibration. If log-transformations of parameters were used during calibration, the same transformations are used for parameter generation. In addition, uncorrelated normal or log-normal "noise" may be optionally applied to additional non-calibrated model inputs, including cost model coefficients.

The performance model is used to simulate soil and/or groundwater concentrations in source zones during thermal treatment, groundwater concentrations at ED injection gallery monitoring locations, and groundwater concentrations at compliance wells, which are used for making "real-time" operational decisions during the simulations (e.g., to turn remediation systems off, terminate monitoring, or incur "penalty costs"). Log-normal noise is added to these simulated concentrations for each parameter set realization using a user-specified "measurement error." For data types employed for model calibration, these estimates are obtained from the residual

calibration error. Otherwise, they are based on independent statistical analyses or the user's experience. NPV cost is computed for each MC realization and the average NPV cost for all realizations is computed as an estimate of the expected NPV cost value.

Chapter 6
Remediation Design Optimization

6.1 Overview

Predictions of remediation performance, no matter how sophisticated the performance model that is employed, are always uncertain to a significant degree. Quantification of performance uncertainty is critical for remediation design, since system "failure" nearly always occurs as a result of deviations from best estimates of performance. Therefore, remediation design (indeed, engineering design in general) is an exercise in determining the optimal degree of overdesign to achieve a "factor of safety" that balances the cost of overdesigning against the cost of failing to meet design objectives. Our approach to this tradeoff problem is to seek a design that minimizes the "expected" cost across the spectrum of equi-probable outcomes considering all sources of prediction uncertainty. More specifically, we seek to minimize the average NPV cost to reach compliance criteria over a finite number of MC realizations.

6.2 Compliance Rules

The overall goal of groundwater remediation is to reduce contaminant concentrations in compliance wells below a risk-based or regulatory-mandated level within a certain timeframe at minimum cost. For a given remediation design, one of three possible outcomes is assumed to apply for a given remedial action at the actual site and hence for each MC model realization:

No Further Action (NFA). If compliance well monitoring data meet specified NFA criteria at a date after t_{nfa} and prior to the maximum simulation date, t_{max}, then all remediation and monitoring activities will be terminated ("no further action").

Non-Compliance (NC). If contaminant concentrations for one or more compliance wells exceed certain noncompliance criteria after a specified "penalty date", $t_{penalty}$, or if NFA has not been achieved prior to t_{max}, then a specified fixed present value "penalty cost" will be added to the cost function and the simulation is terminated. No penalty cost will be considered if $t_{penalty} > t_{max}$.

Implement Conditional Containment (PT). If contaminant concentrations at a designated PT trigger well exceed certain criteria after a specified trigger date t_{PT}, then a pump-and-treat (PT) or other containment system is implemented upgradient of the trigger location. Discounted capital and annual operating costs for the containment system are accrued until NFA or NC conditions occur or t_{max} is reached. Other remedial actions and their costs continue to be simulated until they meet their termination criteria or t_{max} is reached. The PT system is not explicitly simulated, but is assumed to contain the plume. Model-predicted concentrations at compliance wells are computed as though unaffected by the containment system – i.e., attainment of NFA is conservatively assumed to be unaffected by the containment system. No PT costs are considered if $t_{PT} > t_{max}$

We assume site-wide monitoring of contaminant concentrations at a frequency of f_{samp}^{SW} per year at each designated compliance well location. Since concentration measurements at a given well can exhibit considerable temporal variability, compliance rules must be carefully defined to filter out measurement "noise" so that the likelihood of a false NFA determination is small.

Two compliance rule options to filter measurement noise are considered. The first option employs annual averaging of f_{samp}^{SW} compliance well concentrations per year and requires all annual averages within a lookback period of $N_{lookback}$ years to be below a specified target concentration C_{max} to attain NFA. This approach is very conservative, but noisy data may inordinately extend the remediation duration.

The second option which has been recommended by the US EPA (Levine, 2010) involves a linear regression of concentration versus time for all measurements within a lookback period and computes confidence limits of the mean regression value at the end of the regression period. If the upper one-sided α-probability confidence limit of the regression is less than C_{max} for each compliance well, then NFA is attained. This approach effectively handles data noise in the decision process, but is less sensitive to outliers. A complete summary of the compliance rules is given in Table 6-1.

Table 6-1. Compliance rule protocol options.

	Extreme Value (EXV) Rule	Regression Confidence Limit (RCL) Rule[1]
NFA	If annually averaged contaminant concentrations for all compliance wells are less than C_{max} for each of the last $N_{lookback}$ years ending on or after t_{nfa}, then all remediation and monitoring activities are terminated.	If the upper confidence limit of the current value of a regression of contaminant concentration vs. time over the last $N_{lookback}$ years ending on or after t_{nfa} is less than C_{max} for all compliance wells, then all remediation and monitoring activities are terminated.
NC	If annually averaged contaminant concentrations for any compliance wells exceed C_{max} in any of the last $N_{lookback}$ years ending on or after $t_{penalty}$ or if NFA has not been achieved prior to t_{max}, then a specified present value penalty cost $D_{penalty}$ is added to the cost function and the simulation is terminated.	If the upper confidence limit of the current value of a regression of contaminant concentration vs. time over the last $N_{lookback}$ years ending on or after $t_{penalty}$ exceeds C_{max} for any compliance wells or if NFA has not been achieved prior to t_{max}, then a present value penalty cost $D_{penalty}$ is added to the cost function and the simulation is terminated.
PT	If annually averaged contaminant concentrations in a designated PT trigger well exceed C_{PT} for all of the last $N_{lookback}$ years ending on or after t_{PT}, then discounted capital and operating costs for pump-and-treat or other plume containment system are accrued. The simulation continues until NFA is achieved or t_{max} is reached.	If the lower confidence limit of the current value of a regression of contaminant concentration vs. time over the last $N_{lookback}$ years ending on or after t_{PT} exceeds C_{PT} for a designated PT trigger well, then discounted capital and operating costs for pump-and-treat or other plume containment system are accrued. The simulation continues until NFA is achieved or t_{max} is reached.

[1] Based on Levine (2010)

The earliest possible compliance date, t_{nfa}, in Table 6-1 is computed as

$$t_{nfa} = \max_{ij}\left(t_{STP_i} + \Delta t_{ij}\right) + N_{lookback} \tag{6-1}$$

where t_{STPi} is the date that ED injection stops in gallery i, Δt_{ij} is the travel time from ED injection gallery i to the compliance well j, and $\max_{ij}$ is the maximum over all ij pairs with gallery i upgradient of compliance well j. The compliance date is used to ensure that low compliance well concentrations due to upgradient ED injection are not misinterpreted as permanently clean.

Annual average concentrations in the EXV rule are treated as geometric averages. Log-normal measurement "noise" is applied to annual averages in MC realizations with a standard error equal to the ln C standard deviation from model calibration divided by $f_{samp}^{SW\ 1/2}$. Note that the effect of increasing sampling frequency is to decrease measurement noise, which will allow earlier NFA attainment, and hence lower NPV cost. The optimal sampling frequency will depend on the tradeoff between NPV cost reduction and the additional sampling and analytical costs. The same tradeoff occurs with the RCL rule, since increasing sampling frequency decreases the regression uncertainty by $f_{samp}^{SW\ 1/2}$.

The "penalty cost" may be a real cost (e.g., for last ditch containment measures) or a fictitious cost applied to constrain the failure probability. Penalty cost is specified in NPV dollars (i.e., no discount is applied internally). Care should be taken not to specify a penalty date ($t_{penalty}$) that cannot be realistically achieved with current site conditions and proposed remedial technologies lest compliance will be nearly impossible to meet and the optimization problem will be ill-defined. Likewise, if t_{max} is too early to achieve a high NFA probability, low remediation costs may be misleading. An exception may be if long-term containment with institutional controls is under consideration, t_{max} may be set to reach a pseudo-steady state condition, fixed and penalty costs set to zero, and design variables optimized to minimize operating costs.

Note that pump-and-treat, if considered, is not explicitly simulated. Pump-and-treat is assumed to contain the plume, but model-predicted concentrations at compliance wells are treated as though unaffected by the PT system.

Real-time implementation of Option 2 would involve performing regressions of the last $N = f_{samp}^{SW} N_{lookback}$ ln-concentration values after each sampling round versus Julian date, T, to fit a linear trend model

$$\ln C = a + bT \tag{6.2}$$

where a and b are regression coefficients. The regression error is

$$S_{yx}^2 = \frac{SSE}{N-2} \tag{6.3}$$

where SSE is the sum of squared ln C regression residuals. Uncertainty in the mean regression is

$$S_{\hat{y}} = \frac{S_{yx}}{N^{1/2}} \tag{6.4}$$

and one-sided confidence limits at probability α are computed by

$$
\begin{aligned}
LCL_{\alpha} &= \exp\left(a + bT - t(\alpha,\, f_{samp}^{SW} N_{lookback} - 1) S_{\hat{y}}\right) \\
UCL_{\alpha} &= \exp\left(a + bT + t(\alpha,\, f_{samp}^{SW} N_{lookback} - 1) S_{\hat{y}}\right)
\end{aligned}
\tag{6.5}
$$

where $t(\alpha, df)$ is the one-sided Student-t value for probability α with df degrees of freedom.

To reduce computational effort in the MC model, we generate a single (geometric) average concentration value for each year in each realization with noise $S_{lnC}/\ f_{samp}^{SW\ 1/2}$ rather than f_{samp}^{SW} sample values per year with noise S_{lnC}, where S_{lnC} is the posterior ln C calibration error. The regressions are performed on time series with $N = N_{lookback}$ concentration values, which yield a lower SSE due to annual averaging. Equations (6.2) through (6.5) are employed to compute confidence limits using $N = N_{lookback}$. Note that in actual field practice, regressions would be performed on $N = f_{samp}^{SW} N_{lookback}$ concentration values to determine when NFA is met.

It should be self-evident that the duration of time allowed before cleanup criteria are required to be met will have a significant effect on remediation design and cost. Specifically, if $t_{penalty}$ or t_{PT} are decreased or the magnitude of contingent containment or penalty costs are increased, then earlier, more aggressive and more costly remediation will be favored. Likewise, if the time discount factor, d, is decreased, future costs are less sharply discounted, thus favoring earlier and more aggressive action. In the case of no contingent penalty or containment costs (or $t_{penalty} > t_{max}$ and $t_{PT} > t_{max}$) with a positive discount rate, the cost optimal solution will be to simply monitor until t_{max} or NFA is reached, regardless of the probability of achieving NFA. Some cost consequence of "failure" must be stipulated to induce active remediation.

6.3 Site-Wide Costs and Total Cost

The NPV cost for site-wide monitoring, reporting and maintenance are computed as follows

$$
\begin{aligned}
C_{NPV}^{SWtot} &= C_{NPV}^{SWcap} + C_{NPV}^{SWop} \\
C_{NPV}^{SWcap} &= \left(C_{well}^{SWcap} N_{well}^{SW} + C_{other}^{SWcap}\right)(1-d)^{t_{start} - t_{ref}} \\
C_{NPV}^{SWop} &= \sum_{t=t_{start}}^{t_{comp}} \left(C_{samp}^{SWop} f_{samp}^{SW} N_{well}^{SW} + C_{other}^{SWop}\right)(1-d)^{t - t_{ref}}
\end{aligned}
\tag{6.6}
$$

and the total NPV cost for all site remediation activities and penalty costs is

$$
C_{NPV}^{all} = C_{NPV}^{SWtot} + C_{NPV}^{EDtot} + C_{NPV}^{TRtot} + I_{PT} C_{total}^{PTcap} (1-d)^{t_{PT} - t_{ref}} + I_{PT} \sum_{t=t_{PT}}^{t_{nfa}} C_{total}^{PTop} (1-d)^{t - t_{ref}} + I_{pen} C_{NPV}^{pen} \tag{6.7}
$$

where

C_{NPV}^{all} is the total NPV remediation and penalty cost ($K),

C_{NPV}^{SWtot} is the total NPV site-wide cost ($K),

C_{NPV}^{EDtot} is the total NPV ED injection system cost ($K),

C_{NPV}^{TRtot} is the total NPV thermal remediation cost ($K),

C_{total}^{PTcap} is the total PT fixed cost ($K),

C_{total}^{PTop} is the total PT operating cost per year ($K/yr),

C_{NPV}^{pen} is the NPV penalty cost ($K),

C_{NPV}^{SWcap} is the total NPV site-wide fixed cost ($K),

C_{well}^{SWcap} is the fixed cost for monitoring well construction ($K/well),

C_{other}^{SWcap} is any other site-wide fixed costs ($K),

C_{total}^{SWop} is the total NPV operating cost for site-wide monitoring and reporting ($K),

C_{samp}^{SWop} is the cost per sample for site-wide monitoring ($K/sample),

C_{other}^{SWop} is other annual site-wide operating costs ($K/yr),

f_{samp}^{SW} is the number of samples per well per year taken for site-wide monitoring,

I_{pen} is 1 if a penalty cost is triggered, else 0,

I_{PT} is 1 if PT implementation is triggered, else 0,

N_{well}^{SW} is the number of site-wide monitoring wells (including compliance wells),

t_{PT} the year that PT is triggered (yr),
t_{nfa} is the year compliance is achieved or the max simulation date for NC (yr),
t_{start} is the first year capital costs are incurred (yr),
t_{ref} is the basis date for NPV adjustment (yr), and
d is the annual discount rate (fraction).

Total NPV remediation cost with penalty, C_{NPV}^{all}, is the objective function to be minimized.

6.4 Design Optimization

The design optimization problem is formulated by defining the specific NFA, NC and (optionally) PT rules and remediation options to be considered involving possible thermal source remediation, potential locations for ED injection galleries upgradient and/or downgradient of DNAPL source zones, and options for PT or alternative Plan B systems to be employed in the event of failure. Design variables to be optimized will need to be identified and unit costs determined considering site specific factors.

The mathematical objective for the design optimization problem is to find an optimal set of design variables that minimizes total expected NPV (ENPV) cost. NFA, NC and PT rules serve as implicit constraints on the optimization conditioned through the cost and performance models. In addition to any remediation technology specific design variables, site-wide variables (e.g., sampling frequency, f_{samp}, and lookback period, $N_{lookback}$) may also be optimized.

An efficient and robust genetic optimization algorithm, which is resistant to local minima in the response function, is employed to perform the optimization.

Optimization output includes optimal ENPV costs (with and without penalty costs), cost breakdowns, and cost probability distributions, in addition to optimized design variables. Cost and performance for individual MC realization as well as for expected values can be extracted.

Chapter 7
Application to a Hypothetical Problem

7.1 Problem Description

A hypothetical problem is considered involving a TCE plume in an unconfined aquifer. A DNAPL release was assumed to commence in 1965 resulting in a DNAPL pool at the bottom of the aquifer and residual DNAPL in the upper portion of the aquifer designated as Source 1 and Source 2, respectively.

Vertically averaged dissolved plume concentrations were computed using the "true" parameters at 26 monitoring well locations between 1985 and 2009. Simulated concentrations (C) were subjected to ln-normally distributed "noise" to represent deviations due to sampling and measurement error, spatial and temporal variability, and model simplifications with a ln-standard deviation (S_{lnC}) of 0.5. The resulting noisy data were assumed to represent field observations available for model calibration. The hypothetical site characterized by different parameter sets are summarized in Table 7-1. Well locations and "measured" concentrations in 2009 are illustrated in Figure 7-1.

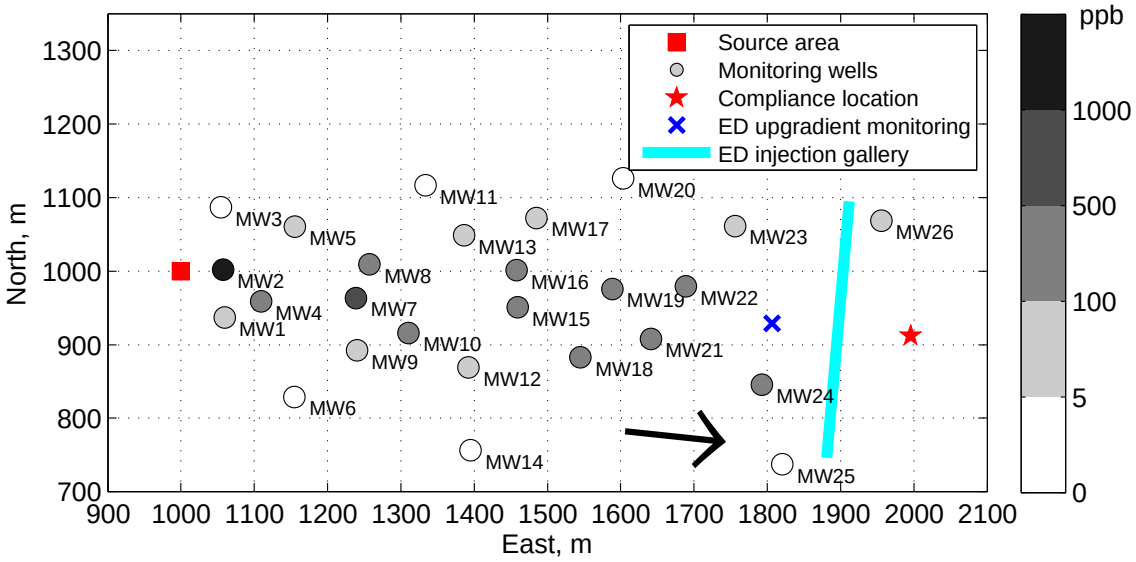

Figure 7-1. TCE concentrations in monitoring wells in 2009 and locations of DNAPL source, compliance well, ED injection galleries, and wells for monitoring upgradient of ED galleries.

Model calibration was performed as described in Chapter 5 using the "data" described above and prior estimates of model parameters summarized in Table 7-1 based on information assumed to be obtained from site characterization and/or literature studies. Final parameter estimates and their estimation standard errors are summarized in Table 7-1 (error covariances between all parameters were also computed but are not shown). The final *a posteriori* estimate of residual error in TCE concentrations not accounted for by the model was S_{lnC} = 0.56. Observed versus calibrated concentrations are compared in Figure 7-2.

Table 7-1. True model parameters, prior information, and final estimates.

Parameter	PDF[1]	True Value	Prior Estimates		Calibrated Values	
			Value	St Dev[3]	Value	St Dev[3]
Source 1 mass on calib. date[2] (kg)	LN	3646	2715	0.60	2948	0.52
Source 1 rate on calib. date[2] (kg/d)	LN	0.088	0.120	0.60	0.067	0.21
Source 1 depletion exponent (-)	N	0.60	0.75	0.25	0.73	0.24
Source 2 mass on calib. date[2] (kg)	LN	56.4	45.0	0.60	44	0.48
Source 2 rate on calib. date[2] (kg/d)	LN	0.012	0.010	0.60	0.008	0.37
Source 2 depletion exponent (-)	N	1.30	1.26	0.25	1.32	0.21
Source length, L_x (m)	LN	20.0	20.0	0.00	20.00	0.00
Source width, L_y (m)	LN	20.0	23.0	0.50	18.3	0.39
Release date (yr)	N	1965.0	1963.0	3.00	1963.9	2.53
Plume darcy velocity (m/d)	LN	0.070	0.065	0.60	0.049	0.15
Aquifer porosity (-)	N	0.30	0.35	0.04	0.36	0.04
Longitudinal dispersivity (m)	LN	20.0	17.0	0.50	19.8	0.08
Transverse dispersivity (m)	LN	2.00	4.00	0.50	2.1	0.03
Coordinate rotation, α (degrees)	N	5.00	5.99	0.00	5.99	0.00
Aquifer thickness (m)	LN	30.0	34.0	0.10	34.7	0.10
H-equiv EA concentration (g/m^3)	LN	2.75	2.39	0.15	-	-
H-equiv O_2 concentration (g/m^3)	LN	0.57	0.49	0.15	-	-
H-equiv ED ratio (-)	LN	0.31	0.26	0.15	-	-
H-equiv ratio CH (-)	LN	0.061	0.051	0.15	-	-
Serial decay fraction (-)	LN	0.32	0.50	0.15	-	-

[1] Assumed probability distributions: N = normal, or LN = lognormal.
[2] Source mass and discharge rate on t_{cal} = 1990.
[3] Standard deviations of LN variables are log-transformed (dimensionless); all other values are in specified units.

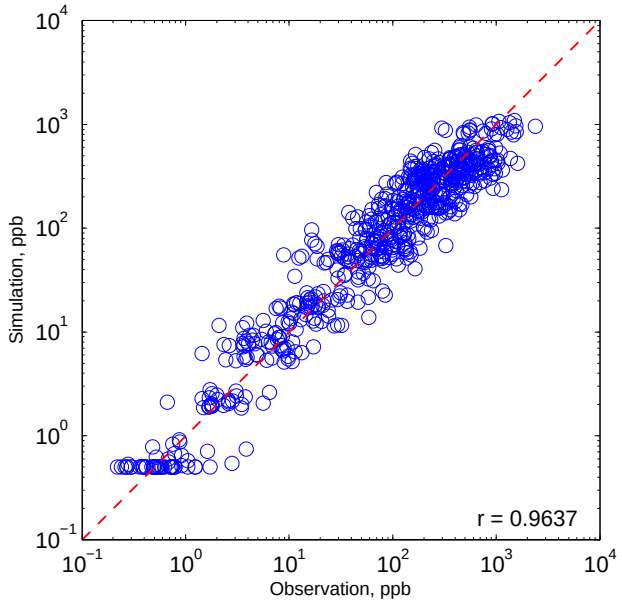

Figure 7-2. Observed versus calibrated TCE concentrations.

7.2 Remediation Options and Unit Costs

Remediation options to be considered in this hypothetical problem are source zone mass reduction using thermal source removal by ERH, and dissolved plume bioremediation with emulsified vegetable oil (EVO) injection as ED in a single injection well gallery. ERH is to be initiated in January 2010. The duration of ERH and timing and operation of ED injection galleries will be determined through optimization of relevant design variables. The remediation goal is to achieve contaminant concentrations in the compliance well below C_{max} = 5 µg/L by $t_{penalty}$ = 2050 with NFA being met by t_{max} = 2110. If the latter is not accomplished, a penalty cost will be incurred. Compliance rules described in Chapter 6, ED operation variables given in Chapter 3, and TSR variables in Chapter 4 will be investigated with cost variables summarized in Table 7-2. Uncertainty of cost variables was not considered in this hypothetical problem.

Table 7-2. Cost variables used in hypothetical problem.

Definition	Variable	Value	Unit
Thermal Treatment Costs			
Fixed costs for design, operation and reporting	C_{site}^{TR}	320	\$K
Treatment volume cost coefficient	$C_{vol_i}^{TR}$	0.025	\$K/m^3
Treatment area cost coefficient[1]	$C_{area_i}^{TR}$	0.188	\$K/m^2
Cost per source soil boring[1]	$C_{bore_i}^{TR}$	3.5	\$K
Analysis cost per soil sample	$C_{SOILsamp}^{TR}$	0.1	\$K/sample
Source monitoring well installation cost per well[1]	$C_{well_i}^{TR}$	7.0	\$K
Analysis cost per groundwater sample	C_{GWsamp}^{TR}	0.5	\$K/sample
ED Injection Costs			
Fixed cost per meter of ED gallery	C_{width}^{EDcap}	0.096	\$K/m
Fixed cost per ED performance monitoring well	C_{mw}^{EDcap}	10	\$K/well
Other fixed cost for ED injection	C_{other}^{EDcap}	65	\$K
Operating cost per ED mass injected	C_{mass}^{EDop}	0.00632	\$K/kg
Other operating cost per year for ED injection	C_{other}^{EDop}	240	\$K/year
Cost per ED monitoring event	$C_{samp}^{EDop} N_{mw}^{ED}$	5	\$K/event
Other Costs			
Penalty cost incurred for non-compliance[2]	C_{NPV}^{pen}	25,000	\$K
Cost per site-wide monitoring event	$C_{samp}^{SWop} N_{well}^{SW}$	20	\$K
Reference year for present value cost	t_{ref}	2010	year
Discount rate used for incurred costs	d	0.03	-

[1] Since sources 1 and 2 are collocated (i.e., pool and residual within the same area), the treatment thickness and indicated costs are allocated 15% to Source 1 and 85% to Source 2.

[2] Penalty cost is a fictitious value employed to limit noncompliance probability.

7.3 Case Study Results

7.3.1 Optimization for different TSR operational monitoring strategies (Cases 1 and 2)

A set of optimization simulations was performed to evaluate effects of the six TSR operational monitoring strategies described in Chapter 4 on performance. The simulations are designated as follows:

- Case 1a - Optimize design using TSR Method 1 with soil concentration data,
- Case 1b - Optimize design using TSR Method 1 with dissolved concentration data,
- Case 1c - Optimize design using TSR Method 1 with soil & dissolved concentration data,
- Case 2a - Optimize design using TSR Method 2 with soil concentration data,
- Case 2b - Optimize design using TSR Method 2 with dissolved concentration data, and
- Case 2c - Optimize design using TSR Method 2 with soil & dissolved concentration data.

A 95% RCL criteria with a 5-yr lookback period ($N_{lookback}$) was employed to define NFA and NC for all simulations. The following design variables were optimized:

- TSR treatment area, A_{TSR} (same for Source 1 and 2),
- TSR removal fractions, $R_{TSR(soil)1}$ for source 1 and $R_{TSR(soil)2}$ for source 2,
- Energy fractions at first sampling during TSR, $E_{frac(init)1}$ and $E_{frac(init)2}$ for sources 1 and 2,
- ED gallery injection start date, t_{EDo},
- ED injection rate, M_{ED},
- TCE concentration in monitoring well(s) upgradient of ED gallery below which injection is stopped, C_{ED}, and
- Compliance and ED monitoring frequency, $f_{samp} = f_{samp}^{ED} = f_{samp}^{SW}$.

The following variables were fixed during optimization:

- TSR start date = 2010,
- Energy increment for sampling after $E_{frac(init)}$ during TSR, $\Delta E_{frac} = 0.2$,
- TSR treatment thickness, Z_{tsr} = 3.6 m for Source 1 and 26.4 m for Source 2,
- Number of source zone soil borings or groundwater wells for TSR, $N_{well_i}^{TR} = N_{bore_i}^{TR} = 5$,
- Number of source zone soil samples per boring or groundwater samples per well for TSR, $N_{samp/well_i}^{TR} = N_{samp/bore_i}^{TR} = 2$ for Source 1 and 15 for Source 2, and
- Width of ED injection gallery, L_{ED} = 350 m.

An initial estimate of the ED injection rate was obtained based on an electron balance to reduce observed levels of EAs and contaminant. Assuming no aqueous-solid partitioning, the required ED injection rate is estimated as

$$M_{ED(est)} = \frac{SF\ qWL_z\left(\sum_i f_{EAi}^{'} C_{EAi} + f_{CH}^{'} C_{CH}^{\max}\right)}{f_{ED}^{'}} \qquad (7\text{-}1)$$

where q is darcy velocity, W is the injection well gallery width, L_z is saturated aquifer thickness, $C_{CH}^{\max}$ is the maximum contaminant concentration entering the gallery, SF is a safety factor, and other variables were defined previously. Employing EA concentrations and stoichiometry from Table 3-1 with SF = 2 yields $M_{ED} \approx 16$ kg/d for a 350 m width gallery. During optimization, if M_{ED} drops below M_{EDmin} = 8 kg/d (SF=1), no ED injection is assumed to be performed and all ED costs are set to zero.

Measurement "noise" (S_{lnC}) for thermal system monitoring in the source zone was assumed to be 0.25 for soil concentrations and 0.15 for groundwater concentrations for Source 1 and 0.50 and 0.30, respectively, for Source 2.

Results of Case 1a-2c optimization simulations are tabulated in Table 7-3. Total EPNV costs, excluding penalty costs, ranged from $1852K to $1939K and maximum NPV costs for 100 MC realizations ranged from $1922K to $2409K. Simulated median concentration at the compliance location versus time with 95 and 99% confidence limits are shown in Figures 7-3a to 7-8a and cost probability histograms are given in Figures 7-3b to 7-8b for all cases. Note that concentrations are truncated at an assumed detection limit corresponding to 10% of the cleanup target.

Probability of noncompliance was 3% for all cases except 1b, which was 2%. For all cases, the optimization algorithm determined that ED injection was not cost effective. The optimum sampling frequency for compliance monitoring was determined to be once per year (f_{samp} = 1) for all cases except 1b, which was semi-annual (f_{samp} = 2).

All six optimizations yielded design thermal treatment areas (A_{TSR}) about 2.35 times the best estimate of source area (A_{cal}) to reduce the probability of leaving untreated DNAPL beyond the treatment zone. The large multiplier reflects relatively large uncertainty in the calibration source area and high sensitivity of total cost to untreated mass. Since the cost of thermal treatment could be reduced on the order of $500K by decreasing the thermal treatment area by half, additional source characterization effort is probably warranted, especially considering that we really do not know exactly where the unaccounted mass occurs.

Optimized values of the soil mass reduction ratio ($R_{TSR(soil)}$) for Source 1 (DNAPL pools) ranged from 0.026 to 0.082 for Method 1 and from 0.009 to 0.031 Method 2. However, this variable is effectively merely a minimum mass reduction factor that is overridden a high initial energy fraction ($E_{frac(init)}$) for the first sampling event after system startup. The fact that the average number of sampling events (including the baseline sampling before heating) is exactly 2 for all cases for Source 1 (Table 7-3) indicates that optimization sets $E_{frac(init)}$ so large (~1.8-3.5 times the estimated energy requirement) that the $R_{TSR(soil)}$ criteria is met for all MC realizations at the first post-startup sampling event. In other words, $E_{frac(init)}$, which is a surrogate for thermal treatment duration, becomes the primary design variable rather than the stipulated mass reduction ratio for Source 1 (DNAPL pool).

This is not as much the case for Source 2 (residual DNAPL), which has a lower $E_{frac(init)}$ (0.82 to 2.99) and an average number of source sampling events between 2.01 and 3.5. The optimized soil mass reduction ratio ranges from 0.020 to 0.096. The computed groundwater reduction ratio ($R_{TSR(gw)}$) for Source 2 is several times lower than $R_{TSR(soil)}$ reflecting a source depletion exponent

(β) greater than 1, while it is several times higher than $R_{TSR(soil)}$ for Source 1 reflecting a source depletion exponent (β) less than 1 (see (4-11)).

The further the source depletion exponent deviates from 1, the greater the difference between soil and groundwater reduction ratios. This is important to recognize when setting and monitoring source cleanup targets. It is notable that a significantly smaller (more aggressive) minimum soil reduction ratio is needed for the low β source (Source 1, pools) than for the high β source (Source 2, residuals) to obtain a comparable reduction in dissolved concentrations. This is somewhat offset by the observation that the optimal minimum groundwater reduction ratio ($R_{TSR(gw)}$) for Source 1 (0.032 to 0.103) is less aggressive (higher) than that for Source 2 (0.012 to 0.046), which likely reflects the fact that the rate of mass flux reduction with time (dJ/dt) increases with time if $\beta < 1$ while it decreases with time if $\beta > 1$.

Comparison of Cases 1a through 2c indicates that monitoring of soil concentration alone during thermal treatment yields the lowest ENPV for Method 1 (turning off all heating units at the same time when the average soil and/or groundwater concentration in the source drops below a specified level), while soil and groundwater data yield the lowest cost for Method 2 (turning off the electrodes incrementally based on local concentration reductions). Method 1 with soil data yields the lowest cost of all six cases studied. Including the probability-weighted penalty cost in the ENPV leads to the same conclusion. Thus, for this particular case, Method 1 with soil data appears most cost effective. Although measurement error for soil concentration data is assumed to be higher than for groundwater data, the average cost per sample for groundwater data is higher due to well construction costs if wells are only sampled 2-3 times.

The average number of sampling events for monitoring Source 2 thermal treatment, hence the average thermal monitoring cost, is significantly higher using Method 2 than Method 1. This reflects greater variability in individual measurements used to incrementally turn off heating units compared to averaged measurements used to turn off the entire system. For the example problem considered here, higher thermal monitoring costs more than offset cost savings associated with incremental shutdown of heating units. Due to the large number of factors and tradeoffs that affect the total expected cost NPV cost, it is no more likely that given sampling strategy will be universally optimal than that any other design variable will be optimal for all conditions.

The difference between the highest and lowest optimized ENPV cost for the six different operational methodologies for monitoring thermal treatment is $426K without including penalty costs, which corresponds to potential cost reduction of 19% relative to the most expensive thermal monitoring strategy. Thus, in addition to optimizing various treatment design parameters, evaluating various options for monitoring thermal performance can result in significant additional cost savings.

Table 7-3. Summary of design simulations

(**bold** = optimized values; *italic* = fixed values, normal type = performance results).

Case	1a	1b	1c	2a	2b	2c	3	4	5a	5b
Results										
$ENPV_{total}$ ($K)[1]	1852	2278	1932	1907	1939	2025	11525	1867	1305	1336
- TSR_{total} ($K)	1435	1450	1514	1490	1521	1607	826	1433	887	888
- ED_{total} ($K)	0	0	0	0	0	0	8377	0	0	0
- $TSR_{monitor}$ ($K)	40	97	135	51	133	208	35	40	34	34
- Site wide ($K)	417	828	418	417	418	418	2322	434	418	448
Max NPV ($K)	1922	2409	2037	1968	2008	2100	13036	1908	1379	1379
Non-compliance (%)	3	2	3	3	3	3	71	8	3	53
Compliance and ED Monitoring										
Compliance	*RCL*	*RCL*	*RCL*	*RCL*	*RCL*	*RCL*	*RCL*	*EXV*	*RCL*	*RCL*
f_{samp} (yr^{-1})	**1**	**2**	**1**	**1**	**1**	**1**	*4*	**1**	**1**	1
Thermal Treatment Parameters (Both Sources)										
TSR Method	*1*	*1*	*1*	*2*	*2*	*2*	*1*	*1*	*1*	*1*
TSR Data	*S*	*C*	*S+C*	*S*	*C*	*S+C*	*S*	*S*	*S*	*S*
A_{TSR}/A_{cal}	**2.37**	**2.34**	**2.35**	**2.35**	**2.34**	**2.35**	*1.00*	**2.12**	*1.00*	*1.00*
Thermal Treatment Parameters (Source 1 - Pool)										
$R_{TSR(soil)}$	**0.0444**	**0.0260**	**0.0824**	**0.0090**	**0.0308**	**0.0217**	*0.0100*	**0.0266**	**0.0320**	0.0320
$R_{TSR(gw)}$	0.1027	0.0693	0.1612	0.0320	0.0786	0.0608	*0.0345*	0.0706	0.0807	0.0807
$E_{frac(init)}$	**3.23**	**1.82**	**3.52**	**2.18**	**2.27**	**3.23**	*0.80*	**3.87**	**2.31**	2.31
Avg sample events	2.00	2.00	2.00	2.00	2.00	2.00	3.48	2.00	2.00	2.00
Thermal Treatment Parameters (Source 2 - Residual)										
$R_{TSR(soil)}$	**0.0712**	**0.0414**	**0.0963**	**0.0199**	**0.0351**	**0.0899**	*0.0100*	**0.0327**	**0.0860**	0.0860
$R_{TSR(gw)}$	0.0306	0.0150	0.0456	0.0057	0.0120	0.0416	*0.0023*	0.0110	0.0392	0.0392
$E_{frac(init)}$	**1.08**	**1.03**	**1.09**	**2.99**	**0.84**	**0.82**	*0.80*	**1.34**	**1.07**	1.07
Avg sample events	2.01	2.08	2.01	2.64	3.3	3.54	3.55	2	2.11	2.11
ED Injection for Plume Bioremediation										
t_{EDo} (yr)	-	-	-	-	-	-	*2010.0*	-	-	-
M_{ED} (kg/d)	-	-	-	-	-	-	*16*	-	-	-
C_{ED} (µg/L)	-	-	-	-	-	-	*5*	-	-	-
Δt_{ED} avg (yr)	-	-	-	-	-	-	71.1	-	-	-

[1] NPV costs do not include penalty cost

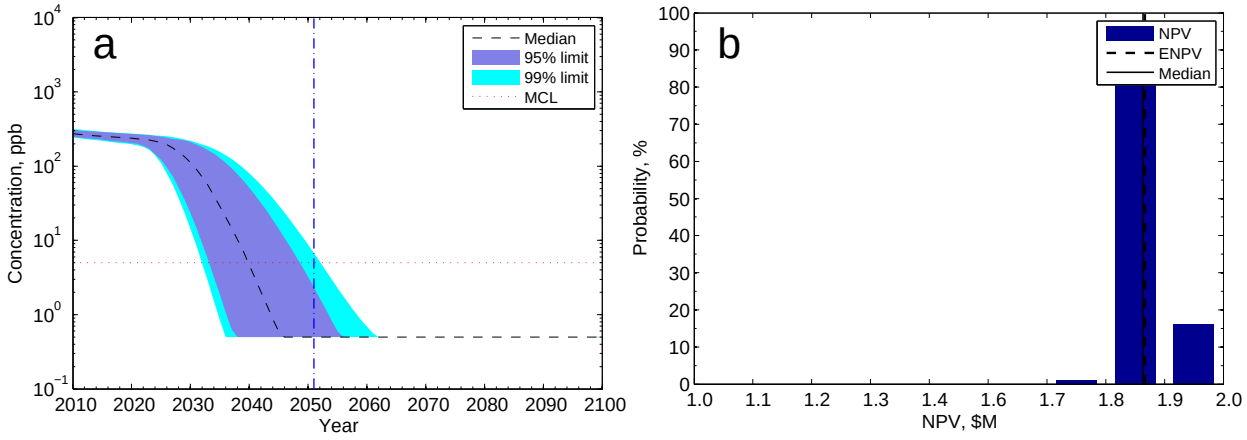

Figure 7-3. Results for Case 1a: (a) TCE concentrations at compliance well and (b) NPV cost distribution (without penalty cost).

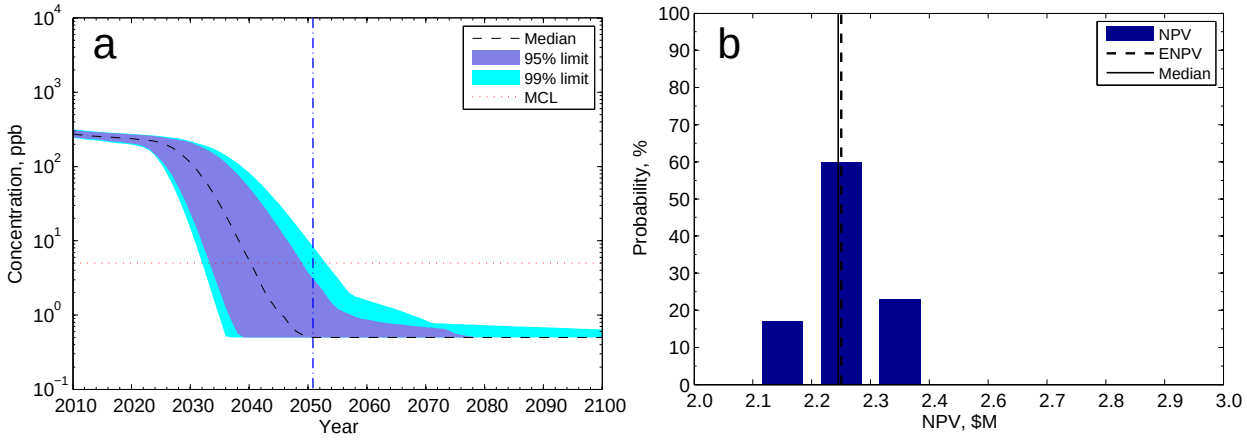

Figure 7-4. Results for Case 1b: (a) TCE concentrations at compliance well and (b) NPV cost distribution (without penalty cost).

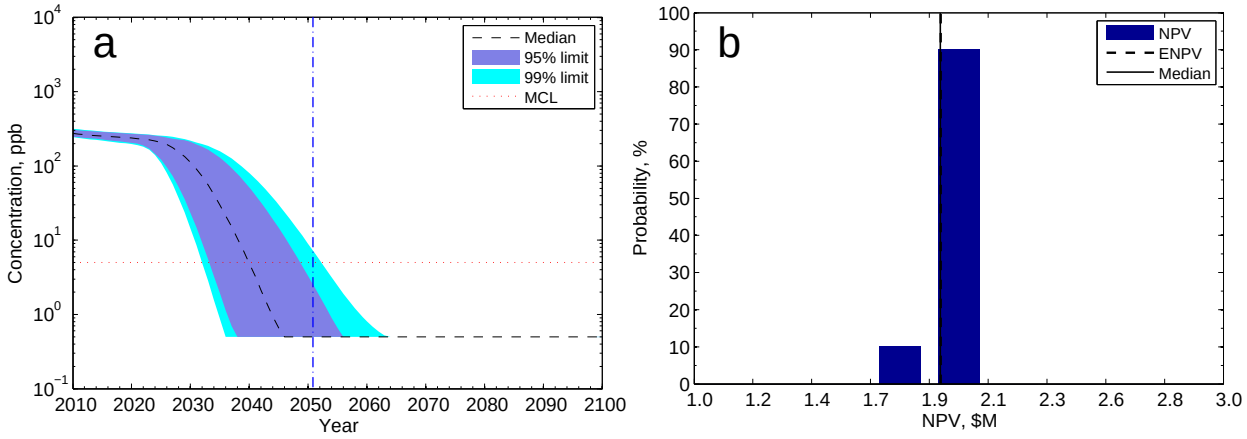

Figure 7-5. Results for Case 1c: (a) TCE concentrations at compliance well and (b) NPV cost distribution (without penalty cost).

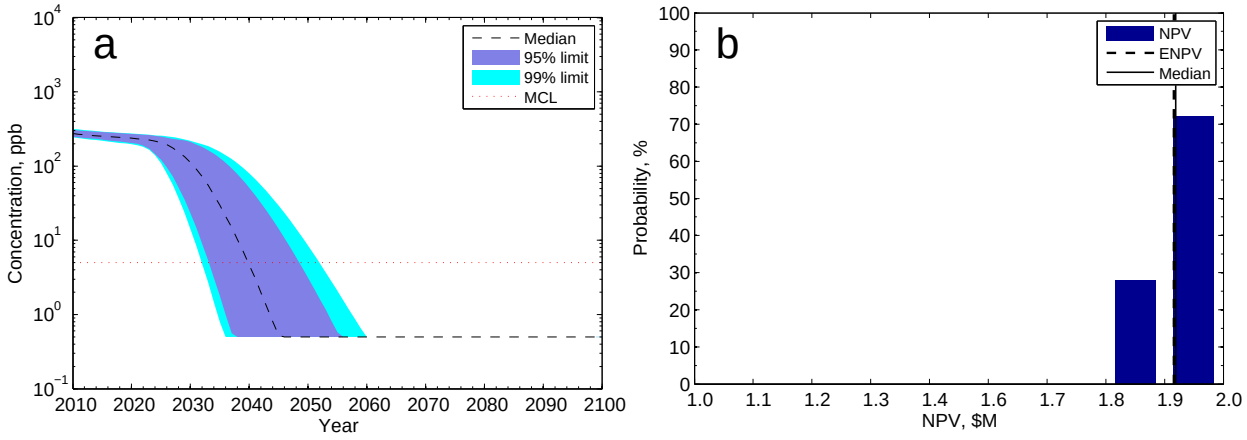

Figure 7-6. Results for Case 2a: (a) TCE concentrations at compliance well and (b) NPV cost distribution (without penalty cost).

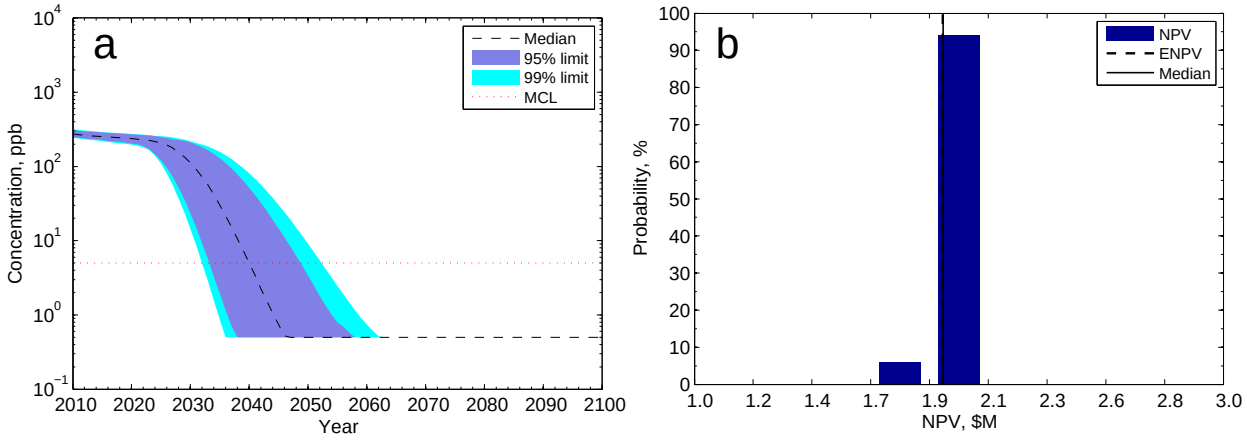

Figure 7-7. Results for Case 2b: (a) TCE concentrations at compliance well and (b) NPV cost distribution (without penalty cost).

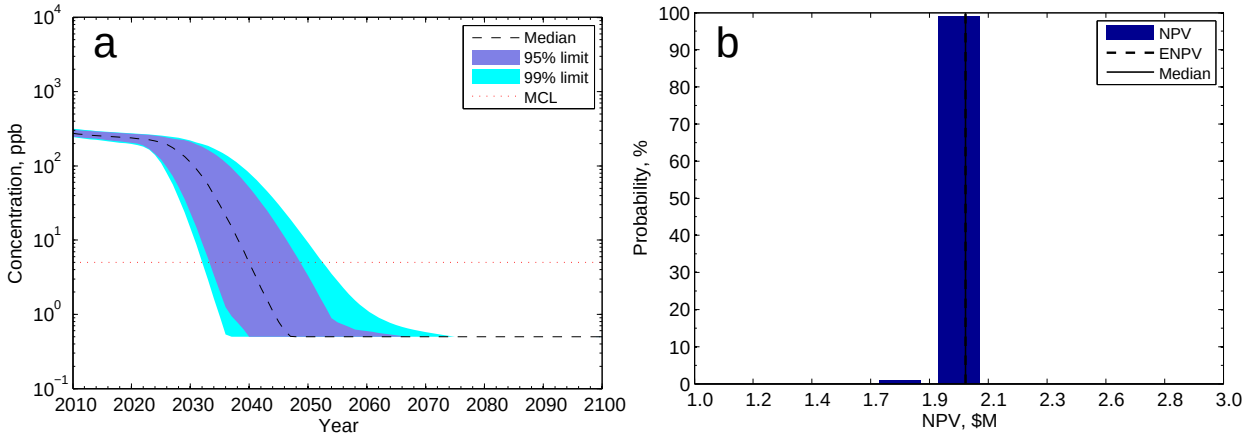

Figure 7-8. Results for Case 2c: (a) TCE concentrations at compliance well and (b) NPV cost distribution (without penalty cost).

7.3.2 Improvement attributable to optimization (Case 3)

A non-optimized MC analysis of remediation performance and cost was performed corresponding to Case 1a using design variables that reflect common field engineering practices (Case 3). Thermal source zone remediation was assumed to start in 2010. Thermal treatment area and volume were taken as their best estimates from model calibration (i.e., A_{TSR}=A_{cal}). The first round of soil sampling after starting thermal treatment is assumed to occur at a fraction $E_{frac(init)}$ = 0.8 of the theoretical energy requirement for each source with additional sampling rounds at intervals ΔE_{frac} = 0.2 until shutdown according to TSR Method 1. Thermal remediation is terminated when the average measured soil concentration in the source zone is below $R_{TSR(soil)}$ = 0.01.

ED injection was also assumed to start in 2010 (t_{EDo}) with an annual average injection rate based on (7-1) with SF = 2 yielding M_{ED} = 16 kg/d. ED injection was terminated when the annually averaged measured (simulated + noise) TCE concentration upgradient of the ED injection gallery dropped below 5 μg/L.

The Case 3 thermal treatment design is considerably less effective than the optimized designs for Cases 1 and 2 even though the source mass reduction target is more aggressive than nearly all of the Case 1 and 2 targets and ED injection is utilized in Case 3. The poor performance is attributable to a high probability of contaminant mass beyond the limited thermal treatment area, which is 60% smaller than the optimized area. Lower thermal costs result, but there is a high probability of source mass remaining above target levels after thermal treatment that cannot be removed by natural source attenuation by 2110. This results in a 71% probability of noncompliance that leads to long durations for ED injection and site-wide monitoring resulted with a total ENPV cost of $11.5M – more than six times higher than for optimized Case 1a. The cost reduction for Case 1a relative to Case 3 is about 84%.

Long duration ED injection can maintain concentrations at the compliance location below the target level with a high probability (Figure 7-9a). However, source mass flux is unlikely to drop low enough to shut down the ED injection gallery prior to the maximum simulation date of 2110, leading to a noncompliance condition. The cost probability distribution has a positive bias (Figure 7-9b) reflecting the large number of cases with operating costs continuing up to 2110.

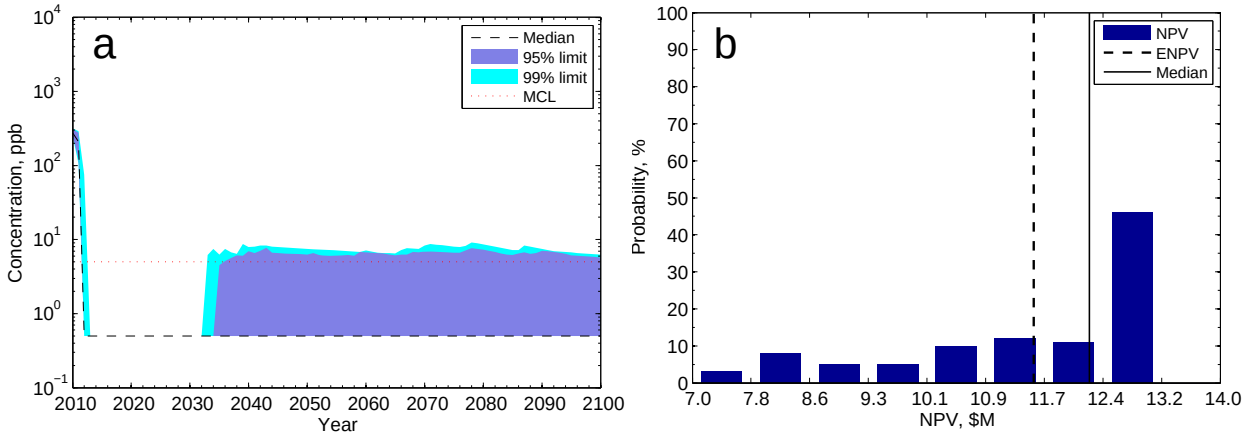

Figure 7-9. Results for Case 3: (a) TCE concentrations at compliance well and (b) NPV cost distribution (without penalty cost).

7.3.3 Effect of compliance rules (Case 4)

To evaluate the effect of compliance rules on remediation design, cost and performance, we performed an optimization identical to Case 1a except that the EXV rule described in Chapter 6 was used in lieu of the RCL rule. The remedial design was similar to that for Case 1a with no ED injection. The optimized thermal treatment area was somewhat less aggressive, while mass reduction targets and $E_{frac(init)}$ were slightly more aggressive. The net result was a very slightly lower average thermal treatment cost and a slightly higher average site-wide monitoring duration and cost (Table 7-3). The 95% upper confidence limit for concentration versus time shift a few years to the right, while the 99% confidence limit becomes nearly flat above the target concentration all the way to 2110 (Figure 7-10). The more stringent and "noisy" EXV rule results in a NC probability that is 5 percentage points higher than for Case 1a.

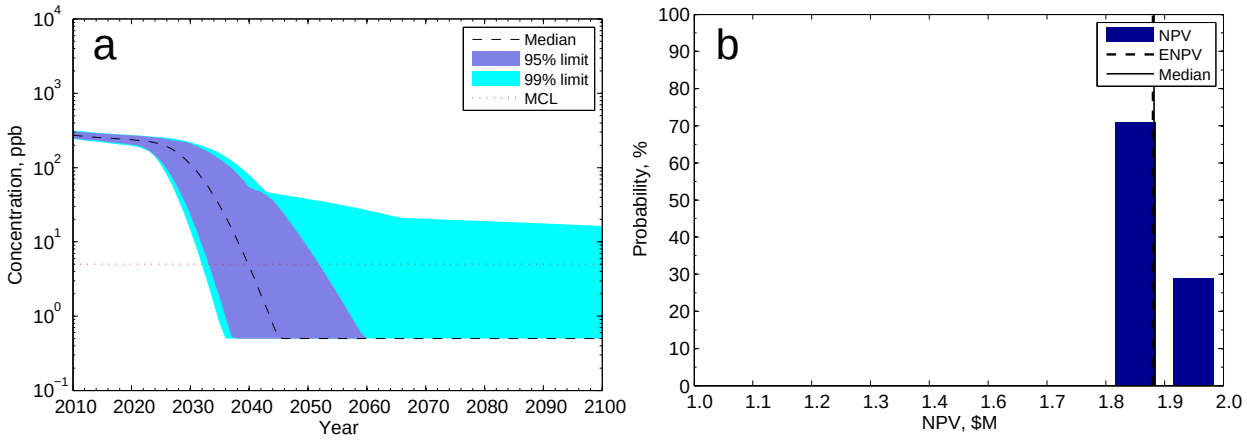

Figure 7-10. Results for Case 4: (a) TCE concentrations at compliance well and (b) NPV cost distribution (without penalty cost).

7.3.4 Effect of source delineation uncertainty on thermal performance (Case 5)

To evaluate the effect of uncertainty in source zone delineation on remediation design, cost and performance, we first performed an optimization identical to Case 1a except that the thermal treatment area was fixed at the best estimate of the source area from calibration and not optimized. However, the treatment area was assumed to fully encompass the region with DNAPL and no "missing mass" outside the treatment area was simulated. This optimization is designated as Case 5a.

The optimized design variables determined in Case 5a were then employed in a MC simulation without further optimization with "missing mass" outside the assumed treatment zone treated as a stochastic variable. This simulation is designated as Case 5b.

Case 5a yields predicted performance comparable to Case 1a. The probability of NC at 3% is the same as Case 1a and concentration versus time probabilities are similar (Figure 7-11). The ENPV cost for thermal treatment is lower due to the smaller system footprint, leading to a lower simulated total ENPV cost.

However, Case 5a is unrealistically optimistic because it disregards uncertainty in source zone delineation and hence in the thermal treatment area necessary to reliably reduce the source mass. The effects of this Pollyannaish treatment of source delineation reliability is seen in Case 5b results, which reveal a high probability of contaminant concentrations above target levels (Figure 7-12) and a 53% probability of NC by 2110 (Table 7-3).

While thermal source treatment is generally very effective at reducing contaminant mass within the treated soil volume, it is sensitive to error in source delineation and disregarding this fact can lead to much poorer performance than expected.

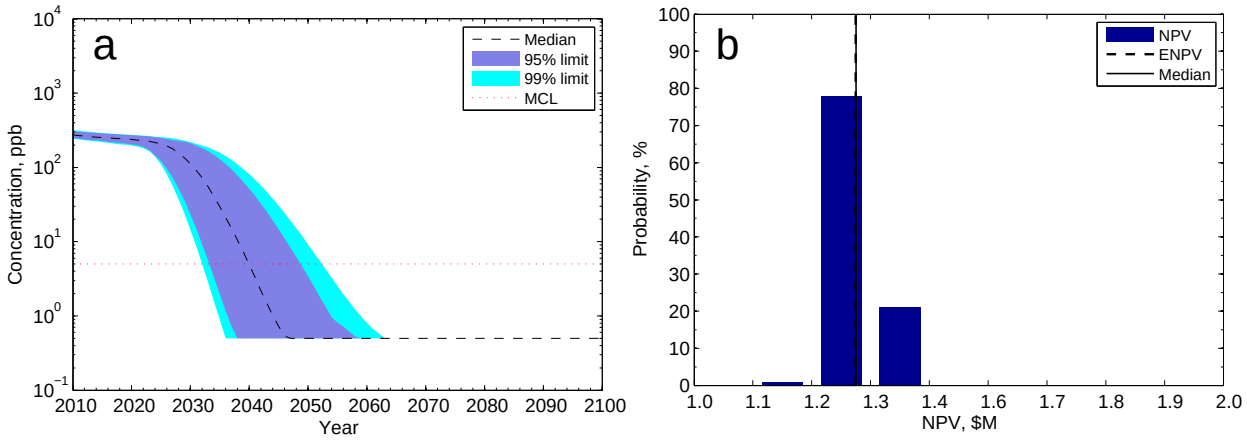

Figure 7-11. Results for Case 5a: (a) TCE concentrations at compliance well and (b) NPV cost distribution (without penalty cost).

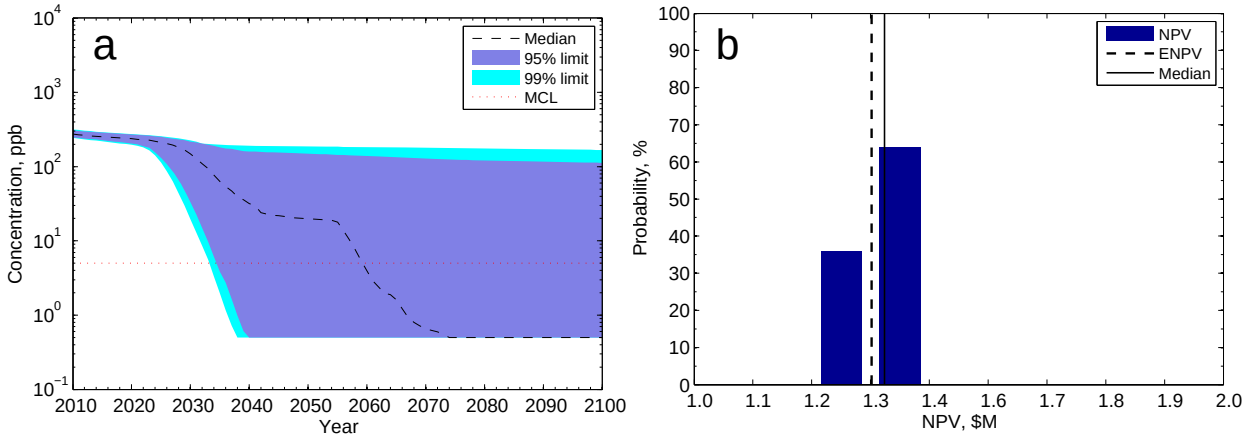

Figure 7-12. Results for case 5b: (a) TCE concentrations at compliance well and (b) NPV cost distribution (without penalty cost).

7.4 Conclusions

Stochastic cost optimization was found to decrease the expected NPV cost for site remediation as much as 85% compared to conventional non-optimized approaches, while also increasing the probability of achieving "no further action" status in a specified timeframe by more than 60%.

Optimizing monitoring frequency for compliance wells used to make *no further action* determinations as well as operational monitoring used to make decisions on individual remediation system components involve tradeoffs between increased direct costs for sampling and analysis versus decreased construction and operating costs that arise because more data increases decision reliability, which ameliorates the extent to which systems must be overdesigned to overcome data uncertainty.

Operational monitoring and heating unit shutdown protocols for thermal source treatment (incremental vs. all-or-none shutdown, soil vs. groundwater sampling, number and frequency of samples) can significantly affect system effectiveness and cost. Optimizing these protocols alone was found to effect cost savings of more than 20%.

The statistical formulation of compliance rules can also significantly affect remediation design, performance and cost. We found that defining compliance based on 95% confidence limits of a regression on a moving time window was more reliable than using measured extreme on a similar lookback period, resulting in decreased expected cost and lower probability of failure.

Disregarding uncertainty in DNAPL source delineation can lead to marked undersign of thermal treatment systems, which can result in a low probability of achieving remediation objectives and ultimately to higher costs to later rectify the misjudgments.

Application of the SCOToolkit methodology on a given site should increase the probability of meeting cleanup objectives with the least cost. Employed over a large number of sites should yield significant total cost reductions.

Chapter 8
Application to Fort Lewis EGDY site

8.1 Site Description

The East Gate Disposal Yard (EGDY) is a source of groundwater contamination at the Logistics Center National Priority List Site located at Fort Lewis, Washington (Figure 8-1). EGDY was used between 1946 and the mid 1970s as a waste disposal site for solvents from cleaning and degreasing operations. Material was transported to the disposal yard in barrels and vats from various areas. About seven barrels of liquid waste per month were disposed during peak operation. A TCE plume in the shallow aquifer evolved from the disposal site with concentrations in the range of hundreds µg/L in the source area and concentrations exceeding 5 µg/L over 4 km downgradient (Dinicola, 2005; USACE, 2008).

The climate of Fort Lewis is characterized by warm dry summers and cool wet winters with a mean annual temperature of about 13 degrees Celsius and mean annual precipitation of about 1000 mm. Fort Lewis is underlain by a complex and heterogeneous sequence of glacial and non-glacial deposits including a shallow aquifer (Vashon) and a deep aquifer (Sea Level Aquifer, SLA). The Vashon aquifer is unconfined and continuous throughout the Fort Lewis area. It ranges in thickness between about 30 to 60 meters. The Vashon and SLA aquifers are separated by a mostly continuous low permeability aquiclude. However, a "window" occurs about 2 km downgradient of the disposal area that allows water and contaminants from the shallow Vashon aquifer to migrate to the deep SLA aquifer.

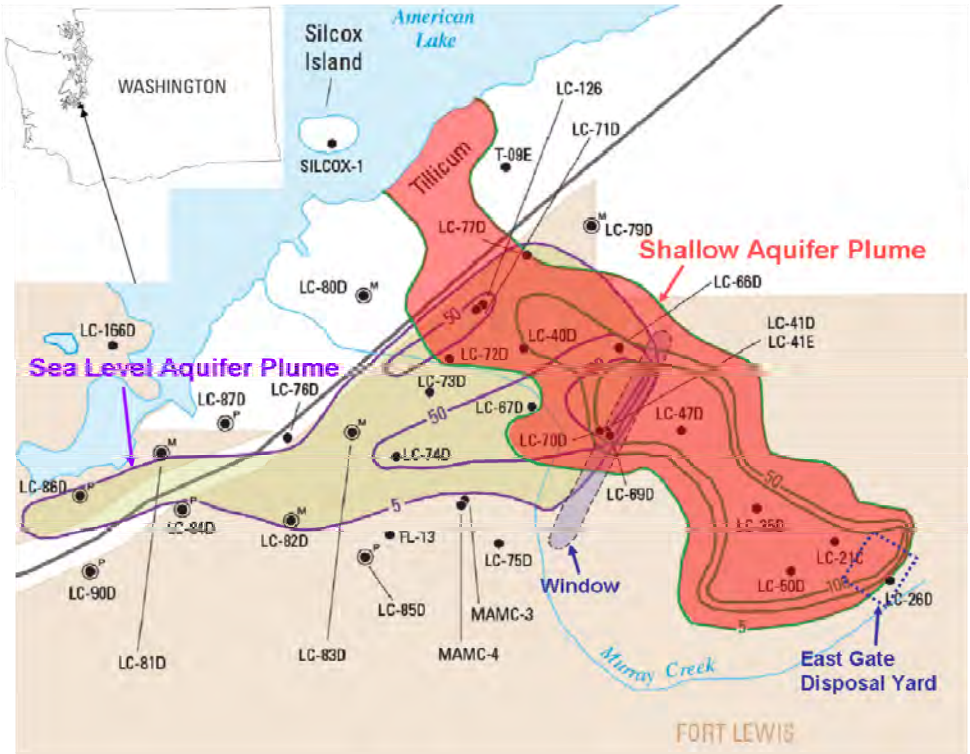

Figure 8-1. Location of EDGY site and TCE plumes as of 2004 (Dinicola, 2005).

Groundwater at Fort Lewis generally flows to northwest in the Vashon aquifer and west-southwest in the SLA aquifer. A simplified geologic cross section of the Fort Lewis site is shown in Figure 8.2. More details on the site geology are found in Dinicola (2005), Truex et al. (2006), and USACE (2008).

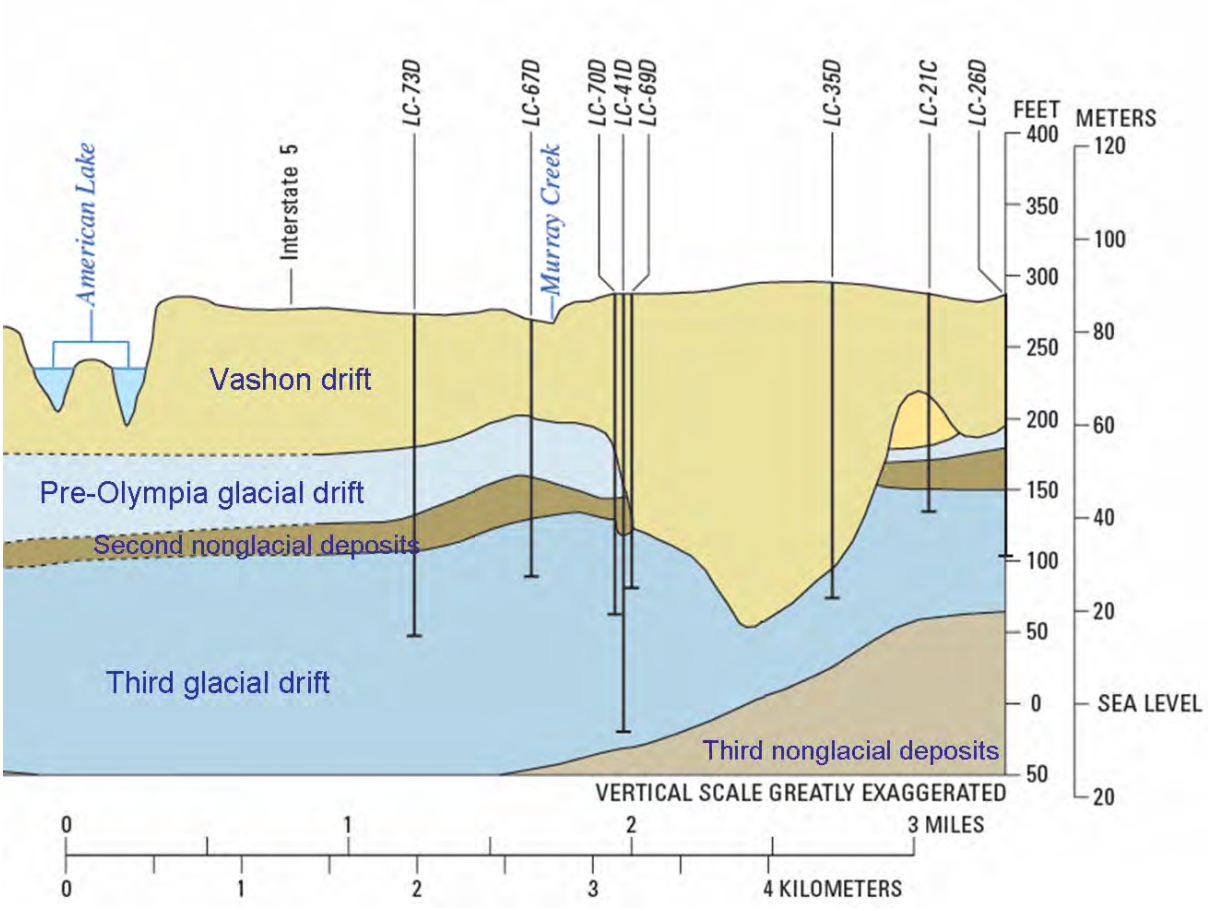

Figure 8-2. Hydrogeologic section of Fort Lewis (Dinicola, 2005).

Several remediation actions have been performed at the EGDY site to contain the existing contaminant plume or reduce DNAPL mass in the source zone. Disposal trenches were excavated in 2000 to remove contaminated waste buried above the water table. About 1260 drums of contaminant were removed. To reduce DNAPL mass below the water table, TSR was implemented for three source zones between late 2003 and early 2007. Tables 8-1 and 8-2 summarize the activities.

Table 8-1. EGDY site remediation history (USACE, 2008)

Date	Activity	Location
1995 - 2005	Pump-and-treat systems installed in Vashon Aquifer	One near EGDY second near highway I-5
2003 - 2005	Integrated pump test in Areas 1 and 3 in Nov 2003 and Sep 2005, respectively	EGDY
2003 - 2005	Source flux measurements in Areas 1 and 3 in Nov 2003 and Sep 2005, respectively	EGDY
2003 - 2006	TSR and monitoring in Areas 1, 2 and 3 in Dec 2003 - Aug 2004, Feb 2005 - Aug 2005, and Oct 2006 - Jan 2007, respectively	EGDY
2005-2006	Whey injection pilot tests	EGDY
2005 - 2007	Post-TSR monitoring in Areas 1,2 and 3 in May 2005, Sep. 2005, and Feb 2007, respectively	EGDY
2006 - 2008	Post-treatment soil coring in Areas 1,2 and 3 in Apr 2006, Apr 2006, and Mar 2008, respectively	EGDY
2009	Pump-and-treat system installed in Sea Level Aquifer	Near hospital

Table 8-2. Summary of TSR operations at EGDY site (USACE, 2008)

Variable	Area 1	Area 2	Area 3
TSR treatment area (m^2)	2360	2080	1691
TSR max depth below ground surface (m)	10	16	9
TSR treatment volume (m^3)	23625	135953	15368
Energy on date	12/17/2003	02/14/2005	10/11/2006
Energy off date	08/04/2004	08/05/2005	01/26/2007
Duration (days)	231	172	107
Mass removal, TCE + DCE (kg)	2990	1340	1120

8.2 Model Calibration

8.2.1 Characterization of groundwater flow field

Groundwater flow at the Fort Lewis site was characterized in USACE (2008). The model used in this project simulates groundwater flow and transport with curvilinear streamlines as described in Chapter 2. Streamlines commencing from each DNAPL source, actual or planned ED injection gallery and from the "window" between the upper and lower aquifer units were digitized and fitted to third order polynomial equations of the form $y = ax+bx^2+cx^3$. The model computes travel distances from sources to the wells of interest along their streamlines. Coefficients of individual streamline equations are presented in Figure 8-3. Since the locations of ED galleries 1 to 3 are immediately upgradient of Areas 1 to 3, their streamlines are similar to those of Areas 1

to 3. The streamline of ED gallery 4 starts upgradient of the "window" and follows the streamline of Area 2. Polynomial coefficients can be estimated using the provided function 'trajectory.exe' or using Excel to solve the nonlinear least squares problem using the SOLVER function.

Origin	a	b	c
Area 1 (Source 1)	4.275E-01	5.615E-04	2.756E-08
Area 2 (Source 2)	2.605E-01	7.257E-04	6.437E-08
Area 3 (Source 3)	1.129E-01	1.244E-03	2.758E-07
Win 1	-9.570E-01	-8.070E-04	-1.510E-07
Win 2	-7.770E-01	-6.800E-04	-1.230E-07
Win 3	-1.171E+00	-9.984E-04	-1.780E-07
ED 1	4.952E-01	5.811E-04	3.097E-08
ED 2	2.448E-01	7.196E-04	5.822E-08
ED 3	3.612E-02	1.270E-03	2.987E-07
ED 4	-1.640E+00	0.000E+00	0.000E+00

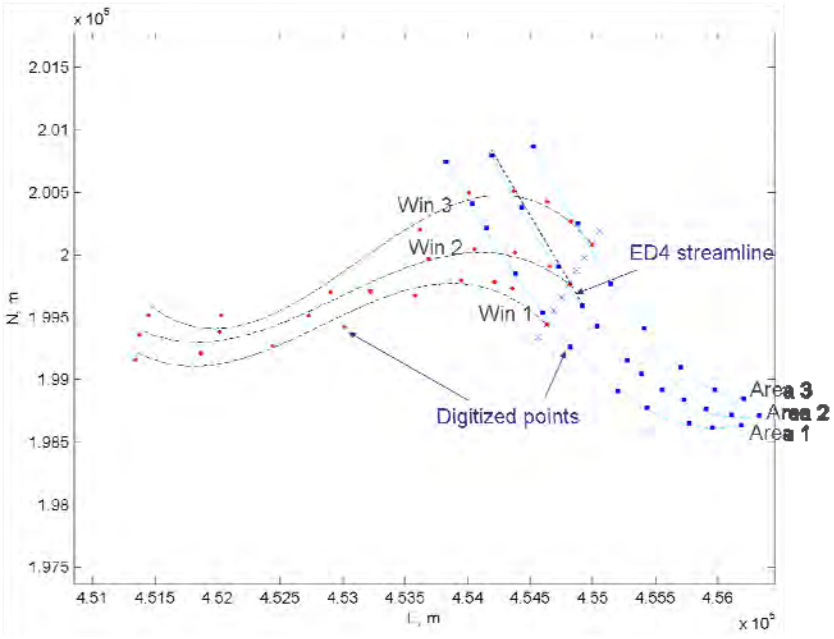

Figure 8-3. Streamlines used to model groundwater flow at the Fort Lewis site.

8.2.2 Calibration using pre- and post-ERH data

Chlorinated solvent concentrations in groundwater reported by Truex et al. (2006) were utilized to construct time-series for each monitoring well. Chlorinated solvent species were converted to "TCE-equivalent" concentrations such that their H-demand for complete reduction is equal to that of TCE. The sum of H-equivalent concentrations of all chlorinated ethenes was taken as the total TCE-equivalent solvent concentration. Locations of monitoring wells with data used for model calibration are shown in Figure 8-4. Pre-ERH data included dissolved concentration measurements from 26 wells from 1995 to late 2001. Post-ERH data included longer time series for pre-ERH wells through 2009, data from 14 additional wells closer to the source areas (Figure 8-4 inset), and measurements of source mass flux and mass removed by ERH.

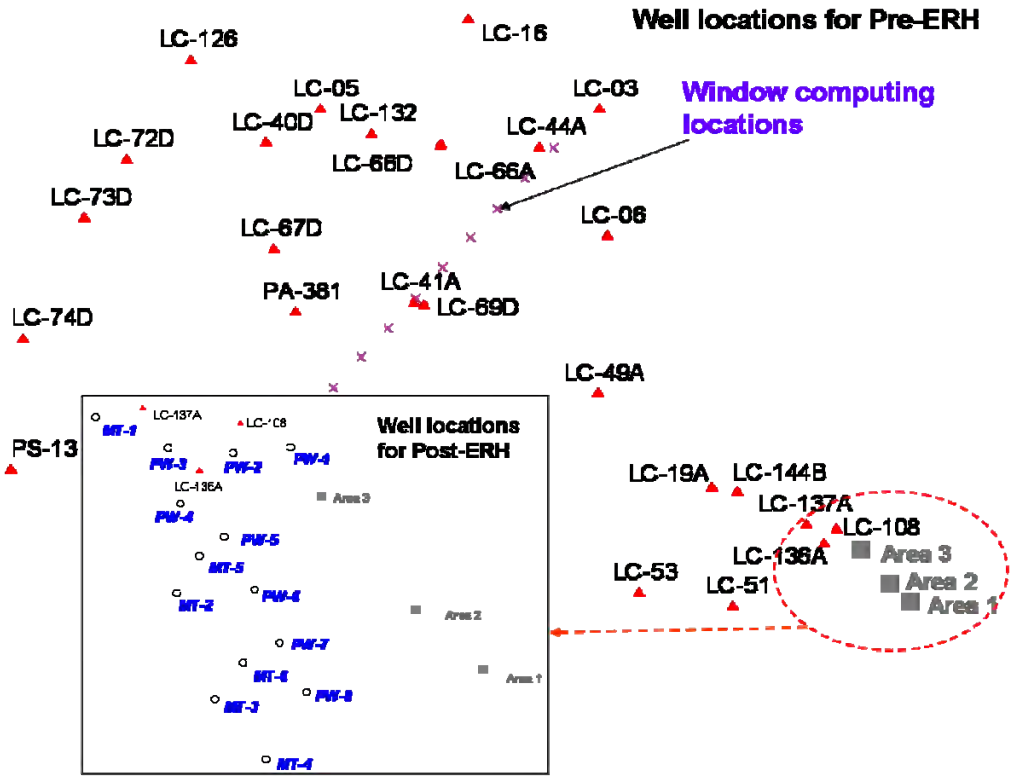

Figure 8-4. Well locations used in calibration.

To model source zone mass dissolution and transport downstream, initial estimates of source and aquifer parameters were estimated from information in various reports (Dinicola, 2005; Truex et al., 2006; USACE, 2008) summarized in Table 8.3. We calibrated model parameters to site data using 2000 as the reference year (t_{cal}) for source mass and source flux using both pre- and post-remediation data. Data include dissolved concentration data (total TCE-equivalents), source flux measurements, and DNAPL mass removed by TSR. Details of calibration data are tabulated in Appendix A.

We assume that most of the contamination present in the SLA was transported from the Vashon aquifer through the "window" in the aquiclude. The Vashon aquifer is divided into three zones with different decay coefficients. Zone 1 extends from the DNAPL sources to the window; Zone 2 encompasses the window itself; and Zone 3 is the region downgradient of the window. The model internally computes a first-order "decay" coefficient for the window zone as described in Chapter 2 to account for the advective flux to the SLA unit. The window zone is divided laterally into three sections to approximate the average TCE flux from the upper to lower aquifer. Fluxes are tabulated at discrete times in a lookup table and interpolated to define a smooth source function for the Vashon aquifer. The model uses 0.0001 d^{-1} as a prior estimate of biodecay coefficients of for Zones 1 and 3.

Table 8-3. Fort Lewis site characterization data.

Area	Parameters	Prior Value[1]	STD[2]	Reference
Area 1	Mass at 2000 (kg)	10330	0.63	USACE, 2008
	Flux at 2000 (kg/d)	0.75	1.00	USACE, 2008
	Release date	1970	3.00	USACE, 2008
	Width (m)	47	0.20	USACE, 2008
Area 2	Mass at 2000 (kg)	6495	0.56	USACE, 2008
	Flux at 2000 (kg/d)	0.32	1.00	USACE, 2008
	Release date	1970	3.00	USACE, 2008
	Width (m)	42	0.20	USACE, 2008
Area 3	Mass at 2000 (kg)	7987	0.60	USACE, 2008
	Flux at 2000 (kg/d)	0.42	1.00	USACE, 2008
	Release date	1970	3.00	USACE, 2008
	Width (m)	34	0.20	USACE, 2008
Vashon	q (m/d)	0.4	0.15	Truex et al., 2006; Dinicola, 2005
	Porosity	0.29	-	Truex et al., 2006; Dinicola, 2005
	Retardation	1.21	0.15	Typical from literature
	Longitudinal dispersivity (m)	20	0.20	Estimated from plume length
	Transverse dispersivity (m)	2	0.20	Estimated fcrom plume length
	Saturated depth (m)	30	0.20	Truex et al., 2006
	ED average (H-eq ppb)	48	0.15	Dinicola 2005
	EA average (H-eq ppb)	1977	0.15	Dinicola 2005
SLA	Darcy velocity (m/d)	1	0.15	Truex et al., 2006; Dinicola, 2005
	Porosity	0.22	-	Truex et al., 2006; Dinicola, 2005
	Retardation	1.27	0.15	Typical from literature
	Longitudinal dispersivity (m)	20	0.20	Estimated from plume length
	Transverse dispersivity (m)	2	0.20	Estimated from plume length
	Saturated depth (m)	30	0.20	Truex et al., 2006
	Avg natural ED (H-eq ppb)	768	0.15	Dinicola, 2005
	Avg natural EA (H-eq ppb)	1977	0.15	Dinicola, 2005
Window	q_z (m/d)	0.05	0.50	Truex et al., 2006

[1] Prior estimates represent arithmetic mean for release date, geometric mean for other parameters.

[2] Standard deviations of prior estimates are dimensionless statistics for ln-transformed values for all parameters except release dates, which are in actual units.

Model calibration yields refined estimates of model parameters as described in Chapter 5. Final estimates of calibrated parameters are tabulated in Table 8-4. Residual uncertainty in dissolved concentration predictions (S_{lnC}) was estimated as 0.79 for the pre-ERH calibration and 0.77 with post-ERH data indicating that additional data during and after ERH improved model calibration. Comparisons of observed and predicted concentrations for pre- and post-ERH calibration are shown in Figure 8-5. The most notable change in the post-ERH calibration is a decrease in the best estimate of total source mass in 2000 and a decrease in source mass uncertainty using post-ERH data. Interestingly, the estimated source flux decreased while its uncertainty increased.

Table 8-4. Calibration summary for Fort Lewis.

	Pre-ERH		Post-ERH		
Parameter	Best	*STD*	Best	*STD*	Post-ERH Data
$M_{cal\ 1}$ (kg)	16580	0.58	3831	0.05	2990 kg removed by Aug 2004
$M_{cal\ 2}$ (kg)	9851	0.55	5339	0.54	1340 kg removed by Aug 2005
$M_{cal\ 3}$ (kg)	3403	0.20	5133	0.25	1120 kg removed by Jan 2007
$M_{cal\ sum}$ (kg)	29834	0.37	14302	0.22	
$J_{cal\ 1}$ (kg/d)	0.81	0.05	0.43	0.23	0.75 kg/d in Nov 2003
$J_{cal\ 2}$ (kg/d)	0.34	0.03	0.06	0.36	0.32 kg/d in Nov 2003
$J_{cal\ 3}$ (kg/d)	0.72	0.10	0.50	0.22	0.42 kg/d in Apr 2006
$J_{cal\ sum}$ (kg/d)	1.87	0.04	0.99	0.15	Additional monitoring well data
β_1	0.924	0.25	0.982	0.24	
β_2	1.001	0.25	1.030	0.25	
β_3	1.150	0.23	1.090	0.24	
A_1 (m^2)	2748	0.20	2736	0.20	
A_2 (m^2)	2754	0.20	2822	0.20	
A_3 (m^2)	2579	0.19	6774	0.08	

Notes: Calibration date t_{cal} is 2000 for both pre- and post-ERH calibrations. *Best* values denote parameter best estimates. *STD* values are posterior estimates of standard deviations of ln-transformed values for all parameters except β which is not transformed. A_i denotes the area of source zone i.

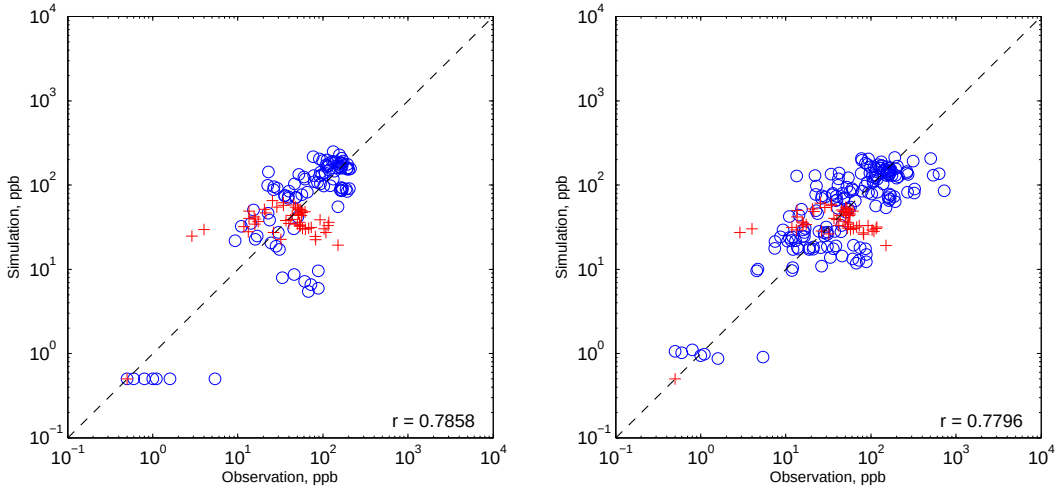

Figure 8-5. Observed vs. simulated concentrations for pre- and post-ERH calibrations. Blue (o) = Vashon aquifer; Red (+) = SLA aquifer.

8.3 Remedial Design Evaluation and Optimization

8.3.1 Long-term Monte Carlo simulations with no further action

Non-optimized MC simulations were performed to assess the long-term effectiveness of ERH source remediation already performed at the site based on pre- and post-remediation parameter estimates. Simulations of ERH were made such that the contaminant mass removed from each source was equal to the measured removal. The following simulations were performed:

- NoOpt 1a - No ERH or any subsequent remedial actions based on pre-ERH calibration,
- NoOpt 1b - Actual ERH with no further remedial actions using pre-ERH calibration,
- NoOpt 2a - No ERH or any subsequent remedial actions based on post-ERH calibration, and
- NoOpt 2b - Actual ERH with no further remedial actions usingpost-ERH calibration.

Long term performance for the NoOpt 1b case differs very little from NoOpt 1a with the predicted time for the median concentration to decrease to 5 µg/L only 10 years earlier in response to ERH (Figure 8-6).

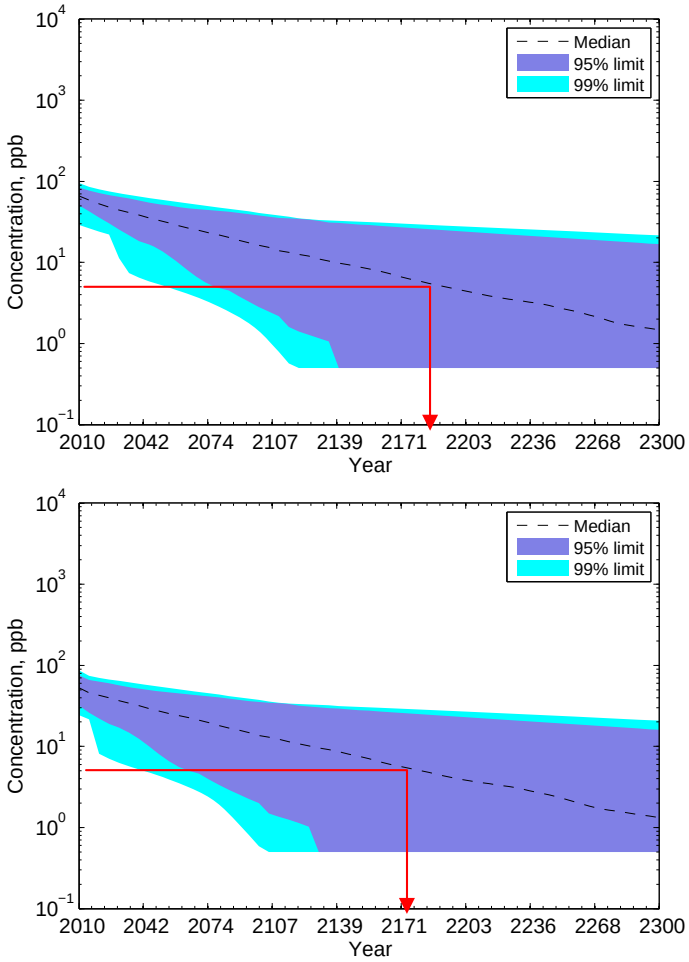

Figure 8-6. TCE-equivalent concentration at the compliance well before (NoOpt 1a, upper panel) and after actual source removal (NoOpt 1b, lower panel) based on pre-ERH calibration parameters (red arrow indicates median time to reach MCL).

The small predicted impact of ERH can be attributed to the small fraction of the calibrated source volume that is recovered by the actual ERH system, which is at least partially due to overestimation of source mass in the pre-ERH calibration. The confidence bands for the pre-ERH simulations are rather wide and increase over time.

Confidence bands for MC simulations based on post-ERH calibration parameters are narrower, reflecting the higher reliability of parameter estimates conditioned on post-ERH data (Figure 8-7). Long-term performance for NoOpt 2b shows the predicted time for the median concentration to reach the MCL is about 80 years shorter than for the no action NoOpt 2a case.

Nevertheless, with a greater than 50% probability of taking more than 100 years to reach the MCL following ERH with no additional remedial action, the performance of thermal treatment conducted at the site taken cannot be judged an unqualified success.

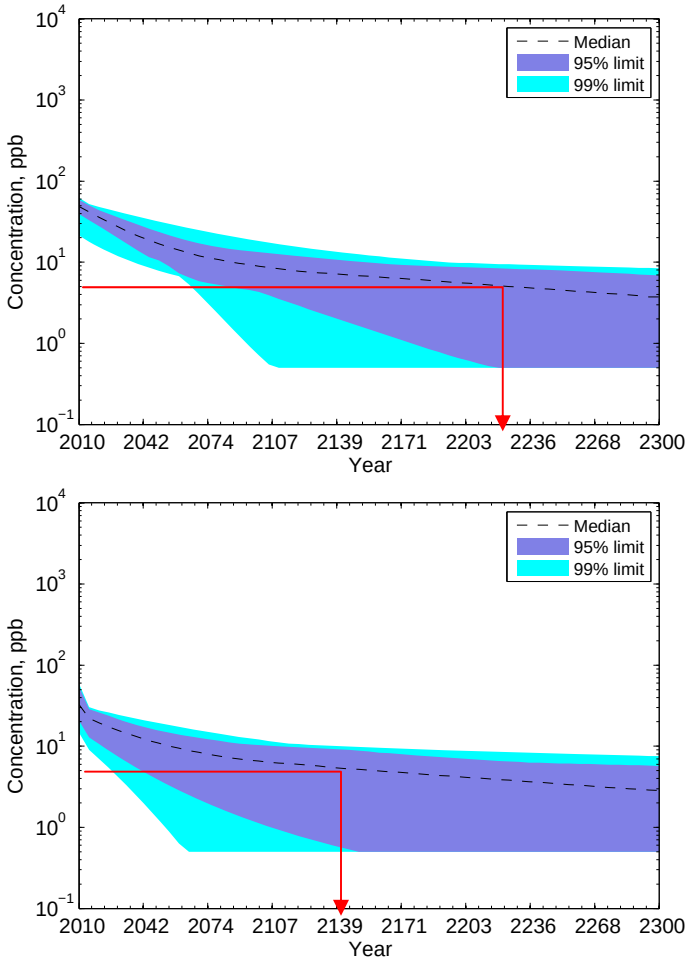

Figure 8-7. TCE-equivalent concentration at the compliance well before (NoOpt 2a, upper panel) nd after actual source removal (NoOpt 2b, lower panel) based on post-ERH calibration parameters (red arrow indicates time to reach MCL).

8.3.2 ERH design optimization

The small mass recovery by ERH at the EGDY site relative to the post-ERH calibrated source mass suggests that a significant quantity of contaminant mass occurs beyond the limits of the various ERH source treatment volumes. Poor performance may also be due to a certain extent to less than optimal mass recovery within the treatment zones. To evaluate the potential for improvement in ERH performance, we turn our attention in this section to ERH design optimization. We will base the optimization analysis on the post-ERH calibration, which is expected to be significantly more reliable than the pre-ERH calibration.

Table 8-5. Cost variables used in design optimization.

Description	Variable	Value	Unit
Thermal treatment costs			
Fixed cost for site	C_{site}^{TR}	320[1]	$K
Thermal system volume cost multiplier	$C_{vol_i}^{TR}$	0.0975[1]	$K/m^3
Thermal system area cost multiplier	$C_{area_i}^{TR}$	0.7332[1]	$K/m^2
Cost per soil boring	$C_{bore_i}^{TR}$	0.1	$K
Analysis cost per soil sample	$C_{SOILsamp}^{TR}$	0.1	$K/sample
Source zone monitoring well installation cost	$C_{well_i}^{TR}$	0.2	$K
Sampling and analysis costs per groundwater sample	C_{GWsamp}^{TR}	0.5	$K/sample
ED injection system costs			
Fixed cost per ED injection gallery width	C_{width}^{EDcap}	3.3[2]	$K/m
Fixed cost per ED performance monitoring well	C_{mw}^{EDcap}	10[2]	$K/well
Other fixed costs for ED injection	C_{other}^{EDcap}	55[2]	$K
Operating cost per mass of ED injected	C_{mass}^{EDop}	0.007427[2]	$K/kg
Operating cost per year per meter ED gallery width	C_{width}^{EDop}	0.733[2]	$K/yr/m
Cost per sample for ED performance monitoring	C_{samp}^{EDop}	2.5[2]	$K/sample
Other operating cost per year for ED injection	C_{all}^{EDop}	61.1[2]	$K/year
Other costs			
Cost per compliance sampling event	$C_{samp}^{SWop} N_{well}^{SW}$	2.5	$K/event
PT operating costs and other site-wide costs	C_{total}^{PTop}	87.5	$K/year
Penalty cost for non-compliance	C_{NPV}^{pen}	50000	$K
Reference year for cost discounting	t_{ref}	2010	year
Discount rate	d	0.03	year^{-1}

[1] Based on G. Bayke, TRS Inc., personal communication (2009) Note: values do not include source characterization costs, post-remediation flux measurements or groundwater pumping at source

[2] Sorenson and Macbeth (2009)

[3] J. Gillie, CTR US USA IMCOM, personal communication (2010)

The optimization simulation assumes ERH operational monitoring following Method 1a (all heating units within a given source treatment zone are turned off at the same time when the average soil concentration drops below a target fraction of the initial concentration – see Chapter 4) and compliance is based on the EXV rule (see Chapter 6) for a 5-year lookback period ($N_{lookback}$) with quarterly groundwater sampling (f_{samp}^{SW} = 4). A cost penalty (C_{NPV}^{pen}) is applied for NC after $t_{penalty}$ = 2050 or if cleanup criteria are not met by t_{max} = 2110.

Cost variables used for design optimization are summarized in Table 8-5. Uncertainty in all unit costs were assumed to follow a uniform probability distribution with a range from 0.9 to 1.1 times the best estimates.

Optimized ERH design variables are summarized in Table 8-6. Optimal mass reduction factors ($R_{TSR(soil)}$) range from 1.35 to 4.59% of the post-ERH estimates of source mass. Optimized thermal treatment areas range from 1.35 times the actual treatment areas used at the site during actual operations in Area 1 to 3.60 times in Area 3. The high ratio for Area 3 suggests a large amount of mass outside the actual treatment zone, which is consistent with the high observed TCE concentrations in wells near Area 3 after thermal treatment.

The model assumes that uncertainty in untreated mass is directly proportional to uncertainty in source area and hence optimizes treatment area to reduce the quantity of untreated mass beyond the treatment perimeter and thus decrease the duration and cost of dissolved plume remediation and the probability of NC. While this assumption is simplistic (mass may be distributed nonuniformly with small "hot spots"), large uncertainty in source area and large spreads between optimized thermal treatment area and the best estimate of source area should raise a warning that additional characterization may be needed to delineate the source more accurately unless characterization costs exceed the cost of overdesigning the thermal system.

The NPV cost ranged from $20M to 26M with an expected value of $22.9M (Figure 8-8), not including costs incurred prior to 2010 or penalty costs. The ENPV for ERH only is about $22M, which is 75% higher than the cost of the actual ERH system (~$12.6M excluding groundwater pumping and source flux measurements), primarily reflecting the larger areal extent of the optimized system. NC probability was estimated to be on the order of 1% and the 99% upper confidence limit of the time to reach NFA was about 30 years after commencing ERH (Figure 8-9).. The results indicate that more refined source characterization, especially in the vicinity of Area 3, followed by additional thermal treatment of "missed" areas could significantly increase the odds of success compared with the actual ERH system that was implemented at the site.

Table 8-6. Optimization of ERH design for EGDY DNAPL sources.

	Thermal Treatment Area ($A_{TSR,}$ m^2)		
Source	Optimized Value	Actual System	$R_{TSR(soil)}$ (%)
Area 1	3175	2360	4.59
Area 2	3108	2080	1.36
Area 3	6099	1691	1.35

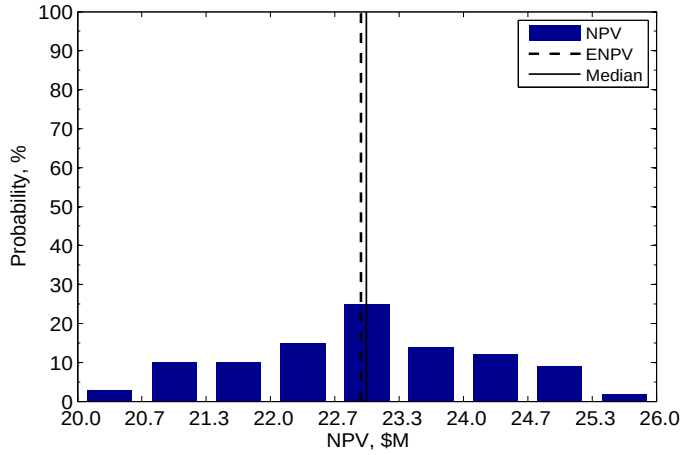

Figure 8-8. Cost distribution of optimized ERH system excluding penalty costs.

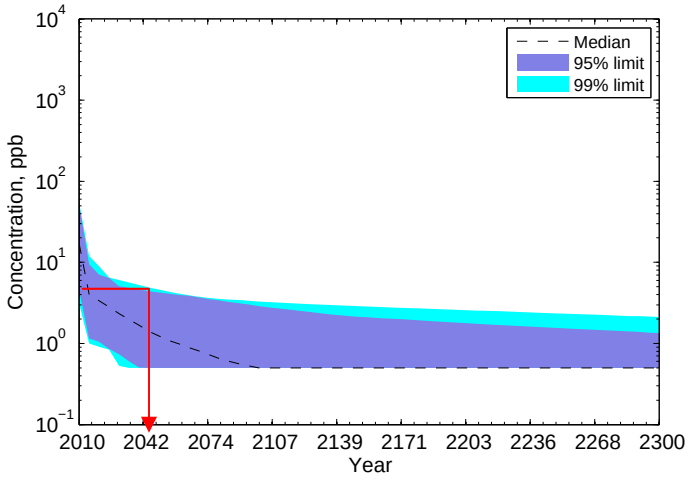

Figure 8-9. TCE-equivalent concentration at the compliance point based on optimized ERH variables in Fort Lewis (red arrow indicates 99% confidence limit of time to reach MCL).

8.3.3 Optimization of enhanced bioremediation with whey injection

Model calibration and optimization analyses indicate that significant amounts of DNAPL were not recovered by past ERH operations at the site, especially near Area 3. Considering the high cost of a second round of source characterization and thermal treatment, we will investigate the effectiveness of employing whey injection to accelerate source zone DNAPL dissolution and to enhance dissolved phase anaerobic dechlorination. Pilot studies in Area 3 indicate that whey injection increases DNAPL dissolution kinetics (Macbeth and Sorenson, 2008).

We consider four potential whey injection gallery locations: three upgradient of each of the three source areas, designated ED1 through ED3, and a fourth upgradient of the "window" from the shallow to deep aquifer, designated as ED4. The purpose of ED1 to ED3 is two-fold. First, we wish to accelerate DNAPL dissolution, and second, we wish to enhance downgradient aqueous plume biodecay. The purpose of ED4 is solely to enhance aqueous plume biodecay and thus reduce the flux of contaminant downgradient of the gallery in the Vashon aquifer and to reduce

the contaminant flux through the window to the SLA. We propose to monitor total TCE and daughter products in performance monitoring wells downgradient of the respective ED gallery and source area and terminate injection when the source is depleted to the point that the annual average concentration is less than a specified concentration C_{EDi} for gallery i. For the ED4 gallery, we propose to monitor a location upgradient of ED4 and to shut off injection after the annual average concentration drops below C_{ED4} and all upgradient ED galleries have been off longer than the max travel time to ED4. A single compliance well is employed for optimization simulations, which is on the plume centerline downgradient of ED4 and upgradient of the "window" (Figure 8-10).

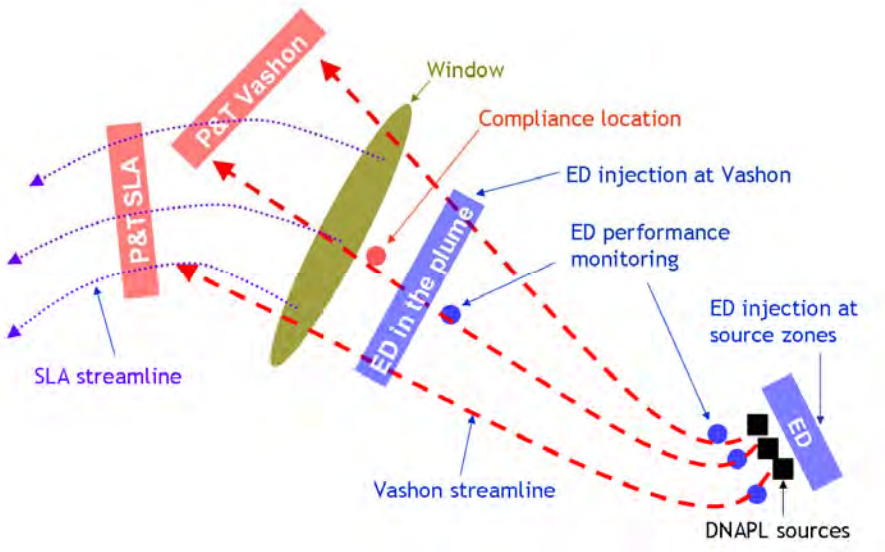

Figure 8-10. Conceptual model of ED injection gallery configuration, ED performance monitoring and compliance monitoring locations.

Mass transfer enhancement is characterized by a factor F_{mt} that represents the ratio of mass transfer under "natural" conditions to that with ED injection as described in Chapter 2. The mass transfer enhancement factor that is assumed to increase proportional the ED concentration as $F_{mt} = 1 + f_{mt} C_{ED}^{net}$. An estimate of f_{mt} was made from a pilot test performed at the site (Area 3 treatment cell 2) in which a 10% whey solution was injected in well IW-2, screened over a 5 m interval, at a rate of 1800 gal/month (22.7 kg whey/day) from Nov 2005 to Feb 2006 (Macbeth and Sorenson, 2008). F_{mt} was determined for wells 2A1 and 2D1 which were 3 and 10 m, respectively downgradient of IW-2, as the ratio of measured TCE concentration after whey injection to that prior to injection. A simulation of whey injection and transport for the pilot test was performed to estimate whey concentrations C_{ED}^{net} at each well and f_{mt} was computed accordingly. Results summarized in Table 8-7 yield an average value of $f_{mt} = 10^{-5}$ L/μg.

Table 8-7. COD measured during whey injection pilot test.

Observation well	Distance from IW-2	F_{mt}	f_{mt} (L/μg)
2A1	3 m	5.6	0.8×10^{-5}
2D1	10 m	4.5	1.3×10^{-5}

The first date of whey injection for optimization simulations was assumed to be 2012. Since ERH was completed prior to 2010, ERH costs were not considered in the ED cost optimization. ERH was simulated by simply removing the measured ERH mass recovery from Area 1-3 sources. ED injection gallery widths were fixed at 70, 90, and 90 m for galleries 1-3 (slightly wider than the calibrated source widths) and 400 m for gallery 4 (about half the 5 μg/L plume width). One kilogram of whey is assumed to have a reducing potential equivalent to 0.078 kg of hydrogen (Table 3-1).

Whey injection rate (M_{ED}), TCE-equivalent concentrations to terminate ED injection (C_{ED}), and ED performance monitoring frequency (f_{samp}^{ED}) were optimized as decision variables. A penalty date ($t_{penalty}$) was set as 2100 and the maximum simulation date (t_{max}) as 2110 since ED injection is considered a long term plume control strategy, but simulation was extended to 2300 to assess longer-term performance. The compliance criteria to terminate monitoring is for the 95% RCL of total TCE-equivalent concentration for a 5-year lookback period ($N_{lookback}$) to be below 5 μg/L.

Optimization results (Table 8-8) indicate only galleries 1 and 2 should be operated with whey injection rates of 25.0 and 29.1 kg/d, respectively, which correspond to 1983 and 2339 gallons per month of 10% whey solution. At these injection rates over the gallery widths, the time-average increase in source mass transfer rates are less than about 20%. Quarterly monitoring of ED performance wells is determined to be optimal with stop criteria (C_{ED}) of 26 and 16 μg/L for galleries 1 and 2, respectively.

The ENPV cost for the optimized whey injection design including costs of site-wide monitoring and existing pump-and-treat system operation but excluding penalty costs is $4667K with a 93% probability of meeting compliance criteria by 2100 and NFA by 2110 and with 7% NC probability (penalty costs applied in optimization). The median date at which compliance is met is about 2040 with 99% probability confidence limits ranging from 2030 to slightly greater than 2300 (Figure 8-11). The range in NPV cost spans from about $1.5M to $10M (Figure 8-12).

Table 8-8. Optimization of ED injection after actual ERH at Fort Lewis.

		ED operation					Average monitoring period (yr)
ENPV* ($K)	Non-compliance (%)	Gallery	Injection (kg/d)	C_{ED} (μg/L)	Avg ED duration (yr)	f_{samp}^{ED} (yr^{-1})	
4667	7	ED 1	25.0	26	1.0	5	46
		ED 2	29.1	16	19.7	5	
		ED 3	-	-	-	-	
		ED 4	-	-	-	-	

* ENPV does not include penalty costs

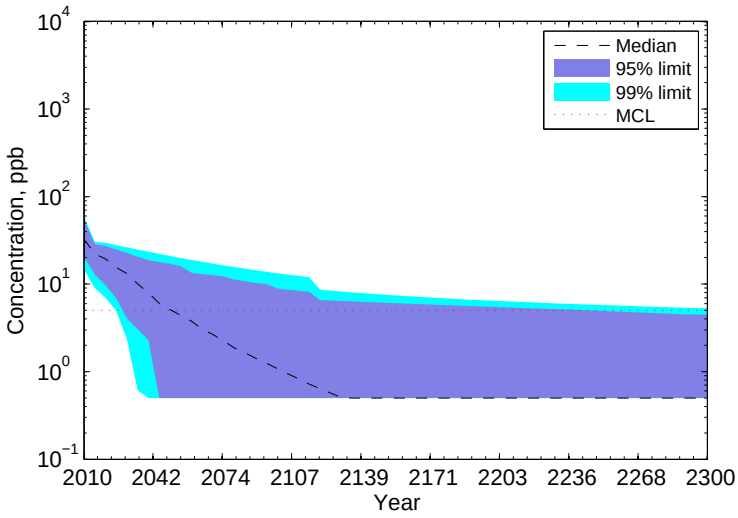

Figure 8-11. Confidence limits of TCE-equivalent concentration at the compliance point versus time.

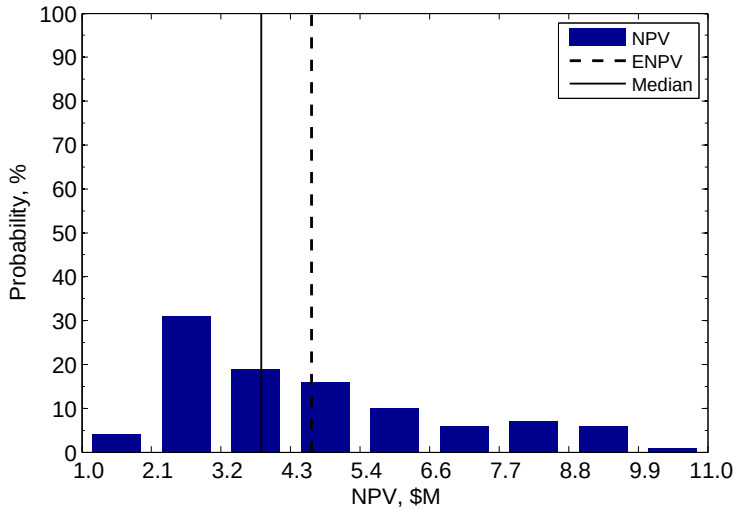

Figure 8-12. Cost probability distribution for whey injection optimization.

8.4 Conclusions

Optimization of thermal treatment for the Fort Lewis EGDY site using pre-thermal treatment calibration parameters indicated that the thermal treatment areas needed to be much larger than the calibrated source areas to successfully capture the source due to uncertainty in source delineation. MC simulations of the thermal system actually implemented at the site indicated that its probability of meeting remediation objectives was low. The actual Implementation of a thermal system Recalibration after thermal treatment provided refined estimates of source mass and other parameters and confirmed that the thermal treatment system implemented at the site failed to capture much of the source mass.

Although not reported here, we also performed model calibration for the three known sources plus a fourth source with an unknown location. Coordinates of the fourth source as well as other source parameters were calibrated. Forward simulations of thermal treatment for the three known sources, even assuming 100% capture by implemented thermal systems, predicted similar poor performance due to mass remaining in the untreated fourth source. Results were not presented because uncertainty in calibrated coordinates of the fourth source were large and the results led to the same conclusions – namely, that further site characterization is needed to better delineate DNAPL sources within the EGDY area.

Prediction uncertainty was reduced by recalibrating the model using data obtained during and after thermal treatment, suggesting that an iterative calibration-optimization approach over time as additional data is collected may allow remediation system design and operation to be refined, increasing the probability of success and reducing cost.

Optimization of whey injection systems indicated that source zone injection galleries could be useful in conjunction with other source zone mass removal technologies, such as thermal treatment, although injection at rates high enough to effect substantial mass transfer enhancement did not appear to be cost effective. Improved source delineation and targeted source treatment appear to be the most pressing needs at the site.

Refinement of the site model calibration with additional source characterization data and stochastic optimization of additional source remedial actions, enhanced bioremediation, monitoring strategies, and their interactions should enable implementation of a remedial action plan that has a high probability of success with the least cost.

Chapter 9
Application to Dover AFB Area 5

9.1 Site Description

Dover Air Force Base (AFB) is located in Kent County, Delaware, and has been in operation since 1942. Base operations have generated numerous wastes, including solvents and hydrocarbons, which were historically buried in drums or disposed in the storm drainage system. Wastes were disposed in various on-base locations, which have resulted in several NAPL sources and contaminant plumes. Our focus in this study is a merged groundwater plume associated with several sources within the West Management Unit (WMU) designated as Area 5 (ORNL, 2008).

Dover AFB is underlain by unconsolidated sediments of the Atlantic Coastal Plain (USGS, 2000). The units of interest are the Columbia Formation and the underlying Calvert Formation. The Columbia Formation is mainly composed of sands, silts and gravels. A clayey silt unit separates it from the Frederica aquifer in the upper Calvert Formation. The water table configuration at Dover AFB is generally controlled by surface water bodies including Little River, St. Jones River, and Delaware Bay (USGS, 2000) and recharge from precipitation. The hydraulic conductivity is variable ranging from 0.03 m/day to 76 m/day and the hydraulic gradient varies over three orders of magnitude with groundwater velocity ranging from about $3x10^{-5}$ m/day to 0.08 m/day.

The five major known contaminant sources in Area 5 are designated as OT51, OT50, SS20, OT44, and OT41 (Figure 9-1). They were formerly oil/water (O/W) separator sites (OT51, OT50, OT44), a vehicle refueling site with underground storage tanks (UST) (SS20), and the Industrial Waste Collection Drain (IWCD) site (OT41).

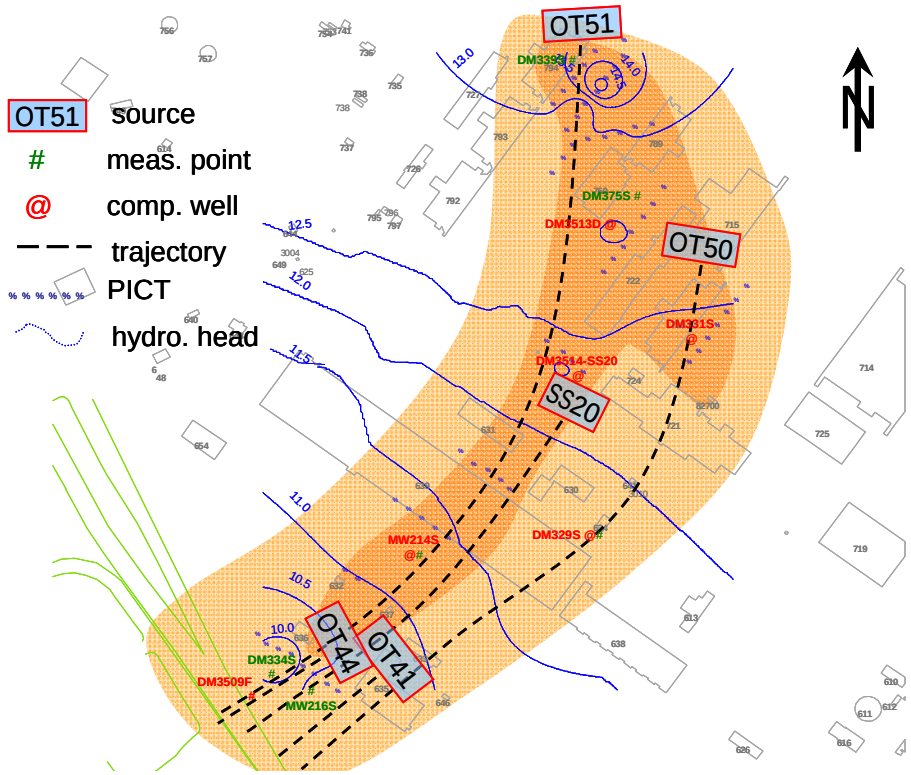

Figure 9-1. Contaminant plume, streamlines, and locations of sources and EVO injection galleries at Dover AFB Area 5.

Chlorinated ethenes, ranging from VC to PCE and soluble fuel hydrocarbons (BTEX) occur throughout the area (Table 9-1). A number of remedial actions have been undertaken, the most important of which are summarized in Table 9-2. Currently, injection of EVO in 10 injection well galleries (Figure 9-1) is being employed to enhance microbial reductive dechlorination of chlorinated ethenes. The system is referred to as Accelerated Anaerobic Bioremediation with Permanent Injection Circulation Transects (AAB PICT).

Table 9-1. Detected contaminants (ORNL, 2008).

Contaminant	OT51	OT50	SS20	OT44	OT41
Benzne	X		X	X	X
cis-1,2-DCE	X	X	X	●	X
PCE	X	X	X		X
TCE	X	X	X	X	X
Toluene	X		X		X
VC	X	X	●	●	●

X Contaminant present at this source.

● Potential contaminants of concern (COC) due to the breakdown of other COCs.

Table 9-2. Chronology of Events (ORNL, 2008).

Date	Event
April 2006	Record of decision (ROD) prepared for OT51, OT50, SS20, OT44, OT41/Motor Pool, and Area 5 (WMU)
May 2006	Finalized Area 5 remedial action work plan (RAWP)
May 8 – 24, 2006	Collected membrane interface probe data delineate Source Areas D and E prior to treatment injections
May 16 – June 9, 2006	AAB direct injection performed at Source Areas E, F, G, and H
May – July 2006	Installation of AAB and monitoring wells
May – October 2006	First round of AAB PICT injections
Week of June 12, 2006	Baseline groundwater sampling conducted in upgradient portion of Area 5 (OT51/OT50)
June 2006 – on going	AAB groundwater monitoring
July 2006	Natural Attenuation monitoring conducted for Area 5
January/February 2007	Natural Attenuation monitoring conducted for Area 5
July 2007 – November 2007	Second round of AAB PICT injections; stopped before completion b ecause of cold weather

9.2 Model Calibration

Groundwater flow and contaminant transport is approximated by the two-dimensional depth-averaged model described in Chapter 2. Groundwater streamlines originating at each contaminant source were estimated from water table contours and the contaminant plume and described by simple polynomial regressions (Figure 9-1). Streamline functions starting from each EVO injection gallery were also determined (not shown in figure).

The forward model at Area 5 simulates DNAPL source dissolution and transport for each source as well as transport of injected ED from each EVO injection gallery. Since the model does not explicitly simulate incomplete dechlorination, we model total chlorinated ethenes as a pseudo-species. Since TCE is the primary contaminant, we sum the concentration of all chlorinated ethene species after converting to their stochiometric equivalent quantity of TCE as described in Chapter 3. Model calibration was performed initially using chlorinated solvent data collected from 1994 to 2006, before ED injection started.

For each contaminant source, we calibrated five parameters: contaminant mass remaining in the source in 2006, source discharge rate in 2006, source width, initial release date, and mass depletion exponent. To reduce the number of parameters, we assume that all sources have the same depletion exponent. Besides parameters related to sources, there are also eight aquifer parameters of which porosity (0.3), natural ED concentration (1200 H-eq ppb) and natural EA concentration (2400 H-eq ppb) levels were assumed known. Prior distributions of all parameters are represented as lognormal except for the source release date, which is represented as normal. Prior best estimates of all parameters and their standard deviations are listed in Table 9-3.

Table 9-3. Parameter prior estimates and their uncertainty.

	Parameters	Prior value[1]	STD[2]	Reference
Site OT51	Mass in 2006 (kg)	3000	1.0	ORNL, 2008
(Source 1)	Source flux in 2006 (kg/d)	0.01	1.0	ORNL, 2008
	Release date (y)	1975	3.0	ORNL, 2008
	Width (m)	50	0.20	ORNL, 2008
	Depletion exponent (-)	1.3	0.10	
Site OT50	Mass in 2006 (kg)	3000	1.0	ORNL, 2008
(Source 2)	Source flux in 2006 (kg/d)	0.01	1.0	ORNL, 2008
	Release date (y)	1975	3.0	ORNL, 2008
	Width (m)	50	0.20	ORNL, 2008
	Depletion exponent (-)	1.3	0.10	
Site SS20	Mass in 2006 (kg)	3000	1.0	ORNL, 2008
(Source 3)	Source flux in 2006 (kg/d)	0.01	1.0	ORNL, 2008
	Release date (y)	1975	3.0	ORNL, 2008
	Width (m)	50	0.20	ORNL, 2008
	Depletion exponent (-)	1.3	0.10	
Site OT41	Mass in 2006 (kg)	3000	1.0	ORNL, 2008
(Source 4)	Source flux in 2006 (kg/d)	0.01	1.0	ORNL, 2008
	Release Date (y)	1975	3.0	ORNL, 2008
	Width (m)	50	0.20	ORNL, 2008
	Depletion exponent (-)	1.3	0.10	
Site OT44	Mass in 2006 (kg)	3000	1.0	ORNL, 2008
(Source 5)	Source flux in 2006 (kg/d)	0.01	1.0	ORNL, 2008
	Release date (y)	1975	3.0	ORNL, 2008
	Width (m)	50	0.20	ORNL, 2008
	Depletion exponent (-)	1.3	0.10	
Aquifer	Darcy velocity (m/d)	0.03	0.10	USGS, 2000
	Retardation factor (-)	1.10	0.56	Typical from literature
	Longitudinal dispersivity (m)	20	0.20	Estimated from plume length
	Transverse dispersivity (m)	2	0.20	Estimated from plume length
	Saturated thickness (m)	12	0.20	USGS, 2000

[1] Prior values are initial best estimates representing the geometric mean for all variables except release date and source-depletion exponent, which are represented by the arithmetic mean.

[2] Standard deviations are for natural logarithms of all variables except release date and source-depletion exponent, which are the standard error of actual values.

For lognormally distributed parameters, prior best estimates represent the geometric mean of the variable and the standard deviation is the statistic for the natural logarithm (S_{ln}). Note that the 99% confidence limit for a log-normally distributed variable ranges from approximately exp(-$3S_{ln}$) to exp($3S_{ln}$) times the geometric mean. For example, the prior estimate of Source 1 contaminant mass in 2006 has a geometric mean of 3000 kg with a standard deviation of ln(mass) equal to 1 (dimensionless) indicating a 99% confidence range of ~0.05 to 20 times 3000 kg or 150 to 60,000 kg.

The calibration approach described in Chapter 5 implemented in SCOToolkit was used to estimate model parameters and their uncertainties as well as the measurement error in concentration data. Best estimates of parameters as well as their posterior standard deviations are summarized in Table 9-4 and the data fit is illustrated in Figure 9-2.

Table 9-4. Summary of calibration results for Dover AFB Area 5.

Parameters	Best Estimates	STD[1]
Mass at source 1 in 2006 (kg)	3065	1.0
Mass at source 2 in 2006 (kg)	3224	1.0
Mass at source 3 in 2006 (kg)	3069	1.0
Mass at source 4 in 2006 (kg)	3017	1.0
Mass at source 5 in 2006 (kg)	3010	1.0
Total Mass	15385	0.45
Flux at source 1 in 2006 (kg/d)	0.006	0.58
Flux at source 2 in 2006 (kg/d)	0.010	0.53
Flux at source 3 in 2006 (kg/d)	0.006	0.61
Flux at source 4 in 2006 (kg/d)	0.002	0.90
Flux at source 5 in 2006 (kg/d)	0.001	0.73
Total Flux	0.025	0.70
Release date of source 1 (y)	1974	2.9
Release date of source 2 (y)	1985	-[2]
Release date of source 3 (y)	1977	2.5
Release date of source 4 (y)	1975	3.0
Release date of source 5 (y)	1975	3.0
Width of source 1 (m)	45	0.19
Width of source 2 (m)	51	0.20
Width of source 3 (m)	81	0.15
Width of source 4 (m)	48	0.20
Width of source 5 (m)	51	0.20
Source depletion exponent (-)	1.3	0.1
Darcy velocity (m/d)	0.015	0.056
Retardation factor	1.10	0.56
Longitudinal dispersivity (m)	11.3	0.18
Transverse dispersivity (m)	1.6	0.15
Saturated thickness (m)	15.8	0.20

[1] Standard deviations are for natural logarithms of all variables except release date and source depletion exponent, which are the standard error of the actual values.

[2] The estimated value is the upper limit constraint set in optimization, so uncertainty estimate from linear analysis is not available.

Darcy velocity and release dates are reasonably well characterized by the calibration. Estimates of source mass and its uncertainty barely changed from the prior estimates, indicating that the available data is insufficient to reliably estimate source mass. Note that 99% confidence limits for the mass of each source in 2006 range from about 150 to 60,000 kg. Other parameters exhibit intermediate reliability.

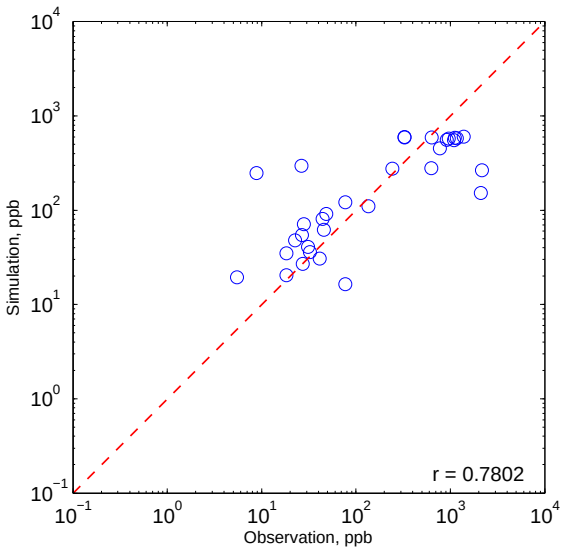

Figure 9-2. Observed versus calibrated contaminant concentrations.

9.3 Design Optimization

Given the large uncertainty in source mass estimates, reliable prediction of the duration of DNAPL dissolution that will feed the dissolved plume is not expected. However, due to the low estimated DNAPL dissolution rates relative to source mass, forward simulations indicate a high probability that without source remediation, ED injection or some other means of plume control will be required for a very long time (decades to centuries). Furthermore, due to the number of known DNAPL sources, a possibility of additional smaller source zones, and difficulty to perform detailed source zone characterization or remediation due to buildings, infrastructure and base operation disruptions, we will focus on investigating remedial options capable of minimizing the cost of long-term plume control using EVO injection with ten of the ED injection galleries that have already been constructed within Area 5.

Specifically, our goal is to minimize total costs over a 100 year period subject to the constraint that after a grace period the TCE-equivalent concentration at each of the five compliance wells, signified by the "@" sign on Figure 9-1, should be less than MCL for each MC realization. Formally, we minimize the expected present value of the total cost over 100 years. Note that this criterion has a conservative bias since other chlorinated ethane species present at levels comparable to TCE have lower MCLs. One hundred realizations, conditioned on the actual data used for calibration, are used in the optimization. By enforcing that all 100 realizations need to meet MCL constraints at compliance wells, we implicitly ensure that the probability of failure of the optimal remediation design is on the order of 1%. The grace period is computed as the travel time of ED from the nearest injection gallery to a compliance well plus 1 year. The MCL value is 5 TCE-equivalent μg/L. Cost variables for Dover site are summarized in Table 9-5.

Table 9-5. Summary of cost variables used in optimization.

	Description	Value
Capital Costs	Gallery construction	\$333/ gallery width (m)
	Injection equipment	\$65,000/ unit[1]
Operating Costs	Fork lift rental and operation	\$21,600/ year
	Generator rental and operation	\$21,600/ year/unit
	Personnel	\$65,000/year/gallery
Material Cost	ED material (in solution)	\$1.3 / kg solution[1]
Annual Discount Rate	Risk-free return minus inflation rate	3%

[1] The H-equiv mass per kg of solution is approximately 0.063kg

Optimization under uncertainty requires a significant amount of computational resources. In this application, where we only consider plume control with constant ED injection over a fixed time period and without source zone remediation, the ED concentration C_{ED}^{net} is a linear function of injection rates at each gallery; thus, the contaminant concentration can be calculated easily by taking advantage of the linear relationship between injection rates and ED concentrations. Once we calculate the DNAPL concentration without ED injection, and the ED concentration due to unit ED injection rate (i.e., 1 kg-solution/day) from each injection gallery over the simulation period, MC simulations can be replaced by a simple linear equation. Furthermore, with the linear relationship between DNAPL concentration and ED injection rate, we can find the optimal ED injection strategy for Dover site using linear programming. More precisely, mixed binary integer programming was used in this study to determine whether one gallery is used or not and the amount of ED injected in case it is used.

We present optimization results for the following optimization scenarios:

- Optimize ED injection rates in the ten existing ED injection galleries at the site over a 100 year time period to minimize overall remediation costs, and
- Optimize ED injection rates in 2011 and implement the optimal strategy for 50 years. In 2061, model parameters are recalibrated using additional data since 2011. Then, with the updated calibration, reoptimize ED injection rates for the next 50 years.

9.3.1 ED injection optimization for 100 years

ED is injected at a constant rate in each gallery for 100 years. Rates can differ from gallery to gallery. The optimal strategy for the operating galleries are shown in Table 9-6. Expected values for capital cost, cumulative NPV operating cost, total NPV cost, and annual operating cost are summarized in Table 9-7. Confidence limits for dissolved TCE-equivalent concentrations at compliance well DM329S (Figure 9-3) indicate that by 2030, there is a high likelihood of meeting the cleanup level. The predicted spatial distribution of groundwater contamination in 2111 using best estimates of model parameters and optimized design variables (Figure 9-4) shows that EVO injection is reasonably successful at containing the dissolved plume, although improvements may be possible if gallery locations were optimized.

Table 9-6. Single-stage optimization of ED injection rates for Dover AFB Area 5.

ED Injection Gallery	Injection Rate (kg-sol/yr)
1	0
2	0
3	620
4	0
5	365
6	219
7	0
8	219
9	0
10	365
All	1788

Table 9-7. Expected cost details for single-stage ED optimization.

Capital Cost (ENPV $K)	Operating Cost (ENPV $K)	Annual Operating Cost ($K/yr)	Total Cost (ENPV $K)
431	17,415	549	17,846

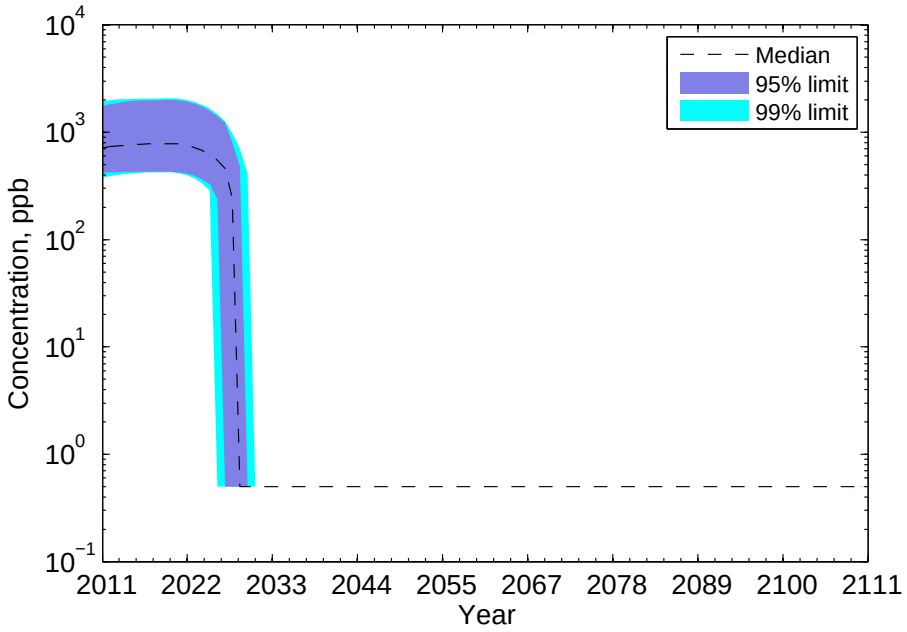

Figure 9-3. TCE-equivalent concentration at a compliance point DM329S.

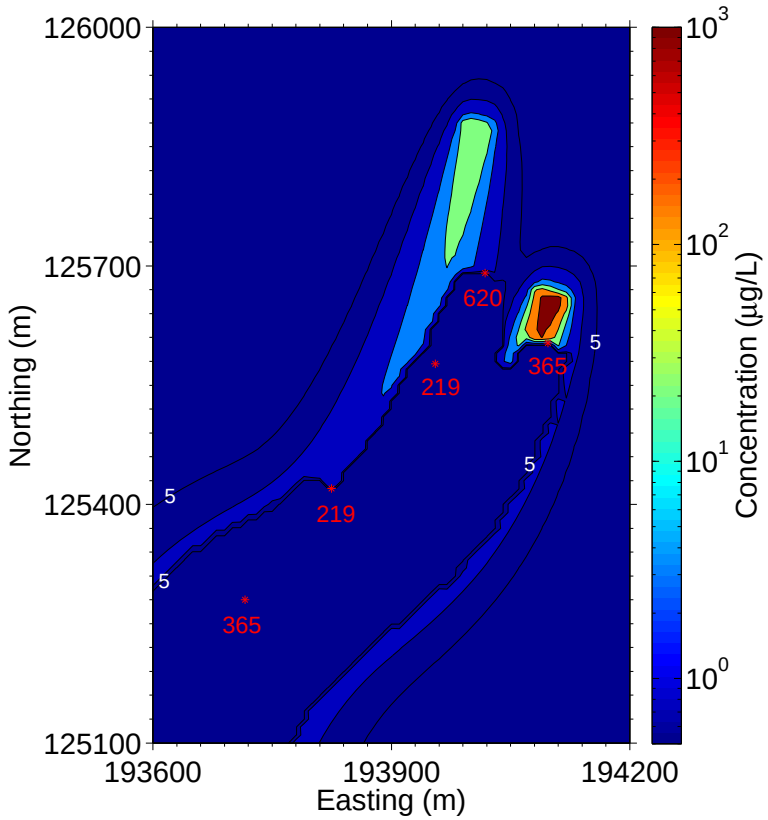

Figure 9-4. Contour plot of TCE-equivalent concentration in 2111 with best parameter estimates (red dots and numbers represent operating gallery locations and corresponding ED injection rates).

9.3.2 ED injection multi-stage optimization with parameter recalibration

In this section, we consider two-stage optimization for ED injection rates. Injection rates determined from the initial calibration/optimization are assumed to be implemented in 2011 for 50 years. In 2061, model parameters are re-calibrated using the additional observed concentrations in monitoring wells since initial implementation. Then, with new model parameters, ED injection rates are re-optimized and applied for the next 50 years. In this way, the remediation strategy can be adjusted based on field observations. This observation-feedback approach should reduce the probability of failure and expected costs. To obtain concentration "observations" for the first 50 years, "true" model parameters are selected from a parameter realization generated from the original calibration which is not used in optimization.

The results show that after recalibration and optimization, ED galleries 6, 8, and 10 are shut down, and the total injection rate is reduced from 1788 kg-sol/yr to 876 kg-sol/yr (Table 9-8), resulting in a reduction in annual (undiscounted) operating costs from $549 K/yr to $207 K/yr (Tables 9-7 and 9-9). It is also observed that after reoptimization, injection rates in injection galleries 3 and 5 were adjusted.

Table 9-8. Two-stage optimization of ED injection rates for Dover AFB Area 5.

ED Injection Gallery	Injection Rate (kg-sol/yr)	
	2011-2060	2061-2111
1	0	0
2	0	0
3	620	803
4	0	0
5	365	73
6	219	0
7	0	0
8	219	0
9	0	0
10	365	0
All	1788	876

Table 9-9. Cost details for two-stage ED optimization.

Capital Cost (NPV $K)	Operating Cost (NPV $K)	Annual Operating Cost[1] ($K/yr)	Total Cost (NPV $K)
431	15,484	207	15,915

[1] Annual operating costs for years 2011-2060 / 2061-2110

The spatial distribution of groundwater contamination in 2061 indicates that some contamination moves beyond the most downgradient monitoring wells before being attenuated by EVO injection (Figure 9-5). Given the paucity of data, this is difficult to confirm or refute. With additional downgradient data, the model accuracy could be evaluated and the calibration refined.

Comparison of the two-stage optimization plume simulation in 2111 (Figure 9-6) with the one-stage optimization (Figure 9-4) reveals that although both cases yield high probabilities of meeting the MCL at the selected compliance locations, fingers of contamination may slip by compliance wells. This risk can be ameliorated by visual inspection of the plume distribution and by using the optimization to select compliance well locations.

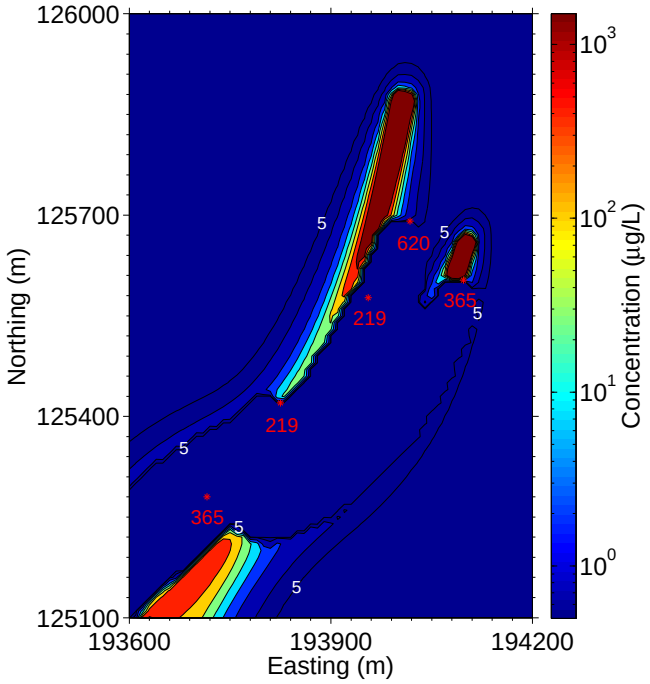

Figure 9-5. Contour plot of TCE-equivalent concentration in 2061 using the best parameter estimate after recalibration in 2061 (red dots and numbers represent operating gallery locations and corresponding ED injection rates).

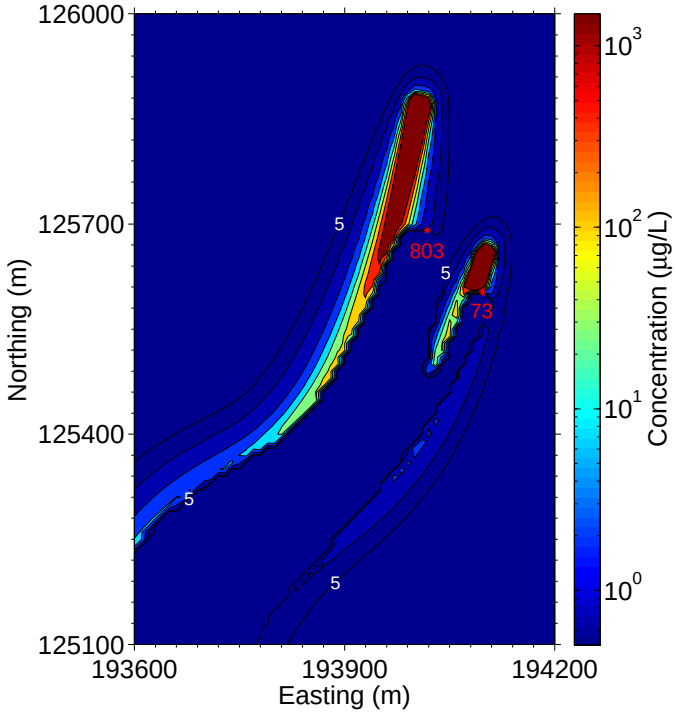

Figure 9-6. Contour plot of TCE-equivalent concentration in 2111 using the best parameter estimate after recalibration in 2061 (red dots and numbers represent operating gallery locations and corresponding ED injection rates assigned in 2061).

9.4 Conclusions

Estimates of source mass could not be calibrated reliably from available site data. Ninety-nine percent confidence limits for the mass of the five identified DNAPL sources in Dover AFB Area 5 ranged from about 150 to 60,000 kg. Forward simulations indicate a high probability that without source remediation, long-term measures are likely to be required to control off-base plume migration. Due to the number of known DNAPL sources, the possibility of additional smaller source zones, and the difficulty to perform detailed source zone characterization or remediation due to infrastructure and base operation disruptions, plume control using EVO injection may be a practical long-term solution.

Optimization of EVO injection rates in ten existing injection galleries indicated a high probability that contaminant concentrations in specified compliance wells could meet cleanup targets with continued injection in only 5 of the current 10 injection galleries, which would reduce operating costs by about 50%.

A multi-stage calibration-optimization strategy was investigated in which indicated that periodic re-calibration and re-optimization using additional monitoring data can further reduce expected costs and improve system performance and the reliability. Re-optimizing after 50 years was predicted to allow a reduction in ED injection rates that reduced (non-discounted) annual operating costs by an additional 60%.

A possible strategy that may be investigated in future studies to reduce source mass and model uncertainty would be to inject EVO immediately upgradient of each of source zones for several injection cycles. High EVO concentrations in the source zones is expected to increase DNAPL dissolution rates and thus accelerate source mass depletion. Recalibration using monitoring data obtained during accelerated source depletion should diminish model uncertainty and enable more reliable system design and perfmroance.

Chapter 10
Conclusions, Future Research and Implementation

A new approach for optimizing the design and operation of DNAPL site remediation systems was developed and implemented in the computer program SCOToolkit, which explicitly considers uncertainty in site and remediation system characteristics, measurement data, performance models and unit costs, and specific compliance criteria. By seeking to minimize NPV cost averaged over equiprobable Monte Carlo realizations of future performance, conditioned on all available site data, with penalties applied for nonattainment of remediation objectives, the approach constrains the probability of failure. Unlike conventional design and operational optimization protocols, the proposed approach takes into account the many complex interactions and tradeoffs among design, monitoring and characterization variables and cleanup criteria. For example, remediation optimization often attempts to minimize sampling frequency, while SCOToolkit can determine an optimum sampling frequency at which the increased cost of additional samples is just offset by cost savings associated with improved decision reliability (i.e., the magnitude of overdesign is adjusted to minimize expected cost).

The method was applied to two well-characterized sites where different remedial technologies were used to evaluate its ability to reduce costs and improve remedial designs. At the first site, the Fort Lewis East Gate Disposal Yard (EGDY) site, optimization of thermal source treatment indicated a need for a much larger treatment area than was actually employed to avoid a high failure probability associated with source delineation uncertainty based on available source characterization data. The method was also used to optimize source and plume bioremediation at the EGDY site, using whey injection without additional source reduction. The results indicated that this remedial strategy is expected to achieve Maximum Contaminant Limits by 2100 with a 93% probability of success when using relatively low whey injection rates. Additional source treatment efforts may be cost effective if additional characterization were undertaken to reduce source zone uncertainty. Further studies may be undertaken using SCOToolkit to evaluate the potential monetary value of additional source zone investigations in conjunction with a second round of thermal or other source zone treatment.

SCOToolkit was also applied to Dover AFB Area 5 to optimize enhanced bioremediation. The results suggested that electron donor injection may be needed indefinitely in the future to meet remediation criteria, as a result of the large uncertainty in estimated source mass and difficulties in characterizing and treating source zones without disrupting base operations. Optimization analyses to minimize long term operating costs indicated a high probability of meeting compliance criteria using only five of the current ten emulsified vegetable oil injection galleries, with approximately half the current annual operating cost. Recalibration and optimization after 50 years, using additional data from this period, was projected to reduce prediction uncertainty allowing further reductions in operating costs. Recommendations for further optimization analyses include investigating EVO injection immediately upgradient instead of downgradient of each source zone to increase DNAPL dissolution rates, reduce source mass more quickly, and recalibrate at shorter time intervals to accelerate operating cost reductions.

Stochastic cost optimization of design and monitoring variables was shown to reduce expected costs by 50% or more compared to conventional design methods, and to substantially increase

the probability of meeting compliance targets. Expected cost reductions were also shown to be possible by judicious specification of statistical criteria for no further action (NFA) and by stipulating procedures for technology deployment, operation and shut-down. For example, source zone soil and/or groundwater monitoring may be used to operationally decide when to terminate electrode heating for thermal treatment all at once, within zones, or individually. The optimal protocol depends on tradeoffs between the magnitude of measurement noise, unit costs for well installation and monitoring, and other variables. Over many sites, minimization of expected cost should yield significant cost savings. For any single site, the probability of failure is reduced to a level that the probability-weighted cost of failure is just offset by the cost of overdesigning the system.

Various enhancements to SCOToolkit could be implemented to extend applicability to a broader range of remedial technologies and to make the program easier to use. With limited effort, the DNAPL source remediation module could be extended to add the capability to simulate in situ chemical oxidation (ISCO), thermal conduction and steam injection performance and cost, in addition to the current electrical resistance heating capability. Pre- and post-processors would simplify problem setup, execution and interpretation of output.

In addition to more extensive technology demonstrations on the Dover AFB and Fort Lewis sites, as discussed above, further testing would be beneficial to demonstrate the applicability and benefits of SCOToolkit on DoD sites that span ranges of site complexity, data availability, and remediation technologies, including enhanced source zone and plume bioremediation, various thermal technologies, and ISCO, used individually or in various combinations. In addition to single-pass calibration-optimization applications, demonstrations of iterative calibration-optimization protocols are desirable to assess potential cost reductions due to additional site characterization efforts.

Finally, technology transfer will be critical to fully realize cost savings promised by SCOToolkit. Responsible parties and regulators must gain an understanding of the technology and its capabilities, and training must be available for consultants and other users to learn how to effectively and efficiently use the software.

11. References

Aly, A. H. and R. C. Peralta, 1999, Optimal design of aquifer cleanup systems under uncertainty using a neural network and a genetic algorithm. Water Resources Research 35 (8), 2523-2532.

Andricevic, R. and P. K. Kitanidis, 1990, Optimization of the pumping schedule in aquifer remediation under uncertainty. Water Resources Research 26, 875-885.

Becker, D. B., B. Minser, R. Greeenwald, Y. Zhang, K. Harre, K. Yager, C. Zheng, and R. Peralta, 2006, Reducing long-term remedial costs by transport modeling optimization. Ground Water 44, 864-875.

Borden, R. C. and P. B. Bedient, 1986, Transport of dissolved hydrocarbons influenced by oxygen limited biodegradation - theoretical development. Water Resources Research 22, 1973-1982.

Cardiff, M., X. Liu, P. K. Kitanidis, J. Parker, and U. Kim, 2010, Cost optimization of DNAPL source and plume remediation under uncertainty using a semi-analytic model. Journal of Contaminant Hydrology 13, 24-43.

Cohen, R. M. and J. W. Mercer, 1993, DNAPL Site Evaluation. C. K. Smoley Publication, Boca Raton, FL, 384 p.

Chan-Hilton, A. B. and T. B. Culver, 2005, Groundwater remediation design under uncertainty using genetic algorithms. Journal of Water Resources Planning and Management 131 (1), 25-34.

Dinicola, R. S., 2005, Hydrogeology and trichloroethene contamination in the sea-level aquifer beneath the Logistics Center, Fort Lewis, Washington: U.S. Geological Survey Scientific Investigations Report 2005-5035, 50 p.

Domenico, P. A., 1987, An analytical model for multidimensional transport of a decaying contaminant species. Journal of Hydrology 91, 49–58.

Erickson, M., A. Mayer, and J. Horn, 2002, Multi-objective optimal design of groundwater remediation systems: Application of the niched Pareto genetic algorithm (NPGA). Advances in Water Resources 25, 51-65.

Feyen, L. and S. M. Gorelick, 2005, Framework to evaluate the worth of hydraulic conductivity data for optimal groundwater resources management in ecologically sensitive areas. Water Resources Research 41, W03019, 16 p.

Gorelick, S. M., C. I. Voss, P. E. Gill, W. Murray, and M. A. Saunders, 1984, Aquifer reclamation design: The use of contaminant transport simulation combined with nonlinear programming. Water Resources Research 20 (4), 415-427.

Heron, G., K. Parker, J. Galligan, and T. C. Holmes, 2009, Thermal treatment of eight CVOC source zones to near nondetect concentrations. Groundwater Monitoring & Remediation 29, 56-65.

Kamanth, R. K., C. J. Newell, B. B. Looney, K. M. Vengelas, and J. Perex, 2006, Biobalance: A Mass Balance ToolKit for Evaluating Source Depletion, Competition Effects, Long-Term Sustainability and Plume Dynamics. GSI Environmental Inc., 61 p.

Kitanidis, P. K., 1987, A first-order approximation to stochastic optimal control of reservoirs. Stochastic Hydrology and Hydraulics 1, 169-184.

Lee, S.-I. and P. K. Kitanidis, 1991, Optimal estimation and scheduling of aquifer remediation with incomplete information. Water Resources Research 27 (9), 2203-2217.

Levine, H., 2010, EPA perspective on site closure: how clean is clean? US Dept of Defense SERDP/ESTCP Partners in Environmental Technology Technical Symposium and Workshop, Washington DC, Nov 30-Dec 2.

Liang, H. and R. W. Falta, 2008. Modeling field-scale cosolvent flooding for DNAPL source zone remediation. Journal of Contaminant Hydrology 96, 1-16.

Liu, X., M. Cardiff, and P. K. Kitanidis, 2010, Parameter estimation in nonlinear environmental problems. Stochastic Environmental Research and Risk Assessment 24 (7), 1003-1022, doi: 10.1007/s00477-010-0395-y.

Mayer, A. and K. L. Endres, 2007, Simultaneous optimization of dense non-aqueous phase liquid (DNAPL) source and contaminant plume remediation. Journal of Contaminant Hydrology 91(3-4), 288-311.

Macbeth, T. W. and K. S. Sorenson, Jr., 2008, Final Report: In Situ Bioremediation of Chlorinated Solvent Source Areas with Enhanced Mass Transfer. ESTCP Project ER-0218.

McKinney, D. C. and M.-D. Lin, 1996, Pump-and-treat ground-water remediation system optimization. Journal of Water Resources Planning and Management 122 (2), 128-136.

Mugunthan, P. and C. A. Shoemaker, 2004, Time varying optimization for monitoring multiple contaminants under uncertain hydrogeology. Bioremediation Journal 8, 129-146.

National Research Council, 1994, Alternatives for Ground Water Cleanup. National Academy Press, Washington D.C., 336 p.

Oak Ridge National Laboratory (ORNL), 2008, Area 5 monitoring report (through January 2008), Dover Air Force Base, Delaware, June 2008.

Park, E. and J. C. Parker, 2005, Evaluation of an upscaled model for DNAPL dissolution kinetics in heterogeneous aquifers. Advances in Water Resources 28, 1280-1291.

Parker, J. C. and E. Park, 2004, Modeling field-scale dense non aqueous phase liquid dissolution kinetics in heterogeneous aquifers. Water Resources Research 40, W05109, doi:10.1029/2003WR002807.

B. P. Flannery, 2007, Numerical Recipes: The Art of Scientific Computing. Cambridge University Press, New York, 1256 p.

Rittman, B. E. and P. L. McCarty, 2001, Environmental Biotechnology: Principles and Applications. McGraw-Hill, 754 p.

Rizzo, D. M. and D. E. Dougherty, 1996, Design optimization for multiple management period groundwater remediation. Water Resources Research 32 (8), 2549-2561.

Sorenson, K. S., 2006, Recent progress in bioremediation of chlorinated solvent DNAPL source areas. Partners in Environmental Technology Symposium and Workshop, Nov 28-30, 2006, US Dept. of Defense – SERDP, C-46.

Sorenson, K. and T. Macbeth, 2009, In Situ Bioremediation of Chlorinated Solvents Source Areas with Enhanced Mass Transfer, Cost and Performance Report, ESTCP Project ER-0218.

Teutsch, G. and M. Finkel, 2002, Integrated physico-chemical-economic modelling for optimal plume management at contaminated sites: a decision support system, ModelCARE 2002: Calibration and Reliability in Groundwater Modeling: A Few Steps Closer to Reality. IAHS Publications, Prague, Czech Republic, 69-78.

Teutsch, G., H. Rugner, D. Zamfirescu, M. Finkel, and M. Bittens, 2001, Source remediation vs. plume management: critical factors affecting cost-efficiency. Land Contamination and Reclamation 9, 128-142.

Thomson, N. R., E. D. Hood, and G. J. Farquhar, 2007, Permanganate treatment of an emplaced DNAPL Source. Ground Water Monitoring & Remediation 27, 74-85.

Truex, M. J., C. D. Johnson, and C. R. Cole, 2006, Numerical Flow and Transport Model for the Fort Lewis Logistics Center, Fort Lewis, Washington. DSERTS NO. FTLE-33. Pacific Northwest National Laboratory, Richland, Washington, 121 p.

Tucciarelli, T. and G. Pinder, 1991. Optimal data acquisition strategy for the development of a transport model for groundwater remediation. Water Resources Research 27, 577-588.

US Army Corps of Engineers (USACE), 2008, East Gate Disposal Yard Thermal Remediation Performance Assessment After Action Report. 248 p.

U.S. Geological Survey, 2000, Hydrogeology and Simulation of Ground-Water Flow at Dover Air Force Base, Delaware. Water-Resources Investigations Report 99-4224.

Wagner, B. J. and S. M. Gorelick, 1987, Optimal groundwater quality management under parameter uncertainty. Water Resources Research 23 (7), 1162-1174.

Wagner, B. J., U. Shamir, and H. R. Nemati, 1992, Groundwater quality management under uncertainty: Stochastic programming approaches and the value of information. Water Resources Research 28, 1233-1246.

Wymore, R. A., T. W. Macbeth, J. S. Rothermel, L. N. Peterson, L. O. Nelson, K. S. Sorenson Jr., N. Akladiss, and I. R. Tasker, 2006. Enhanced anaerobic bioremediation in a DNAPL residual source zone: Test Area North case study. Remediation Journal 16, 5-22.

Appendix A. Concentration and Source Data for Fort Lewis Calibration

Table A-1. TCE-equivalent concentrations used for Fort Lewis site calibration.

No.	Well	East (m)	North (m)	Date	Concentration (ppb)	Aquifer
1	LC-03	455341.94	200345.95	06/01/1995	0.80	1
2	LC-03	455341.94	200345.95	06/01/1996	0.50	1
3	LC-03	455341.94	200345.95	06/01/1997	0.60	1
4	LC-03	455341.94	200345.95	06/01/1998	1.10	1
5	LC-03	455341.94	200345.95	06/01/1999	1.00	1
6	LC-03	455341.94	200345.95	06/01/2000	5.40	1
7	LC-03	455341.94	200345.95	06/01/2001	1.60	1
8	LC-05	454413.21	200342.91	06/01/1995	46.50	1
9	LC-05	454413.21	200342.91	06/01/1996	22.40	1
10	LC-05	454413.21	200342.91	06/01/1997	26.50	1
11	LC-05	454413.21	200342.91	06/01/1998	29.00	1
12	LC-05	454413.21	200342.91	06/01/1999	26.30	1
13	LC-05	454413.21	200342.91	06/01/2000	39.80	1
14	LC-05	454413.21	200342.91	06/01/2001	65.70	1
15	LC-06	455369.37	199917.10	06/01/1995	88.50	1
16	LC-06	455369.37	199917.10	06/01/1996	46.00	1
17	LC-06	455369.37	199917.10	06/01/1997	33.40	1
18	LC-06	455369.37	199917.10	06/01/1998	61.30	1
19	LC-06	455369.37	199917.10	06/01/1999	72.50	1
20	LC-06	455369.37	199917.10	06/01/2000	88.50	1
21	LC-06	455369.37	199917.10	06/01/2001	67.30	1
22	LC-108	456129.11	198922.98	06/01/1995	151.00	1
23	LC-108	456129.11	198922.98	06/01/1996	15.30	1
24	LC-108	456129.11	198922.98	06/01/1997	22.80	1
25	LC-108	456129.11	198922.98	06/01/1998	50.50	1
26	LC-108	456129.11	198922.98	06/01/1999	23.70	1
27	LC-108	456129.11	198922.98	06/01/2000	14.30	1
28	LC-108	456129.11	198922.98	06/01/2001	11.00	1
29	LC-132	454582.08	200260.81	06/01/1995	23.00	1
30	LC-132	454582.08	200260.81	06/01/1996	52.30	1
31	LC-132	454582.08	200260.81	06/01/1997	59.80	1
32	LC-132	454582.08	200260.81	06/01/1998	62.00	1
33	LC-132	454582.08	200260.81	06/01/1999	79.00	1
34	LC-132	454582.08	200260.81	06/01/2000	93.50	1
35	LC-132	454582.08	200260.81	06/01/2001	102.00	1
36	LC-137A	456031.98	198938.29	06/01/1995	191.43	1
37	LC-137A	456031.98	198938.29	06/01/1996	93.47	1
38	LC-137A	456031.98	198938.29	06/01/1997	78.20	1
39	LC-137A	456031.98	198938.29	06/01/1998	132.27	1
40	LC-137A	456031.98	198938.29	06/01/1999	86.70	1
41	LC-137A	456031.98	198938.29	06/01/2000	122.17	1
42	LC-137A	456031.98	198938.29	06/01/2001	205.33	1
43	LC-144B	455799.22	199047.83	06/01/1995	195.25	1
44	LC-144B	455799.22	199047.83	06/01/1996	148.40	1
45	LC-144B	455799.22	199047.83	06/01/1997	136.15	1
46	LC-144B	455799.22	199047.83	06/01/1998	97.00	1
47	LC-16	454905.47	200648.62	06/01/2001	9.30	1
48	LC-19A	455718.37	199063.36	06/01/1998	90.57	1
49	LC-19A	455718.37	199063.36	06/01/1999	136.77	1
50	LC-19A	455718.37	199063.36	06/01/2000	108.27	1

Table A-1. TCE-equivalent concentrations used for Fort Lewis site calibration (continued)

No.	Well	East (m)	North (m)	Date	Concentration (ppb)	Aquifer
51	LC-19A	455718.37	199063.36	06/01/2001	163.30	1
52	LC-41A	454723.34	199690.05	06/01/1995	165.00	1
53	LC-41A	454723.34	199690.05	06/01/1996	170.00	1
54	LC-41A	454723.34	199690.05	06/01/1997	187.50	1
55	LC-41A	454723.34	199690.05	06/01/1998	160.00	1
56	LC-41A	454723.34	199690.05	06/01/1999	167.50	1
57	LC-41A	454723.34	199690.05	06/01/2000	162.50	1
58	LC-41A	454723.34	199690.05	06/01/2001	193.30	1
59	LC-44A	455141.99	200214.59	06/01/1995	45.50	1
60	LC-44A	455141.99	200214.59	06/01/1996	30.00	1
61	LC-44A	455141.99	200214.59	06/01/1997	16.80	1
62	LC-44A	455141.99	200214.59	06/01/1998	16.00	1
63	LC-44A	455141.99	200214.59	06/01/1999	24.50	1
64	LC-44A	455141.99	200214.59	06/01/2000	28.30	1
65	LC-44A	455141.99	200214.59	06/01/2001	30.70	1
66	LC-49A	455336.76	199380.35	06/01/1995	133.00	1
67	LC-49A	455336.76	199380.35	06/01/1996	155.90	1
68	LC-49A	455336.76	199380.35	06/01/1997	166.15	1
69	LC-49A	455336.76	199380.35	06/01/1998	173.00	1
70	LC-51	455784.81	198661.63	06/01/1995	99.00	1
71	LC-51	455784.81	198661.63	06/01/1996	130.00	1
72	LC-51	455784.81	198661.63	06/01/1997	142.50	1
73	LC-51	455784.81	198661.63	06/01/1998	162.50	1
74	LC-51	455784.81	198661.63	06/01/1999	170.00	1
75	LC-51	455784.81	198661.63	06/01/2000	162.50	1
76	LC-51	455784.81	198661.63	06/01/2001	153.30	1
77	LC-53	455473.31	198707.04	06/01/1995	115.00	1
78	LC-53	455473.31	198707.04	06/01/1996	167.50	1
79	LC-53	455473.31	198707.04	06/01/1997	155.00	1
80	LC-53	455473.31	198707.04	06/01/1998	162.50	1
81	LC-53	455473.31	198707.04	06/01/1999	195.00	1
82	LC-53	455473.31	198707.04	06/01/2000	210.00	1
83	LC-53	455473.31	198707.04	06/01/2001	200.00	1
84	LC-66A	454812.20	200218.85	06/01/1995	76.75	1
85	LC-66A	454812.20	200218.85	06/01/1996	112.00	1
86	LC-66A	454812.20	200218.85	06/01/1997	115.90	1
87	LC-66A	454812.20	200218.85	06/01/1998	111.75	1
88	LC-66A	454812.20	200218.85	06/01/1999	119.15	1
89	LC-66A	454812.20	200218.85	06/01/2000	106.65	1
90	LC-66A	454812.20	200218.85	06/01/2001	91.20	1
91	PA-381	454330.00	199657.72	06/01/1995	56.50	1
92	PA-381	454330.00	199657.72	06/01/1996	35.80	1
93	PA-381	454330.00	199657.72	06/01/1997	35.50	1
94	PA-381	454330.00	199657.72	06/01/1998	39.30	1
95	PA-381	454330.00	199657.72	06/01/1999	48.50	1
96	PA-381	454330.00	199657.72	06/01/2000	47.80	1
97	PA-381	454330.00	199657.72	06/01/2001	39.00	1
98	LC-137B	456035.56	198940.36	03/25/2004	263.60	1
99	LC-137B	456035.56	198940.36	08/29/2005	630.67	1
100	LC-137B	456035.56	198940.36	08/29/2006	538.27	1

Table A-1. TCE-equivalent concentrations used for Fort Lewis site calibration (continued)

No.	Well	East (m)	North (m)	Date	Concentration (ppb)	Aquifer
101	LC-137B	456035.56	198940.36	08/31/2007	326.51	1
102	LC-137B	456035.56	198940.36	09/02/2008	727.02	1
103	LC-137B	456035.56	198940.36	08/31/2009	269.33	1
104	LC-137B	456035.56	198940.36	03/02/2010	322.48	1
105	LC-160	456044.89	198862.04	12/18/2006	77.73	1
106	LC-160	456044.89	198862.04	12/12/2007	42.51	1
107	LC-160	456044.89	198862.04	12/10/2008	34.22	1
108	LC-160	456044.89	198862.04	12/07/2009	22.11	1
109	LC-160	456044.89	198862.04	03/02/2010	13.40	1
110	LC-27	456110.34	198690.28	09/28/2006	28.53	1
111	LC-27	456110.34	198690.28	03/02/2007	16.59	1
112	LC-27	456110.34	198690.28	03/19/2008	8.70	1
113	LC-27	456110.34	198690.28	02/24/2009	12.09	1
114	LC-27	456110.34	198690.28	03/02/2010	11.01	1
115	MT-1	455984.84	198929.11	12/12/2006	127.66	1
116	MT-1	455984.84	198929.11	12/12/2007	106.31	1
117	MT-1	455984.84	198929.11	12/10/2008	139.14	1
118	MT-1	455984.84	198929.11	12/07/2009	41.07	1
119	MT-1	455984.84	198929.11	06/07/2010	85.83	1
120	MT-2	456065.61	198750.19	12/12/2006	15.75	1
121	MT-2	456065.61	198750.19	12/12/2007	11.58	1
122	MT-2	456065.61	198750.19	12/10/2008	13.02	1
123	MT-2	456065.61	198750.19	12/07/2009	10.51	1
124	MT-2	456065.61	198750.19	06/07/2010	7.51	1
125	MT-3	456103.63	198642.71	12/18/2006	21.22	1
126	MT-3	456103.63	198642.71	12/12/2007	13.65	1
127	MT-3	456103.63	198642.71	12/10/2008	7.42	1
128	MT-3	456103.63	198642.71	12/07/2009	14.17	1
129	MT-3	456103.63	198642.71	06/07/2010	12.20	1
130	MT-4	456154.73	198581.30	12/18/2006	26.30	1
131	MT-4	456154.73	198581.30	12/12/2007	12.05	1
132	MT-4	456154.73	198581.30	12/10/2008	4.68	1
133	MT-4	456154.73	198581.30	12/07/2009	11.84	1
134	MT-4	456154.73	198581.30	06/07/2010	4.57	1
135	PW-3	456057.00	198897.68	12/20/2006	505.04	1
136	PW-3	456057.00	198897.68	12/18/2007	265.24	1
137	PW-3	456057.00	198897.68	12/10/2008	271.59	1
138	PW-3	456057.00	198897.68	12/07/2009	176.84	1
139	PW-4	456069.12	198840.78	12/20/2006	314.34	1
140	PW-4	456069.12	198840.78	12/18/2007	162.52	1
141	PW-4	456069.12	198840.78	12/10/2008	103.84	1
142	PW-4	456069.12	198840.78	12/07/2009	54.26	1
143	PW-4	456069.12	198840.78	09/20/2010	41.53	1
144	PW-5	456112.97	198807.55	12/20/2006	118.60	1
145	PW-5	456112.97	198807.55	12/28/2007	114.49	1
146	PW-5	456112.97	198807.55	12/10/2008	57.65	1
147	PW-5	456112.97	198807.55	12/07/2009	40.63	1
148	PW-5	456112.97	198807.55	09/20/2010	54.72	1
149	PW-6	456143.41	198753.97	12/18/2006	74.60	1
150	PW-6	456143.41	198753.97	12/18/2007	86.56	1

Table A-1. TCE-equivalent concentrations used for Fort Lewis site calibration (continued)

No.	Well	East (m)	North (m)	Date	Concentration (ppb)	Aquifer
151	PW-6	456143.41	198753.97	12/10/2008	35.99	1
152	PW-6	456143.41	198753.97	12/07/2009	20.90	1
153	PW-6	456143.41	198753.97	09/20/2010	18.76	1
154	PW-7	456168.18	198700.00	12/20/2006	37.79	1
155	PW-7	456168.18	198700.00	12/18/2007	44.40	1
156	PW-7	456168.18	198700.00	12/10/2008	30.77	1
157	PW-7	456168.18	198700.00	09/20/2010	16.57	1
158	PW-8	456195.19	198649.27	12/18/2006	62.05	1
159	PW-8	456195.19	198649.27	12/14/2007	38.89	1
160	PW-8	456195.19	198649.27	12/10/2008	30.81	1
161	PW-8	456195.19	198649.27	12/07/2009	25.82	1
162	PW-8	456195.19	198649.27	09/20/2010	18.86	1
163	LC-126	453981.55	200510.92	06/01/1995	93.00	2
164	LC-126	453981.55	200510.92	06/01/1996	117.50	2
165	LC-126	453981.55	200510.92	06/01/1997	115.00	2
166	LC-126	453981.55	200510.92	06/01/1998	103.00	2
167	LC-126	453981.55	200510.92	06/01/1999	108.80	2
168	LC-126	453981.55	200510.92	06/01/2000	81.80	2
169	LC-126	453981.55	200510.92	06/01/2001	82.30	2
170	LC-40D	454232.17	200231.42	06/01/1995	15.50	2
171	LC-40D	454232.17	200231.42	06/01/1996	16.00	2
172	LC-40D	454232.17	200231.42	06/01/1997	17.30	2
173	LC-40D	454232.17	200231.42	06/01/1998	15.90	2
174	LC-40D	454232.17	200231.42	06/01/1999	11.80	2
175	LC-40D	454232.17	200231.42	06/01/2000	4.00	2
176	LC-40D	454232.17	200231.42	06/01/2001	13.30	2
177	LC-66D	454815.25	200223.18	06/01/1995	42.00	2
178	LC-66D	454815.25	200223.18	06/01/1996	53.00	2
179	LC-66D	454815.25	200223.18	06/01/1997	53.00	2
180	LC-66D	454815.25	200223.18	06/01/1998	57.80	2
181	LC-66D	454815.25	200223.18	06/01/1999	26.30	2
182	LC-66D	454815.25	200223.18	06/01/2000	2.90	2
183	LC-66D	454815.25	200223.18	06/01/2001	32.00	2
184	LC-67D	454256.85	199869.25	06/01/1995	50.50	2
185	LC-67D	454256.85	199869.25	06/01/1996	52.30	2
186	LC-67D	454256.85	199869.25	06/01/1997	56.50	2
187	LC-67D	454256.85	199869.25	06/01/1998	61.80	2
188	LC-67D	454256.85	199869.25	06/01/1999	51.80	2
189	LC-67D	454256.85	199869.25	06/01/2000	51.30	2
190	LC-67D	454256.85	199869.25	06/01/2001	55.70	2
191	LC-69D	454756.91	199682.96	06/01/2001	150.00	2
192	LC-72D	453770.55	200173.05	06/01/1995	45.50	2
193	LC-72D	453770.55	200173.05	06/01/1996	47.80	2
194	LC-72D	453770.55	200173.05	06/01/1997	54.00	2
195	LC-72D	453770.55	200173.05	06/01/1998	57.30	2
196	LC-72D	453770.55	200173.05	06/01/1999	43.80	2
197	LC-72D	453770.55	200173.05	06/01/2000	13.60	2
198	LC-72D	453770.55	200173.05	06/01/2001	37.00	2
199	LC-73D	453627.71	199977.88	06/01/1995	25.50	2
200	LC-73D	453627.71	199977.88	06/01/1996	34.30	2

Table A-1. TCE-equivalent concentration selected in Fort Lewis (continued)

No.	Well	East (m)	North (m)	Date	Concentration (ppb)	Aquifer
201	LC-73D	453627.71	199977.88	06/01/1997	34.30	2
202	LC-73D	453627.71	199977.88	06/01/1998	28.80	2
203	LC-73D	453627.71	199977.88	06/01/1999	20.60	2
204	LC-73D	453627.71	199977.88	06/01/2000	13.50	2
205	LC-73D	453627.71	199977.88	06/01/2001	21.30	2
206	LC-74D	453425.18	199565.97	06/01/1995	40.00	2
207	LC-74D	453425.18	199565.97	06/01/1996	50.30	2
208	LC-74D	453425.18	199565.97	06/01/1997	54.50	2
209	LC-74D	453425.18	199565.97	06/01/1998	53.50	2
210	LC-74D	453425.18	199565.97	06/01/1999	72.70	2
211	LC-74D	453425.18	199565.97	06/01/2000	68.00	2
212	LC-74D	453425.18	199565.97	06/01/2001	62.30	2
213	PS-13	453382.38	199122.79	06/01/2001	0.50	2

Notes:
1. When a measuring date is not clear or an annual average is used, the date set to the middle of the year, e.g., June 1
2. Aquifer 1 and 2 indicate Vashon and SLA, respectively.

Table A-2. Source flux measurement at EGDY in For Lewis

Source	Date	Source flux (kg/day)
1	11/01/2003	0.754
1	04/01/2006	0.005
2	11/01/2003	0.323
2	04/01/2006	0.003
3	04/01/2006	0.420

Notes:
1. Nov 1, 2003 is pre-ERH for Areas 1 to 3 and Apr 1, 2006 is post-ERH for Areas 1 and 2 and pre-ERH for Area 3.
2. The model uses numeric years, e.g., 08/04/2004 = 2004.59, etc.

Table A-3. DNAPL mass removed by TSR at EGDY in For Lewis

Source	Date	Mass removal (kg)
1	08/04/2004	2990
2	08/05/2005	1340
3	01/26/2007	1120

Note: The model uses decimal years, e.g., 08/04/2004 = 2004.59, etc.

Appendix B. Publications Resulting From Project

Cardiff, M., and P.K. Kitanidis, 2008, Efficient Solution of Nonlinear Underdetermined Inverse Problems with COMSOL Multiphysics, Computers and Geosciences, 34, 1480-1491.

Parker, J.C. and R.W. Falta, 2008, Comparison of alternative formulations for modeling DNAPL sources with biodecay, Adv. Water Resources, 31, 1325-1332.

Parker, J.C, U. Kim, M. Widdowson, and F. Chappel, 2008, A practical modeling approach for NAPL dissolution kinetics, microbially-mediated redox reactions and aquifer-aquitard diffusion to assess remedial options, Amer. Geophys. Union, Fall Meeting, San Francisco, Dec 17, 2008.

Parker, J., P. Kitanidis, X. Liu , M. Cardiff, U. Kim, D. Becker, A. Bloom, and K. Gorder, 2008, Practical cost-optimization of characterization and remediation decisions at DNAPL sites with consideration of prediction uncertainty, SERDP Environmental Symposium, Washington DC.

Liu, X., M. Cardiff, J. Parker, P. Kitanidis, 2008, NAPL remediation cost optimization under uncertainty using a semi-analytic model, Amer. Geophys. Union, Fall Meeting, San Francisco, Dec 17, 2008.

Parker, J.C., E. Park, and G. Tang, 2008, Dissolved plume attenuation with DNAPL source remediation, aqueous decay and volatilization -- Analytical solution, model calibration, and prediction uncertainty, J. Contam. Hydrol., 102, 61-71.

Parker, J., P. Kitanidis, U. Kim, X. Liu, M. Cardiff, and M. Widdowson, 2009, DNAPL source strength vs. time model formulation, calibration and uncertainty. SERDP Annual Meeting, Dec 1-3, Washington DC.

Parker, J., P. Kitanidis, U. Kim, X. Liu, M. Cardiff, 2009, Cost optimization of DNAPL site remediation with consideration of prediction uncertainty. SERDP Annual Meeting, Dec 1-3, Washington DC.

Cardiff, M., X. Liu, P. K. Kitanidis, J. Parker, and U. Kim, 2010, Cost optimization of DNAPL source and plume remediation under uncertainty using a semi-analytic model, J. Contam. Hydrol., 13, 24-43.

Liu, X., M. Cardiff, and P.K. Kitanidis, 2010, Parameter estimation in nonlinear environmental problems, Stochastic Environmental Research and Risk Assessment, 10.1007/s00477-010-0395-y.

Kitanidis, P, J. Parker, U. Kim, X. Liu, and J. Lee, 2010, Context-specific quantification of uncertainty, value of information, and total-cost optimization of DNAPL site remediation. SERDP Annual Meeting, Nov 30- Dec 2, Washington D.C.

Parker, J., U. Kim, P. Kitanidis, and X. Liu, 2010, Practical cost-optimization of remediation and monitoring decisions at DNAPL sites with consideration of prediction uncertainty. SERDP Annual Meeting, Nov 30- Dec 2, Washington D.C.

Parker, J.C., U. Kim, M. Widdowson, P. Kitanidis, and R. Gentry, 2010, Effects of model formulation and calibration data on uncertainty in predictions of DNAPL source dissolution rate, Water Resour. Res. W12517. DOI: 10.1029/2010WR009361.

Parker, J.C., U. Kim, P.K. Kitanidis, M. Cardiff, and X. Liu, 2010, Stochastic cost optimization of multi-strategy DNAPL site remediation, Ground Water Monitoring and Remediation, 10.1111/j.1745-6592.2010.01287.x.

Parker, J.C., P.K. Kitanidis, and U. Kim, 2010, Joint optimization of remediation design and monitoring for DNAPL sites considering model and data uncertainty, Meeting of the Americas, Foz do Iguassu, Brazil, Aug 8-13, 2010.

Lee, J., X. Liu, P.K. Kitanidis, U. Kim, J. Parker, A. Bloom, R. Lyon, 2011, Cost optimization of DNAPL remediation at Dover Air Force Base, Ground Water Remediation and Monitoring, in review.

Liu, X., J.L., P.K. Kitanidis, J. Parker , and U. Kim, 2011, Value of information as a context-specific measure of uncertainty in groundwater remediation, Water Resources Management, in review.

Kitanidis, P. K., 2011, A second-moment asymptotically optimal nonlinear filter (discrete time), Stoch Envir Res and Risk Assessment, in review.

Parker, J.C., U. Kim, P.K. Kitanidis, M. Cardiff, X. Liu, and G. Beyke, 2011, Stochastic cost optimization of DNAPL site remediation: I. Method description and sensitivity studies. J. Contam. Hydrol., in review.

Kim, U., J.C. Parker, P. K. Kitanidis, M. Cardiff, X. Liu, and J. Gillie, 2011, Stochastic cost optimization of DNAPL site remediation: II. Field application, J. Contam. Hydrol., in review.